



Norwegian University
of Life Sciences

Master's Thesis 2023 60 ECTS

Faculty of Biosciences

Department of Animal and Aquacultural Sciences

Development of CRISPR screenable phenotypes for PCV2 in pig cells and detection of latent BVDV contamination in commercial FBS

Andrine Martinsen

Biotechnology

Acknowledgments

This master's thesis marks the end of an incredible journey as I pursued my Master's degree in Biotechnology at the Norwegian University of Life Sciences (NMBU). As a part of the GeneInnovate project at the Center for Integrative Genetics (CIGENE), with funding's from BIONÆR, I had the privilege of working under the supervision of Matthew Kent.

I want to take a moment to express my gratitude to everyone who has been a part of this adventure. My heartfelt thanks go to my main advisors, Thomas Harvey and Victor Boyartchuk, who have been my guidance, offering their wisdom, support, and patience throughout. They have truly helped me grow and navigate my way through the research and writing process.

Lastly, I cannot forget to mention my amazing family. Their love, understanding, and constant encouragement kept me going during the educational and demanding times, and their faith in me has been a source of inspiration. Thank you for being there every step of the way.

Ås, May 2023

Andrine Martinsen

Abstract

Genome-wide CRISPR screening is a powerful research tool that enables scientists to investigate the roles of specific genes in various biological processes, such as cell survival, phenotype development, or disease pathways. By using CRISPR technology to knockout or modify genes on a genome-wide scale, researchers can identify potential drug targets or uncover novel insights into cellular mechanisms. This study is a part of a bigger project where the main goal is to discover gene candidates for PCV2 resistance in pigs using genome-wide CRISPR knockout screening (GeCKO) as a tool for more precise and efficient breeding. This study aims to develop a protocol for PCV2 cultivation in PK-15 cells and identify a suitable cell line with detectable cytopathic effects upon infection. In addition, the study sought to find a BVDV-free source of FBS to prevent contamination in MDBK cells, a cell line that will be used in GeCKO screening.

The evaluation of cell viability in PCV2 infection experiments demonstrated the presence of viral-induced cytopathic effects, particularly at lower cell densities. However, further optimization and scaling up of the experimental procedure are needed to ensure reproducibility and reliability for GeCKO screening applications. We attempted to develop a screenable phenotype based on virus mediated actin remodeling, however these experiments were unsuccessful, and require optimization of the method. We revealed significant differences in cell growth and viability in PK-15 cells infected with PCV2 compared to mock infected cells, indicating the substantial impact of PCV2 infection on cellular health. PCR and agarose gel electrophoresis confirmed the presence of PCV2 in infected PK-15 cells, and Real-Time PCR demonstrated successful amplification of PCV2 viral DNA showing successful replication. BVDV contamination was identified in the initial testing of MDBK cells grown with different FBS batches. Subsequent testing using a BVDV-free MDBK cell line confirmed FBS as the source of contamination. A BVDV-free batch of FBS was obtained, resolving the contamination issue for future use in GeCKO screening.

This research contributes to the development of CRISPR tools for production animals, paving the way for more gene-editing possibilities and potentially leading to better animal health and cost savings in the breeding industry.

Sammendrag

Genome-wide CRISPR screening er et kraftig forskningsverktøy som gjør det mulig å undersøke virkningen av spesifikke gener i ulike biologiske prosesser, som for eksempel overlevelsessevne, fenotypeutvikling eller sykdomsprosesser. Ved å bruke CRISPR-teknologi for å slå ut eller modifisere gener, kan forskere identifisere potensielle mål for legemidler eller avdekke ny innsikt i cellulære mekanismer. Dette studiet er en del av et større prosjekt der hovedmålet er å oppdage genkandidater som gir griser resistens mot PCV2 ved bruk av Genome-wide CRISPR knockout screening (GeCKO) som er et verktøy for mer presis og effektiv avl. Studiet hadde som mål å utvikle en protokoll for dyrking av PCV2 i PK-15 celler og identifisere en passende cellelinje med detekterbare cytopatiske effekter ved infeksjon av PCV2. prosjektet. I tillegg ønsket vi å finne en BVDV-fri kilde til FBS for å forhindre kontaminasjon i MDBK-celler, en cellelinje som vil bli brukt i GeCKO screening.

Evaluerings av levedyktighet i PK-15 celler infisert med PCV2 viste tilstedeværelse av virusinduserte cytopatiske effekter, spesielt ved lavere celletetthet. Det er nødvendig med ytterligere optimalisering og oppskalering av den eksperimentelle prosedyren for å sikre reproducerbare og pålitelige resultater for GeCKO screeningapplikasjoner. Vi forsøkte å utvikle en screenbar fenotype basert på virusinduserte aktinforandringer, men disse eksperimentene var mislykkede og krever optimalisering av prosedyre. Vi avdekket betydelige forskjeller i cellevekst og levedyktighet i PK-15-celler infisert med PCV2 sammenlignet med mock infiserte celler, noe som indikerer den betydelige effekten av PCV2-infeksjon på cellulær helse. PCR og agarose gelelektroforese bekreftet tilstedeværelsen av PCV2 i infiserte PK-15 celler, og Real-Time PCR hadde vellykket amplifisering av PCV2 viralt DNA og viste suksessfull virusreplikasjon. BVDV kontaminasjon ble identifisert i den første analysen av MDBK celler dyrket med forskjellige FBS batcher. Påfølgende testing ved hjelp av en BVDV-fri MDBK cellelinje bekreftet FBS som kilden til kontaminasjon. En BVDV-fri batch av FBS ble innhentet og løste kontamineringsproblemet for fremtidig bruk i GeCKO screening.

Forskningen i dette studiet bidrar til utvikling av CRISPR-verktøy for produksjonsdyr og legger grunnlaget for flere genredigeringsmuligheter, noe som potensielt kan føre til bedre dyrehelse og kostnadsbesparelser i avlsindustrien.

Abbreviations

ATP	Adenosine Tri-Phosphate
BVD	Bovine Viral Diarrhea
BVDV	Bovine Viral Diarrhea Virus
Cap	Capsid protein
Cas12a	CRISPR-Associated protein 12a
Cas9	CRISPR-Associated protein 9
cDNA	Complementary DNA.
CRISPR	Clustered Regularly Interspaced Short Palindromic Repeats
Ct	Cycle threshold
DAPI	4',6-Diamidino-2-Phenylindole, Dilactate
DMSO	Dimethylsulfoxide
DNA	Deoxyribonucleic acid
DS	Dermatan sulfate
EDTA	Ethylenediaminetetraacetic acid
FBS	Fetal Bovine Serum
FBS-G	FBS-Gold
GAGs	Glycosaminoglycans
GeCKO	Genome-wide CRISPR knockout screening
gRNA	Guide RNA
HPI	Hour post infection
HS	Heparan sulfate
IPEC-J2	Intestinal Porcine Epithelial Cell Line – J2
MDBK	Madin-Darby Bovine Kidney
mRNA	Messenger RNA
NTC	No template control
ORF1	Open reading frame 1
ORF2	Open reading frame 2
PBS	Phosphate-buffered Saline
PCR	Polymerase Chain Reaction

PCV	Porcine circovirus
PCV1	Porcine circovirus type 1
PCV2	Porcine circovirus type 2
pH	Potential hydrogen
PK-15	Porcine Kidney-15
PLC-IP3R-Ca ²⁺	Phospholipase C- Inositol 1,4,5-trisphosphate receptors- Ca ²⁺
PMWS	Postweaning multisystemic wasting syndrome
POMECs	Primary porcine oral mucosal epithelial cells
PPV	Porcine parvovirus
PRRSV	Porcine reproductive and respiratory syndrome virus
Rep	Replicase protein
RLU	Relative Light Units
RNA	Ribonucleic acid
RT-PCR	Reverse transcription PCR
TAE	Tris-Acetate-EDTA
TBS	Tris-buffered saline
TBST	TBS TWEEN® 20
TET	Tetracycline-controlled transcriptional

Table of context

Acknowledgments	i
Abstract.....	ii
Sammendrag.....	iii
Abbreviations.....	iv
Table of Context	vi
1 Introduction.....	1
1.1 Aim of study	1
1.1.1 Pooled CRISPR screening.....	1
1.1.2 Porcine circovirus type 2 (PCV2).....	3
1.1.3 Bovine viral diarrhea virus (BVDV)	4
1.1.4 Aim of study.....	4
1.2 Cells.....	5
1.2.1 PK-15 cells	5
1.2.2 IPEC-J2 cells.....	6
1.2.3 MDBK cells.....	6
1.2.4 Cell culturing.....	6
1.3 Virus.....	8
1.3.1 Porcine circovirus type 2 (PCV2).....	8
1.3.2 PCVE replication cycle	8
1.3.3 PCV2 cultivation.....	12
1.3.4 Bovine viral diarrhea virus (BVDV)	12
1.3.5 BVDV contaminations	13
1.4 Methods of analysis.....	14
1.4.1 PCR and nested RT-PCR	14
1.4.2 Real-Time PCR.....	14
1.4.3 Cell viability assay.....	15
1.4.4 Fluorescence microscopy and flow cytometry	16
2 Methods.....	19
2.1 Cell culture.....	19
2.2 Cultivation of PCV2.....	20
2.2.1 Sample collection and DNA extraction.....	20
2.2.2 PCR and Real-Time PCR.....	21
2.2.3 Investigating PCV1 contamination.....	24
2.2.4 PCV2 infection in PK-15 cells.....	24
2.2.5 Concentrating PCV2 virus	25
2.3 Cell viability assay	26

2.4 Actin filament changes by fluorescence microscopy	26
2.5 BVDV detection in FBS	27
3 Results	31
3.1 Cultivation of PCV2.....	31
3.1.1 Investigating PCV1 contamination.....	31
3.1.2 PCV2 infection in PK-15 cells.....	31
3.1.3 Concentrating PCV2 virus	38
3.2 Cell viability	40
3.3 Actin filament changes by fluorescence microscopy	42
3.4 BVDV detection in FBS	42
4. Discussion	44
4.1 Cell viability assay	44
4.2 Actin filament changes by fluorescence microscopy	47
4.3 BVDV contaminations in FBS	48
4.4 Cultivation of PCV2.....	49
4.4.1 PCV1 contamination.....	49
4.4.2 Microscopic insights.....	50
4.4.3 PCR.....	51
4.4.4 Real-Time PCR.....	51
4.4.5 Concentrating PCV2.....	53
4.5 Further Work	54
4.5.1 Cell viability	54
4.5.2 Actin filament changes.....	54
4.5.3 Cultivation of PCV2	55
6 Conclusion	56
7 Bibliography	59
Appendix A: Cell lines, Materials, Reagents, and Instruments.....	66
Appendix B: Real-time PCR raw data	69

1 Introduction

1.1 Aim of study

1.1.1 Pooled CRISPR screening

Genome-wide Clustered Regularly Interspaced Short Palindromic Repeats (CRISPR) knockout screening is a discovery tool that scientists use to understand and investigate processes where specific genes are involved, such as cell survival, specific phenotypes or biological processes and can be used to identify drug targets (Bock et al., 2022; Yu & Yusa, 2019). One specific area of interest is the utilization of CRISPR screening to uncover pathogen-related genes in order to comprehend the intricate relationship between hosts and viruses. A notable example is the study by Zhu et al., where they employed a genome-wide CRISPR screening to identify host factors that regulate SARS-CoV-2 entry (Zhu et al., 2021). Viral infections in production animals are a common problem, thus GeneInnovate initiated in 2018, a project aiming to utilize genome-wide CRISPR screening to improve the breeding of fish, plants, and animals in Norway. Selective breeding has been a long-standing practice to develop desired traits in plant, fish, and animal breeding. By using genome-wide CRISPR screening to identify pathogen related genes, a more precise and effective selective breeding can be achieved resulting in both better animal health and potential large cost savings. Given that the genome-wide CRISPR screening system is currently restricted to human and mouse applications, the development of similar CRISPR tools for production animals paves the way for more gene-editing possibilities.

The prevalent method for genome-wide CRISPR screening is pooled CRISPR screening, which is the approach GeneInnovate intends to employ in their project (Synthego, n.d.). Pooled CRISPR screening is a highly cost-effective method that allows for the interrogation of entire genomes with no special equipment required (Annie Zhang Bargsten, 2020; Mah, 2021). A pooled CRISPR screen can either be a loss-of-function or gain-of-function screening. In this study we focus on genome-wide CRISPR knockout screening (GeCKO) using CRISPR-associated protein 9 (Cas9), which is a loss-of-function screening where the genes are knocked out of the genome and the consequences of these losses is studied (Puschnik et al., 2017). The CRISPR Cas9 system comprises a Cas9 enzyme and a guide RNA (gRNA) (Xu & Li, 2020). Researchers found a way to utilize this system to modify genes by constructing these gRNAs that guides the Cas9 nuclease to a specific target gene. This initiate cutting of DNA followed by an automatic DNA repair response

in the cell which alters the reading frame of the protein causing a premature stop codon thus inactivating the protein (Wang et al., 2016). While Cas9 is the most studied and commonly used Cas protein in CRISPR-based genome editing, it is important to notice that pooled CRISPR screening can use other proteins besides Cas9, such as CRISPR-associated protein 12a (Cas12a) (Bock et al., 2022; Dede et al., 2020).

To initiate a CRISPR screening, scientists typically introduce a library of CRISPR gRNAs into a cell culture that already expresses Cas9 proteins (**Figure 1A** and **3B**), however, the Cas9 protein can also be introduced with the lentiviral CRISPR library (Bock et al., 2022; Synthego, n.d.). Each gRNA targets a different gene in the genome, allowing researchers to knock out all genes simultaneously, one gene per cell. The resulting cell culture contains a pool of cells where each cell has a different gene knocked out (**Figure 1C**). The cells are then exposed to a selective pressure, such as a viral infection, that reveals cells with a certain trait or function of interest (**Figure 1D**). After the selective pressure is applied, the researchers can identify the cells that have the desired trait or function and sequence the CRISPR gRNAs to determine which genes have been knocked out (**Figure 1E** and **F**). The selective pressure and selection is a crucial step in GeCKO screening for successful screening (Bock et al., 2022). To identify the genes responsible for a specific phenotype, researchers need a way to select cells that have undergone a successful knockout of the gene or genes potentially involved. Screenable phenotypes are characterized to enable selection of such cells. For example, in this project, pooled CRISPR screening will eventually be used to identify genes involved in the viral infection process of PCV2. In cases where a viral infection leads to cell death, the surviving cells may possess crucial genes that enable successful resistance to the viral infection, thereby helping to identify specific genes responsible for the infection. By comparing the sequences of the guide RNAs in the surviving cells to those in the original pool, researchers can identify the specific genes associated with the trait or function of interest. This allows for the identification of potential drug targets or characterization of genes involved in complex biological processes (Bock et al., 2022; Synthego, n.d.). An overview of a GeCKO screening is presented in **Figure 1**.

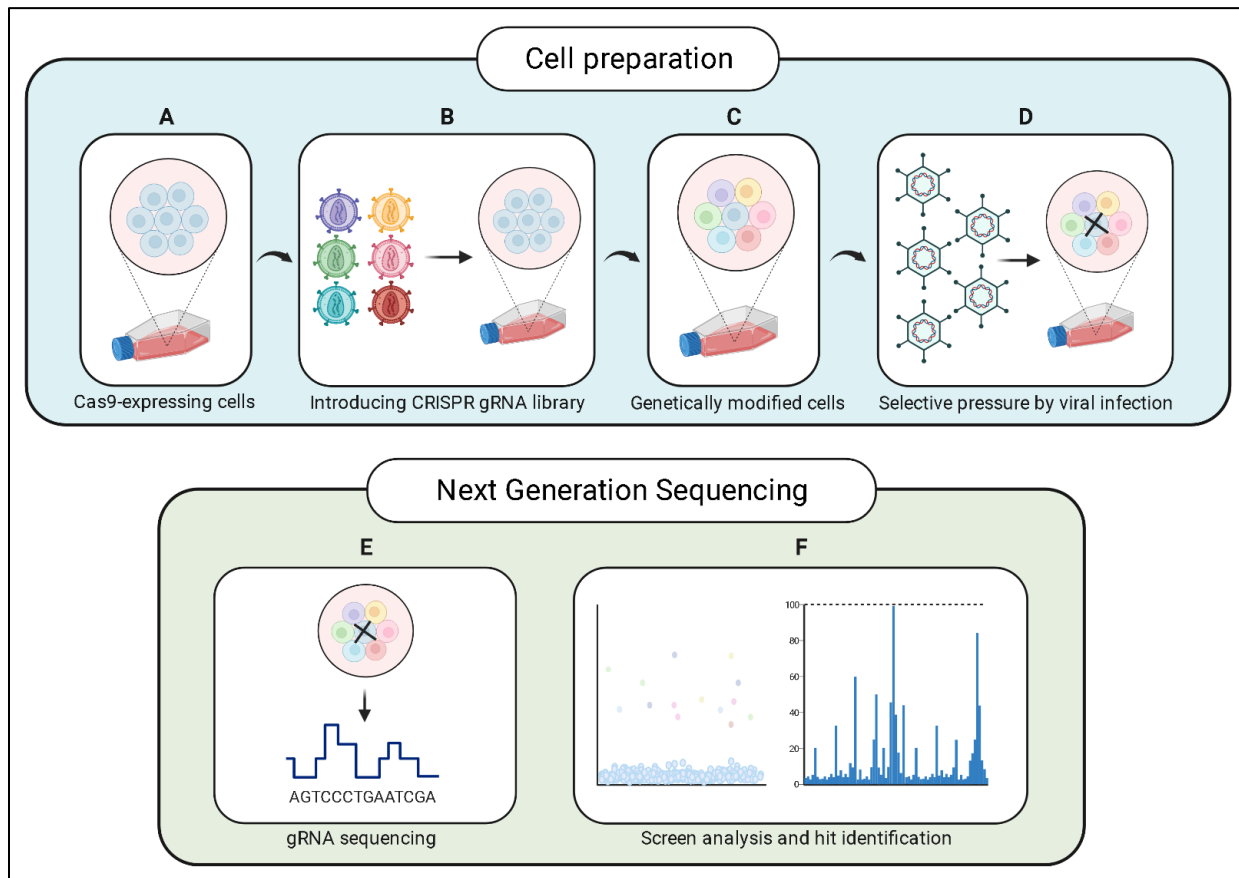


Figure 1 – Genome-wide CRISPR knockout screening: A Cas9-expressing cell culture prepared for CRISPR screening (A) is hit with a CRISPR gRNA library (B) causing knock out of all genes simultaneously, one gene per cell (C). The genetically modified cell pool is then infected with the wanted virus (D) and the cells with desired traits are identified. The gRNA from the experiment is sequenced (E) and a screen analysis and hit identification is performed (F). The figure is adapted from “Blank Panels (Layout 4x2)”, by BioRender.com (2023), retrieved from <https://app.biorender.com/biorender-templates>.

1.1.2 Porcine circovirus type 2 (PCV2)

PCV2 is known to be a cause of post-weaning multisystemic wasting syndrome (PMWS). PMWS is a common porcine industry disease that causes wasting, pallor, dyspnea, rough hair coat, diarrhea, and jaundice (Segales & Domingo, 2002). These symptoms are often seen in 2-3.5-month-old piglets and can result in lethality rates ranging from 4-80% depending on the farm and herd. (Rodriguez-Arriola et al., 2002; Segales & Domingo, 2002). While there is currently no known

cure for PMWS, measures of prevention are recommended. These include improving hygiene, reducing animal density, isolating sick pigs, avoiding cross-fostering, and mixing of separated groups, as well as developing vaccines against PCV2. Vaccination has been shown to increase immunity against PCV2 infections, but it is not a cure for PMWS (Fort et al., 2012; Fort et al., 2009; Kekarainen et al., 2010; Ménard, 2006). PCV2 is also associated with other diseases in pigs, including porcine dermatitis nephropathy syndrome (PDNS) (Segales, 2012). A study conducted in 2013 on the English pig industry found that PMWD and PCV2 were the most economically damaging diseases, resulting in losses of approximately £88 million between 2001 and 2004 (Alarcon et al., 2013).

1.1.3 Bovine viral diarrhoea virus (BVDV)

Bovine viral diarrhoea virus (BVDV) is known to cause Bovine Viral Diarrhoea (BVD) in cattle, resulting in immunosuppression and reproductive disorders. Because of this BVD is a disease that causes considerable economic losses in the cattle industry and the extent of these losses depends on the severity of the outbreak and the herd affected. However, it is estimated that BVD can cost the global cattle industry billions of dollars each year in direct losses (Yarnall & Thrusfield, 2017). These losses include decreased milk production, decreased weight gain, and increased veterinary expenses. In addition to direct losses, BVD also results in indirect losses such as decreased reproductive efficiency and increased susceptibility to other diseases (Houe, 2003).

1.1.4 Aim of study

Due to the significant economic and clinical impact of PCV2 and BVDV and the lack of treatment options, GeneInnovate aims to develop CRISPR technology to enhance the resistance of pigs to PCV2 virus and cattle to BVDV virus by selective breeding. The aim of this study is to find a suitable cell line that exhibits detectable cytopathic effects after infection with PCV2. To ensure continuous access to the virus, a sub-goal of the study is to develop a protocol for PCV2 cultivation.

Madin-Darby Bovine Kidney (MDBK) cells are susceptible to BVDV infection, making them a suitable cell line for detecting cytopathic effects for use in GeCKO screening (La Polla et al., 2022; Munyanduki et al., 2020; Workman et al., 2021). However, Fetal bovine serum (FBS) has been reported to have small BVDV contaminations as a result of fetal infection (Zabal et al., 2000). The

FBS contaminations will lead to contaminations of the complete growth media produced, thus resulting in contaminating the cell line it is used in (Bolin et al., 1991; Nuttall et al., 1977; Xia et al., 2011). Since MDBK cells are susceptible to BVDV infections, the contaminations from FBS will infect the cell line, rendering them unsuitable for BVDV experiments. Therefore, solving this problem is crucial to conducting research on BVDV infections in MDBK cells. In addition to the research on PCV2, the study includes testing for BVDV contamination in MDBK cells using different FBS in the growth media before conducting nested reverse transcription polymerase chain reaction (RT-PCR) with agarose gel electrophoresis to test for the presence of contamination.

Summary of main goals in this study:

1. Develop a protocol for PCV2 cultivation in PK-15 cells for our laboratory.
2. Find a suitable cell line that has detectible cytopathic effects after infection of PCV2.
3. Find an FBS without BVDV contaminations.

1.2 Cells

Immortalized cells are cells that have either been altered in the laboratory or spontaneously mutated, resulting in an indefinite lifespan and the ability to renew (Segeritz, 2017; Udayangani, 2021). Such cells are widely used for research purposes, and there are numerous cell lines available. In this study, we used three immortalized cell lines: Porcine Kidney-15 (PK-15), Intestinal Porcine Epithelial Cell Line – J2 (IPEC-J2), and MDBK cell lines to conduct various experiments.

1.2.1 PK-15 cells

PK-15 is a spontaneously immortalized cell line derived from kidney cells of an adult *Sus scrofa* (pig) (*Cellosaurus PK-15 (CVCL_2160)*, 2023). This cell line has been extensively used in viral research, such as viral replication, pathogenesis, and host-virus interaction studies, as well as gene expression studies (Jiang et al., 2019; Misinzo et al., 2009). One common and well-studied virus in the PK-15 cell line is PCV2 (Chen et al., 2013; Cruz & Araujo, 2014; Misinzo et al., 2009). Previous studies have suggested that the release of replicated virus in PK-15 cells leads to cell apoptosis (Misinzo et al., 2005; S. Wang et al., 2021). Given the widespread use of PK-15 cells in

PCV2 research, we aimed to investigate whether this could be a potential cytopathic effect for GeCKo screening. Additionally, since PK-15 has been described as a cell line suitable for PCV2 replication, we were interested in developing a method of cultivating PCV2 in PK-15 cells (Zhu et al., 2007).

1.2.2 IPEC-J2 cells

IPEC-J2 cells are non-transformed and self-renewing intestinal porcine enterocyte cells that originate from the small intestines of a one-day-old piglet (Brosnahan & Brown, 2012; Vergauwen, 2015). Due to the similarities between the cell line and pig intestinal functions in vivo, IPEC-J2 cells are commonly used for in vitro experiments (Vergauwen, 2015). Similar to PK-15, IPEC-J2 cells have been used in viral research and gene expression studies (Mariani et al., 2009; Yan et al., 2014). In 2014 a research paper published by Yan et al. suggested that PCV2 infection in IPEC-J2 cells leads to microfilament changes that can be detected using fluorescence microscopy and flow cytometry. We wanted to investigate whether this change could be a potential cytopathic effect to use for GeCKO screening. Specifically, we aimed to determine whether this change is detectable by fluorescence microscopy, with the eventual end goal being to separate infected and uninfected cells using cell sorting.

1.2.3 MDBK cells

MDBK cells are epithelial kidney cells from *Bos taurus* (cow) and is a spontaneously immortalized cell line (Fay et al., 2020; Saif et al., 1988; P. Wang et al., 2021). MDBK cell line has been used for viral research, viral vaccine production and gene expression studies and has commonly been used for studying BVDV (Miroslaw et al., 2022). BVDV have been reported to have cytopathic effect on MDBK cells that potentially is suitable for genome-wide CRISPR knockout screening, however to be able to do this research it is critical that the cell line is free of BVDV contaminations (Gao et al., 2011).

1.2.4 Cell culturing

Working with cell cultures requires strict antiseptic techniques to maintain a sterile environment and avoid contamination. The success of culturing cell lines is also dependent on providing a

growth environment that mimics the cells' natural conditions. To do this a complete growth medium that contains the appropriate pH, nutrients, amino acids, and glucose levels is used. The use of FBS is essential in the growth medium as it provides growth-promoting factors, carrier proteins, amino acids, macromolecular proteins, vitamins, hormones, carbohydrates, lipids, and more to ensure the success of cell culturing (Segeritz, 2017). FBS also supports growth by having low levels of antibodies and other growth-inhibiting components, however the down sides of using FBS is that it can contain unwanted viral contaminations (Fang et al., 2017). FBS is derived as a by-product from the cattle industry and has been used in long-term cell culturing since 1958 when Theodore Puck published his work on somatic mammalian cells (Jochems et al., 2002; Puck et al., 1958). To prevent unwanted bacterial growth, antibiotics are added to the complete growth medium, and studies have shown that lower concentrations of antibiotics does not impact cell growth (Jedrzejczak-Silicka, 2017; Keilová, 1948).

Cryopreservation is a widely used method for long-term storage of cell cultures, as it can keep cell viability for years and prevent the formation of intracellular ice crystals (Matsumura et al., 2021). When necessary, cell cultures can be revived from cryopreservation by thawing them in a 37°C water bath and cultivating them in cell culture flasks or plates of various sizes containing complete growth medium. During growth, temperature and gas composition are carefully controlled using incubators to maintain an optimal environment for the cell culture (Segeritz, 2017). For mammalian cells, a gas mixture of 5-10% CO₂ is recommended to maintain physiological pH in the growth medium, and the temperature should be adjusted according to the origin of the cell culture, although most mammalian cell lines grow at 37°C (Jedrzejczak-Silicka, 2017). Once the cell culture reaches a density of 70-90%, it is necessary to passage the cells, allowing the cells to grow without being overcrowded. This removes dead cells, debris, and waste products, and provides fresh nutrients to support further cell growth. Cell counting is a common method used in cell culture for accurate seeding of cells.

1.3 Virus

1.3.1 Porcine circovirus type 2 (PCV2)

Porcine circovirus (PCV), the smallest known virus to affect mammalian cells, was first discovered in 1974 by Tischer et. al. in the cell line PK-15 today known as Porcine circovirus type 1 (PCV1) (Tischer, 1974). PCV2 was discovered 8 years later and is a *Circovirus* belonging to the *Circoviridae* family (Ramamoorthy & Pineyro, 2019). A study by Allan et al. (1998), demonstrated the first connection between PCV2 and PMWS by experimentally infecting piglets with a PCV2 isolate and observing clinical signs consistent with PMWS (Allan, 1998). Multiple subsequent research papers published after Allan et al. supports the connection between PCV2 infection and PMWS (Krakowka et al., 2000; Rodriguez-Arrijoja et al., 2002). It has been suggested that PCV2 alone may not be sufficient to cause PMWS and that other viruses may also play a role in the development of the disease, suggesting PMWS is a multifactorial disease. Studies examining the combined effect of PCV2 with other viruses, such as Porcine parvovirus (PPV) and Porcine reproductive and respiratory syndrome virus (PRRSV), versus the independent effect of PCV2 or other viruses alone have shown that the combined effect can worsen the clinical symptoms of PMWS in pigs. These secondary viruses do not cause PMWS on their own, suggesting that PCV2 is the primary factor. These experiments have also revealed that not all pigs infected with PCV2 show clinical symptoms, indicating that individual differences can play a role in the development of the disease (Allan et al., 1999; Allan et al., 2000; Bolin et al., 2001; Harms et al., 2001; Kennedy et al., 2000; Krakowka et al., 2000; Rodriguez-Arrijoja et al., 2002; Segales & Domingo, 2002).

1.3.2 PCVE replication cycle

Compared to other organisms, viruses are uniquely dependent on the host organism to reproduce and PCV2 is no exception (N.J. Dimmock, 2016). PCV2 is a small, non-enveloped, icosahedral virus, measuring approximately 17 nm in diameter, with a circular, single-stranded DNA genome of around 1700 nucleotides (Chen et al., 2012; Pineyro, 2019; Tischer et al., 1982). Although the virus's replication cycle is not entirely understood, a proposed model of PCV2s replication in PK-15 cell lines is shown in **Figure 2**. It is important to note that different steps of replication can vary from cell line to cell line and most of the research on PCV2 replication cycle has been conducted in epithelial PK-15 and monocytic 3D4/31 cells.

Several glycosaminoglycans (GAGs), including heparan sulfate (HS) and dermatan sulfate (DS) have been identified as important receptors for PCV2 attachment to host cells (**Figure 2 – 1**) (Misinzo et al., 2006; Ouyang & Nauwynck, 2023). While these studies have shown that HS and DS are involved in epithelial PK-15 cells, it is unknown whether GAGs are involved in the infection of IPEC-J2 cells. The virus is believed to enter cells via clathrin-mediated endocytosis, a pathway used for uptake of transmembrane receptors and transporters, remodeling of the plasma membrane composition in response to changes, and maturation of clathrin-coated pits (Mettlen et al., 2018; Misinzo et al., 2008; Misinzo et al., 2005). Recent research, however, suggests that clathrin-mediated endocytosis may trap the virus inside epithelial cells, and other entry mechanisms may lead to infection (Misinzo et al., 2009). The research concluded that PCV2 is mediated by actin polymerization, indicating that actin reorganization is critical for PCV2 infection. Although the exact mechanism by which PCV2 enters PK-15 and IPEC-J2 cells remains uncertain, it is believed to be mediated by actin polymerization (**Figure 2 – 2**) (Misinzo et al., 2009).

Once the endosome containing the PCV2 has entered the cell, disassembly is needed for the replication cycle to continue. It is suggested that low pH is required for activation of serine proteases in monocytic 3D4/31 cells, while a neutralized pH is required for epithelial PK-15 cells (**Figure 2 – 3**), suggesting that two different serine proteases are present in monocytic and epithelial cells (Misinzo et al., 2008; Misinzo et al., 2005). Following this, the viral genome is released and translocated to the nucleus, where genome replication occurs. The PCV2 genome contains open reading frame 1 (ORF1) and open reading frame 2 (ORF2), which code for the replicase protein (Rep) and capsid protein (Cap), respectively, with an intergenic region in between (Faurez et al., 2009). PCV2 is a class 2 virus with a single-stranded DNA of either positive or negative sense. Rolling circle replication, similar to *Geminiviridae* and *Nanoviridae*, is believed to be the mechanism by which the PCV2 genome is replicated (**Figure 2 – 7**). Although the synthesis of the lagging strand in PCV replication remains unknown, the product is suggested to be a supercoiled double-stranded replication form (Faurez et al., 2009). Then, a complex composed of Rep proteins binds to the stem of the loop structure, leading to the initiation of viral DNA replication. The Rep complex then closes the cleaved loop, resulting in a circular positive parental single-stranded DNA molecule and a circular double-stranded DNA molecule consisting of the negative parental strand and the newly synthesized positive strand. The positive parental DNA molecule can either be involved in a second replication cycle or be encapsulated to create a new virus (Faurez et al., 2009).

As PCV2 lacks its own DNA polymerase, it is entirely dependent on the host's own polymerases to achieve the replication of DNA (Tischer et al., 1987).

In addition to genome replication, the Rep and Cap proteins need to be synthesized. To synthesize the Rep and Cap protein, it needs to be converted to double-stranded DNA before further processing (*Figure 2 – 4*). The DNA is transcribed to mRNA in the nucleus (*Figure 2 – 5*) and transported to the cytoplasm for protein synthesis (translation) (*Figure 2 – 6*). Studies of the expression of the Cap protein over time suggest that both Rep and Cap are transcribed in the cytoplasm and then imported back into the nucleus for viral assembly (Huang et al., 2015; Meerts et al., 2005). The assembled virions (*Figure 2 – 8*) are then translocated to the cytoplasm and further released into the extracellular environment outside of the cells (*Figure 2 – 9*) (Finsterbusch et al., 2005). The release of PCV2 in PK-15 cells is suggested to be by cell lysis, however there is no literature suggesting what mechanism releases PCV2 in IPEC-J2 cells (Misinzo et al., 2005).

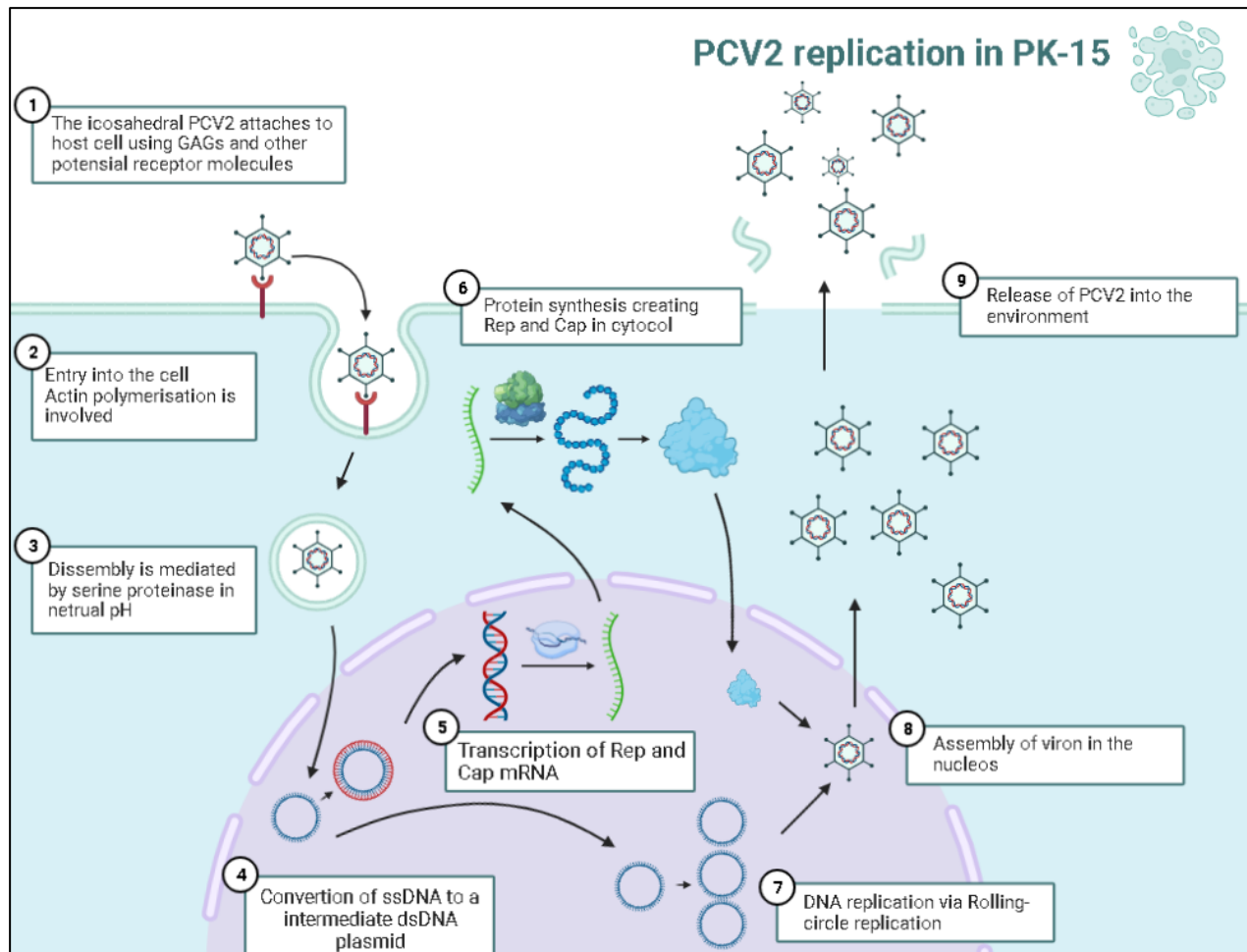


Figure 2 - Suggested model of PCV2 replication in PK-15 cells: The virus attaches to host cells via glycosaminoglycans (GAGs), such as heparan sulfate (HS) and dermatan sulfate (DS) (1). PCV2 enters cells via unknown mechanisms but is possibly actin mediated (2), and the endosome containing the virus is then disassembled by serine proteases active in neutral pH (3). The viral genome is released and translocated to the nucleus, where the plasmid is either used to make a double stranded (ds) intermediate (4) for protein synthesis or used for genome replication (7). The double stranded intermediate is then used for mRNA production (5) used for translation of Rep and Cap proteins (6). The synthesized protein is translocated into the nucleus and assembled (8). The assembled virions are then translocated to the cytoplasm and released into the extracellular environment outside of the cells, with the release in PK-15 cells suggested to be by cell lysis (9). The figure is adapted from “Oncolytic Viruses: Mix and Match to Design Your Own”, by BioRender.com (2023), retrieved from <https://app.biorender.com/biorender-templates>.

1.3.3 PCV2 cultivation

When cultivating viruses in cell lines, the separation of cell debris and virus particles is necessary for the purification of the virus stock produced. The method used for virus purification depends on whether the virus is cytopathic or highly cell-associated (Payne, 2017). Highly cell-associated viruses reproduce without appearing in the medium as free-floating viruses and require a gentle lysis of the cells for release before purification (Anderson & Le Grand, 2014; Payne, 2017). While there is no specific research determining whether PCV2 is a highly cell-associated virus or not, the common approach used for separation is freeze-thawing before centrifugation. A low-speed (approximately 5000xg) differential centrifugation is commonly used to separate cell and cell debris from the virus, which has been proven to be efficient for PCV2 despite its small size (Hu et al., 2019; Payne, 2017; Tischer et al., 1987).

A possible method to creating a high concentration virus stock is by concentrating the low concentration virus stock produced. Low-speed centrifugation, a 16–24 hour centrifugation at around 5000xg, has been reported to work for purification and concentration of Alphavirus (Rayaprolu et al., 2018; Wang et al., 2015). Considering that PCV2 is 17nm in diameter compared to Alphavirus being 65-70 nm in diameter, this is most likely not a good method (Jose et al., 2009). Ultrafiltration is another option where a cutoff filter with a fine pore size is used to keep the viruses above the filter and let the liquid flow through (Meade et al., 2021). This has already been successful for adenoviruses in our lab and a concentration method for adenoviruses has been developed by Merck (*Virus Concentration by Ultrafiltration*, n.d.). Considering PCV2 is 17nm, a pore size of 10kDa will most likely be too small, while 100kDa will most likely be too wide, thus a pore size of 50kDa is suggested to give the best results accordingly to Merck (*Virus Concentration by Ultrafiltration*, n.d.).

1.3.4 Bovine viral diarrhea virus (BVDV)

BVD is an illness observed in bovine and was first described in 1946 in Canada by Childs and was later described in Switzerland (Bürki, 1964; Childs, 1946). BVD is caused by BVDV, a small enveloped virus around 50 nm in diameter with a single-stranded positive RNA at around 12.5kb (Khodakaram-Tafti, 2017). Severe and acute outbreaks of BVD caused by BVDV have been reported with symptoms such as bloody diarrhea, high fever, mouth ulcers, and pneumonia, especially in unvaccinated cattle (Driskell, 2006). The morbidity and mortality rates of BVD vary

among herds and range from high morbidity and low mortality to considerable mortality during severe outbreaks (da Silva Silveira et al., 2020; Yitagesu et al., 2021). Cattle that survive BVD can have severe clinical manifestations, including susceptibility to infections, reproductive disorders, congenital defects, increased neonatal mortality, and non-thriving and dying young stock. Preventive measures, such as vaccination, keeping herds closed, and maintaining strict hygiene practices, have been developed to provide some sort of protection against BVD, however, it should be noted that vaccination is not a cure (Moennig & Becher, 2018). In addition to vaccination, it is recommended to keep herds closed and maintain strict hygiene practices to prevent the introduction of new individuals carrying the virus to a herd and reduce the risk of BVD outbreaks. Regular monitoring of the herd is important to detect BVD infections early and implement appropriate measures to prevent further spread. Testing of individual animals, particularly those in high-risk populations such as pregnant cows, is recommended to identify BVDV carriers and remove them from the herd (Lanyon et al., 2014; Ménard, 2006).

1.3.5 BVDV contaminations

BVDV can have different effects on infected cells, depending on the strain. Some strains of BVDV are cytopathic, causing significant damage to infected cells, visible as rounding up of the cells, formation of syncytia (multi-nucleated giant cells), detachment of the cells from the surface, and cell death (Miroslaw et al., 2022). Other strains of BVDV are non-cytopathic, meaning they do not cause significant damage to the infected cells, and as a result, the infected cells may continue to grow and divide normally at the same time as replication of BVDV occurs. This makes non-cytopathic BVDV strains harder to detect without proper screening methods, as there may be no visible changes in the infected cells. FBS is produced by collecting blood from the fetus of a pregnant cow during slaughter or cesarean section (Jochems et al., 2002). BVDV is highly contagious and can be present in the blood, saliva, urine, and other bodily fluids of infected animals. During pregnancy, cows are more susceptible to infections, including BVDV, due to the suppression of their immune system. If the cow is infected with BVDV during pregnancy, the virus can cross the placenta and infect the developing fetus, resulting in the presence of BVDV in the blood of the calf (Khodakaram-Tafti, 2017). This can lead to the contamination of FBS with BVDV when it is collected from the calf's blood after slaughter.

1.4 Methods of analysis

1.4.1 PCR and nested RT-PCR

PCR has long been an important tool in various fields of DNA research, including medical diagnostics, forensic science, and environmental studies, due to its ability to amplify and detect nucleic acids from a single sample. For this study, PCR and agarose gel electrophoresis was utilized to test for the presence of PCV1 in PK-15 cells. PCR is known for its high sensitivity and specificity, depending on the primer pair used, making it ideal for detection of nucleic acids from pathogens.

To test for the presence of BVDV contaminations and ensure specificity, a nested RT-PCR method was employed. This approach involves two rounds of amplification using two sets of primers, where round one is an RT-PCR to convert the RNA to complementary DNA (cDNA) before a larger region of cDNA is amplified using outer primers (Green & Sambrook, 2019; Mo et al., 2012). During the cDNA synthesis a specific primer can be used to amplify the RNA, however in this study random hexanucleotide primers were used. Then round two amplifies a smaller region within the first PCR product using inner primers. Nested PCR enhances the specificity and sensitivity of the amplification reaction, making it particularly suitable for applications where the target RNA is present in low abundance (Carr et al., 2010). The nested RT-PCR method used in this study was developed and used in the research paper published by Kadir et al. (Kadir et al., 2008).

1.4.2 Real-Time PCR

Real-Time PCR is a method commonly used for amplification, detection, characterization, and quantification of nucleotides in multiple samples simultaneously. Unlike PCR, Real-Time PCR uses fluorescent signals to collect data in real-time, providing the opportunity to detect the product after each amplification cycle (Neidler, 2017). The traditional method for viral titration is using a plaque assay, which is a time-consuming and complex method (Baer & Kehn-Hall, 2014). However, in this study, a fast and sensitive virus titration method was required. Real-Time PCR is also a method used for viral titration, and ideally, the titration is done by comparing the Real-Time PCR results of the sample to a standard curve generated from known amounts of purified virus

particles (Gilpin et al., 2003). In this study, Real-Time PCR with concentration comparison was used to give an indication of viral concentration compared to a reference with an unknown concentration. In this case, the expression levels of the target gene in different samples were compared by analyzing the cycle threshold (Ct) values obtained from Real-Time PCR. The sample with the lowest Ct value indicates the highest expression level of the target gene, while the sample with the highest Ct value indicates the lowest expression level. This approach provides a rapid and sensitive method to compare the expression level of a specific gene in a sample and can be used to monitor the replication kinetics of viruses in cell cultures.

To identify nonspecific and specific PCR products, a melting curve analysis was included to monitor the temperature required to melt the PCR product at the end of a Real-Time PCR analysis. This approach is used to decide whether primer-dimers interfere with the reaction and alter the Ct results (Downey, 2016; *Real-Time PCR Application Guide*, 2006). The study also included four types of controls during PCR and Real-Time PCR: No Template Control (NTC), positive control, negative control, and mock infection. NTC detects DNA contamination or background noise, negative control ensures PCR amplification specificity to the target DNA and positive control confirms that the primer pair targets the specific DNA and minimizes false-negative outcomes (Brunstein, 2013). A mock infection control imitates the virus infection process without viral particles to determine if changes in cell behavior are due to the virus or other factors and is used as a baseline for comparison to infected cells (Wang et al., 2020).

1.4.3 Cell viability assay

Viral infections can cause cell death in the host through a process known as apoptosis, which is a programmed cell death mechanism (Barber, 2001). The virus may disrupt normal cellular processes and induce cellular stress, leading to the activation of apoptotic pathways. There are several mechanisms by which apoptosis can occur, such as death receptors, mitochondria, interferons, and interferons regulatory factors. PCV2 has been shown to induce various cytopathic effects in different cell lines. For example, in CPK-NK cells, PCV2 can cause cell detachment, while in IPEC-J2 cells, it can result in microfilament changes (Hosono et al., 2019; Yan et al., 2014). In primary porcine oral mucosal epithelial cells (POMECs), PCV2 can lead to cell elongation and intercellular space increases (Cui et al., 2019). Through the study of the cytopathic effects of PCV2

on PK-15 cells, it has been suggested that the virus can induce cell apoptosis and was later confirmed by further investigations by S. Wang et al., which showed that PCV2 triggers cell death in PK-15 cells through the Phospholipase C- Inositol 1,4,5-trisphosphate receptors- Ca^{2+} (PLC-IP3R- Ca^{2+}) signaling pathway. (Misinzo et al., 2005; S. Wang et al., 2021; Zhu et al., 2007).

To determine whether PCV2-induced apoptosis can be used as a potential cytopathic effect for GeCKO screening in PK-15 cells, a cell viability assay can be employed. Cell viability assays are often used to evaluate changes in cell conditions, including viral infections, that may affect cell culture viability. Various methods have been developed for cell viability assays, but in this study, an adenosine triphosphate (ATP) detection method was utilized. ATP is continuously produced by the mitochondria in living cells and serves as the energy source for cell function. When a cell dies, ATP production ceases, and any remaining ATP is removed by ATPase. Therefore, the amount of ATP present in a cell culture can be used to directly assess cell viability after viral infection (Koksharov & Ugarova, 2011; Riss TL, 2013). CellTiter-Glo® is a cell viability assay that consists of, amongst other, Beetle Luciferin and Ultra-Glo™ Recombinant Luciferase. Beetle Luciferin is catalyzed by the Luciferase when Mg^{2+} , ATP and molecular oxygen creates a stable glow that can be measured using a plate reader for luminescence (*CellTiter-Glo® Luminescent Cell Viability Assay*, 2023). The more luminescence produced, the greater the number of living cells present in the sample. Using a known amount of living cells as a standard can provide an estimate of the number of living cells in unknown samples.

1.4.4 Fluorescence microscopy and flow cytometry

Mammalian cells possess a complex cytoskeletal system consisting of various structures that serve critical functions in maintaining cell shape, mechanical support, movement, and division. The cytoskeleton consists of protein fibers composed of three main components: microtubules, microfilaments, and intermediate filaments that build up various types of cytoskeletons (*4.5: The Cytoskeleton*, 2023; *Cytoskeleton*, 2022). One important cytoskeletal structure is the cortical actin network, which provides mechanical support and participates in cell signaling and adhesion. Stress fibers are essential for maintaining cell structure and strength, as well as playing a role in cell migration and contractility. Microtubules serve in cell division and intracellular transport, while intermediate filaments are important for maintaining cell shape, strength, and gene expression.

Although a viral infection can lead to cell death, infected cells can also survive and display a different cytopathic effect that can be used as a screenable phenotype (Heaton, 2017). When a virus infects a cell, it can interfere with various cellular processes, including the organization and stability of cytoskeletal structures. For instance, viruses can induce the formation of abnormal structures, such as actin comet tails or filopodia, that facilitate viral entry or exit (Taylor et al., 2011). Disrupting cytoskeletal structures and functions can facilitate viral replication and movement, contributing to the pathogenesis of viral diseases.

In November 2014 Yan et al. published a study demonstrating promising results regarding a detectable cytopathic effect of PCV2 infection in IPEC-J2 cells. They demonstrated that the replication and release phase of PCV2 infection reduce stress fibers in IPEC-J2 cells and induce the production of new actin structures. This research suggests that the altered cytoskeletal structures induced by viral infection could be a potential target for GeCKO screening. To detect this cytopathic effect, Yan et al (2014) used Alexa Fluor™ 488 phalloidin, which is commonly used to stain F-actin in fixed cells. They found that there is a notable difference in F-actin structures between infected and mock infected cells detected with fluorescence microscopy, as shown in **Figure 3A** (Yan et al., 2014). They also discovered that a significant higher fluorescent intensity detected using flow cytometer, as seen in **Figure 3B**. On basis of this, the end goal is to use flow cytometry to detect and separate infected and non-infected cells by the difference in fluorescence intensity of F-actin stained cells and potentially using this in GeCKO screening.

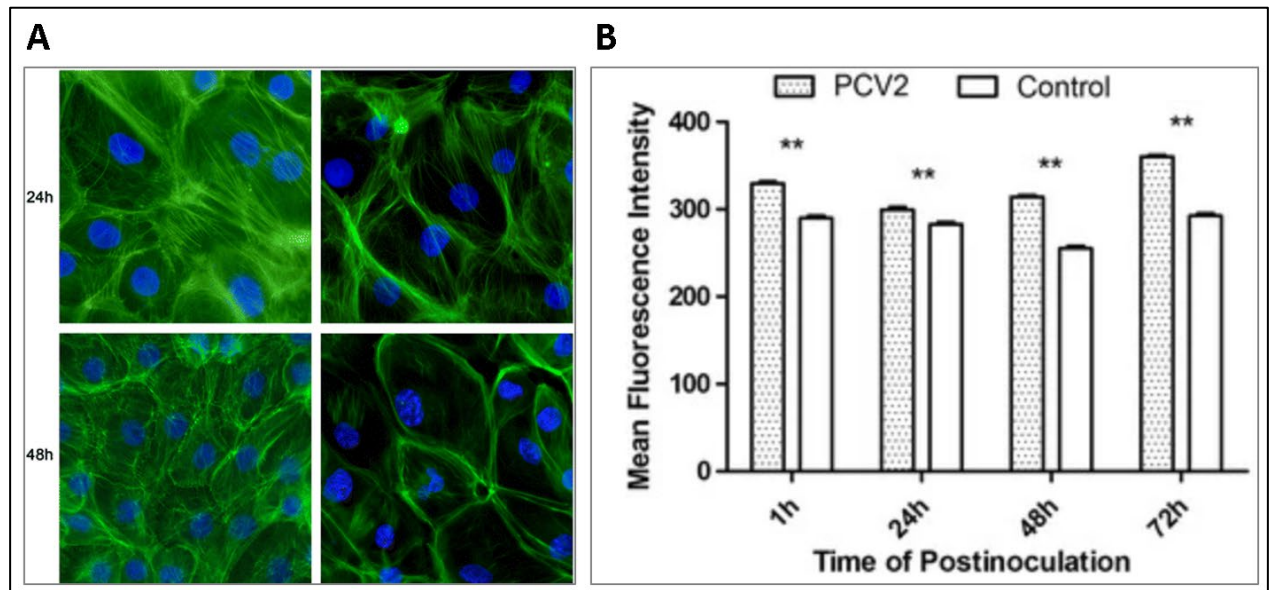


Figure 3 – Difference in F-actin structure between mock infected and PCV2 infected PK-15 cells: **Panel A** shows results obtained from fluorescence microscopy, where the green stain is F-actin, while the blue stain is the nucleus. The two pictures on the left shows mock infected cells, while the two pictures on the right shows PCV2 infected cells. The two pictures at the top are 24 HPI and the two at the bottom are 48 HPI. **Panel B** displays results from flow cytometry, where gray represents PCV2, and white represents mock infection (control). This figure is a modified version of figure 2 in the research paper published by Yan et al. in 2014 (Yan et al., 2014).

2 Methods

All cell lines, materials, and reagents with reference numbers, and instruments used in this study is listed in *Appendix A: Cell lines, Materials, Reagents, and Instruments*.

2.1 Cell culture

MDBK (ATCC CCL-22), PK-15 (ATCC CCL-33), and IPEC-J2 (Lab collection) cell lines were cultured in this study. The complete growth medium was made of Dulbecco's Modified Eagle Medium (DMEM) (SIGMA-ALDRICH, US) with 10% serum and 1% antibiotics. MDBK cells was grown in complete growth media created using FBS-Gold (FBS-G) (Bio&SELL, Germany), while PK-15 and IPEC-J2 used FBS (SIGMA-ALDRICH, US). All three cell lines used a mix of the antibiotic's penicillin and streptomycin (Thermo Fisher Scientific, US) in the complete growth media. All solutions in direct contact with the cells were prewarmed to 37°C, including the growth medium, Trypsin-ethylenediaminetetraacetic acid (EDTA) (0.25%), phenol red (Thermo Fisher Scientific, US), and phosphate-buffered saline (PBS) (SIGMA-ALDRICH, US). The cells were grown at 37°C with 5% CO₂ and passaged when reached 80-90 % confluency.

All the cell lines in this study arrived frozen and were stored at -150°C. The cells were gently and quickly thawed in a 37°C water bath until a few small ice crystals were left, typically after 2 minutes. These cells were transferred into a 15mL falcon tube with 5-10mL of pre-warmed medium. MDBK cells were centrifuged at 200xg for 8 min, PK-15 at 125xg for 8 min, and IPEC-J2 at 100xg for 5 min. The supernatant was then discarded, and the cell pellet was resuspended in 10mL complete growth medium accordingly to each cell line and transferred to a culture flask or plates for growth.

To subculture, MDBK cells were washed with PBS twice and then twice with Trypsin-EDTA. After removing the Trypsin-EDTA solution, the cells were incubated at room temperature for 10 min. Pipetting at full force, complete growth medium was added to detach the visible white layer of cells on the surface of the cell culture flask/plate, ensuring that the MDBK cells were completely detached from the surface. When sub-culturing PK-15 and IPEC-J2, the cells were first washed twice with PBS and then once with Trypsin-EDTA solution. 2-3mL of Trypsin-EDTA solution was added and left in the cell culture flask/plate as it incubated for 5 min at 37°C. Complete growth medium was added when the cells were visibly detached in the microscope. The cells were then

split accordingly to the recommended ratio, applying to MDBK (1:3 or 1:5), PK-15 (1:2 or 1:4), and IPEC-J2 (1:3 or 1:5), or counted on Countess™ 3 FL Automated Cell Counter (Thermo Fisher Scientific, US) and distributed as needed. Appropriate amounts of cells were added to the cell culturing flask/plate.

The cells were collected at a concentration between $1-5 \times 10^6$ cells/mL for cryopreservation when needed. 5% Dimethyl sulfoxide (DMSO) (SIGMA-ALDRICH, US) was added and gently mixed by pipetting. This was distributed in cryovials with 1mL in each tube. The tubes were placed into a Mr. Frosty™ Freezing Container (Thermo Fisher Scientific, US) and placed into a -80°C freezer for 24 hours. After 24 hours all tubes were moved into a -150°C freezer for storage.

2.2 Cultivation of PCV2

The original PCV2 virus stock was kindly provided to us from Professor Lars E. Larsen from a research group in Denmark and was stored at -80°C upon arrival.

2.2.1 Sample collection and DNA extraction

Collection of the samples was done by using Cell scraper, 2-position blade, size: S (Sarstedt, Germany) to detach the cells from the surface of the cell-culturing flask/well before they were collected using pipetting. All samples were collected in cryovials and stored at -80°C . Samples were freeze-thawed 3 times at -80°C , including the freezing required for storing. These samples were centrifuged at $5\,000\times g$ for 15 min. The supernatant was carefully collected in new Eppendorf tubes and the cell debris was discarded. Both the supernatant collected directly from the cell culture flask/plate and samples freeze thawed were then run through a $0.45\ \mu\text{m}$ pore size Filtropur S syringe filter (Sarstedt, Germany) using BD Luer-Lok™ syringe, with concentric tip and PC barrel, 1mL (VWR, US) before DNA was extracted.

DNA extraction of Viral DNA or RNA was performed using Purelink Viral RNA/DNA Mini Kit (Thermo Fisher Scientific, US) following the manufacturer's description. During the elution of the DNA/RNA $50\ \mu\text{L}$ of RNase-free water was used. Purelink is a DNA and RNA extraction kit designed for isolation of high-quality viral DNA and/or RNA by using carrier RNA. Because

carrier RNA will affect UV-based methods for quantification and purity control only PCR was used to control DNA quality when using the PureLink Viral RNA/DNA Mini Kit.

DNA extraction on cellular DNA was performed using DNeasy Blood and Tissue (Qiagen, Netherlands) following the manufacturer’s description. This was done to create negative controls for PCR and Real-Time PCR. The quality of the DNA was determined by qubit, nanodrop, and PCR. DNA extracted with DNeasy Blood and Tissue was quantified on Qubit 4 Fluorometer (Thermo Fisher Scientific, US) following the manufacturer’s protocol. The purity of the DNA was determined using NanoDrop™ 8000 Spectrophotometer (Thermo Fisher Scientific, US) following the manufacturer’s protocol.

2.2.2 PCR and Real-Time PCR

Primers used for all PCV related research in this study were prepared as described in 2.5 *BVDV detection in FBS* and are listed in **Table 1** ordered and produced by Thermo Fisher Scientific using Custom Standard DNA Oligos.

Table 1 – Primers used for PCV2 research: *Primer name, amplification site, organism, primer sequence and product size are listed. The primers are taken from the research paper published by Larochelle et al. (Larochelle et al., 1999).*

Primer name	Amplification site/ Organism	Primer sequence	Product size
PCV2	ORF 2/ PCV2	Forward: PCV2-F: 5' TAGGTTAGGGCTGTGGCCTT 3' Reverse: PCV2-R: 5' CCGCACCTTCGGATATACTG 3'	263nt
PCV1	ORF 1/ PCV1	Forward: PCV1-F: 5' TTGCTGAGCCTAGCGACACC 3' Reverse: PCV1-R: 5' TCCACTGCTTCAAATCGGCC 3'	349nt

2.2.2.1 PCR

Using PCR with agarose gel electrophoresis the primers in **Table 1** were tested to confirm that they were amplifying the correct product size. The master mix were mixed first as described in **Table 2** where DNA polymerase was added lastly straight out of the freezer. The master mix was distributed into the PCR tubes after gently and thoroughly mixing by pipetting up and down. 2 μ L of DNA and 2 μ L of ddH₂O was used as DNA template from uninfected PK-15 and was used as negative control. DNA from PCV2 was used extracted using Purelink Viral RNA/DNA Mini Kit and 4 μ L of DNA was used as template. The tubes were placed into GeneAmpTM PCR system 9700 (Applied Biosystems, US) and amplified using 5 min hot start at 95°C followed by 35 cycles of 1 min denaturation at 95°C, 1 min annealing at 65°C, and 1 min extension at 72°C ending with a 10 min final extension at 72°C.

A 2% agarose gel was made with 1X Tris-Acetate-EDTA (TAE) buffer was made out of 50x TAE Electrophoresis Buffer (Thermo Fisher Scientific, US) in ddH₂O and 2% Standard Agarose – Type LE (BioNordika, Denmark) placed in a gel electrophoresis chamber with 1x TAE buffer to cover the gel. The 1 μ L of the PCR product was mixed with 5 μ L of Gel Loading Solution (SIGMA-ALDRICH, US), pipetted into the gel wells, and was run at 80V for 30 to 40 min in Horizontal Electrophoresis Systems (BIO-RAD, US) using PowerPacTM Basic Power Supply (BIO-RAD, US) before pictures was taken on ChemiDoc XRS+ Gel Imaging System (BIO-RAD, US) using the software Image Lab 6.0 (BIO-Rad, US).

Table 2 – PCR master mix: Master mix components and volume used per PCR reaction and final concentrations in the total reaction volume.

Reagent	Volume	Final concentration
ddH ₂ O	16.6μL	-
10xBuffer	2.5μL	1 x
dNTP	0.2μL	0.2 mM
MgCl ₂	0.5μL	0.05 mM
Forward primer	0.5μL	0.04μM
Reverse primer	0.5μL	
Taq Pol (Hot start, Qiagen)	0.2μL	2.5 U
Total vol master mix	21.0μL	
DNA	XμL	
Total volume per reaction	25.0μL	

2.2.2.2 Real-Time PCR

Real-Time PCR was carried out on C1000 Touch™ Thernal Cycler CFX96™ Real-Time System (BIO-RAD, US) by using SsoAdvanced Universal SYBR® Green Supermix (BIO-RAD, US) following the manufacturer’s protocol. All components were first thawed, including SsoAdvanced Universal SYBR® Green Supermix, forward primer, and reverse primer. The master mix was prepared as described in **Table 3** with primer pair PCV2 from and distributed in Hard-Shell® PCR Plates, 96-Well, thin-wall (BIO-RAD, US) as needed. The proper DNA was then added to the appropriate wells and the plate was sealed. The plate was then placed into the Real-Time PCR machine and the wells were marked with their contents. Initial denaturation was set to 98°C for 3 min followed by 40 cycles with denaturation at 95°C for 15 sec, annealing and extension at 60°C for 1 min with a plate read at the end of each cycle. A melting curve was produced from 65°C to 95°C with an increase of 0.5°C per 5 sec with plate read.

Table 3 – Real-Time PCR master mix: Master mix components and volume used per Real-Time PCR reaction.

Reagent	Volume
ddH ₂ O	6.0μL
SSoAdvanced universal SYBR® Green Supermix	10.0μL
Forward primer	1μL
Reverse primer	1μL
Total vol master mix	18.0μL
DNA	2μL
Total volume per reaction	20.0μL

The Ct values were further processed using the following function: $2^{Ct_{Original\ sample} - Ct_{sample}}$ inspired from function “Real-Time PCR Applications Guide” by Bio-RAD $Ratio_{(test/calibrator)} = 2^{Ct_{(calibrator)} - Ct_{(test)}}$ resulting in calculated fold change (*Real-Time PCR Application Guide*, 2006).

2.2.3 Investigating PCV1 contamination

To investigate if the PK-15 cell line was contaminated with PCV1, DNA from 200μL cell suspension collected from PK-15 cells at passage number 3 was extracted using Purelink Viral RNA/DNA Mini Kit as described in 2.2.1 *Sample collection and DNA extraction*. PCR was performed as described in 2.2.2 *PCR and Real-Time PCR* using only the PCV1 primers. Negative controls from MDBK cells at passage number 4 was included.

2.2.4 PCV2 infection in PK-15 cells

PK-15 cells were seeded in a 24-well plate with 9×10^4 cells/well. 24 hours later all growth medium was removed, and the well was washed with PBS before 1mL of fresh complete growth medium was added to all wells. 6 wells were infected with 200μL of PCV2 from the original stock. 6 wells were infected with 200μL of PCV2 from the original stock diluted 1:10 in complete growth

medium. The complete growth medium in the last 12 wells were first removed before being infected with PCV2: 6 wells with 200 μ L of PCV2 from the original stock and 6 wells with 200 μ L of 1:10 diluted PCV2 from the original stock. These 12 wells were incubated with the virus for 1 hour at 37°C before the virus was removed and fresh complete growth medium was added.

Samples were collected 1, 24, 48, 72, and 96 HPI using a scraping tool to scrape the cells from the growth surface and stored at -80°C before DNA was extracted as described in *2.2.1 Sample collection and DNA extraction*. Samples were measured with Real-Time PCR as described in *2.2.2 PCR and Real-Time PCR*. Two negative controls from PK-15 and MDBK DNA, mock infection from the experiment, positive control from the original virus stock, and no template control was included, and all samples were run with two technical repeats. A standard curve was produced from the original PCV2 virus stock using a 10-fold dilution series with 8 dilutions.

2.2.5 Concentrating PCV2 virus

A PCV2 supernatant collected during a separate experiment was used to test two different ways of concentrating the virus in suspension. PK-15 cells that were treated with a CRISPR library and were infected with a 1:10 dilution of the original PCV2 virus stock. Only the supernatant from this experiment was collected and run through 0.45 μ m pore size Filtropur S syringe filters and stored at -80°C until use.

The method tested for concentrating the virus was using Amicon® Ultra-15 Centrifugal Filter Unit (Merck Millipore, US) with 10kDa and 100kDa pore size, as this is the sizes we had at hand. Before filtration a sample of the unfiltered supernatant was collected. The virus stock was thawed in a 37°C water bath before use. Before use, each Amicon® Ultra-15 Centrifugal Filter Unit was rinsed with 10mL of PBS and centrifuged at 1,000xg for 10 min (10kDa filter) or 2,000xg for 10 min (100kDa filter), followed by discarding the PBS. 4.5mL of the virus sample was added to the filter column and centrifuged at 1,500xg for 70 min (10kDa filter) or 10 min (100kDa filter). After centrifugation, the filter was removed and the media under the filter was discarded. Then, 10mL of PBS was added to the filter column and centrifuged at 1,500xg for 90 min (10kDa filter) or 10 min (100kDa filter). The procedure was repeated once more to ensure complete removal of residual media. The remaining sample in the filter was collected and stored at -80°C until DNA extraction.

DNA from the samples were extracted as described in 2.2.1 *Sample collection and DNA extraction* and samples were measured with Real-Time PCR as described in 2.2.2 *PCR and Real-Time PCR*. Negative control from PK-15 DNA, mock infections from the experiment, positive control from the original virus stock, and no template control was included, and all samples were run with two technical repeats. A standard curve was produced from the original PCV2 virus stock using a 10-fold dilution series with 8 dilutions.

2.3 Cell viability assay

Because of the cell death observed when first infecting PK-15 cells with PCV2 as seen in **Figure 5**, a cell viability assay was performed. PK-15 cells were seeded in 4 different 96-well plates containing 21 wells with $7.5 \cdot 10^3$ cells and 21 wells with $1.5 \cdot 10^4$ cells. The old medium was removed from each well 24 hours later and washed with PBS. 200 μ L of different dilutions of the original virus stock (1:3, 1:6, 1:9, 1:12 and 1:15 dilutions) was added to respected well and incubated for 1 hour at 37°C. The virus was removed, and fresh complete growth medium was added. Cell viability assay was performed 24, 48, 72, and 96 HPI. 100 μ L of the complete growth medium in each well was removed and 100 μ L of CellTiter-Glo® Luminescent Cell Viability Assay (Promega, US) was added. The plate was placed on IKA Digital Orbital Plate Shaker (IKA, Germany) at 600rpm for 5 min, before incubation at room temperature for 25 min. The plate was inserted into Synergy H1 Hybrid Multi-Mode Reader (BioTek, US) and the luminescence (Relative Light Units, RLU) was measured.

2.4 Actin filament changes by fluorescence microscopy

IPEC-J2 cells were thawed and passaged twice then used for seeding in three 8 Well Chamber, removable (Ibidi, Germany) with $1.0 \cdot 10^4$ cells in each well. After 24 hours the cells were infected by first removing the old medium from each well and then washed with PBS. To infect the cells 200 μ L of 1:10 dilution of original PCV2 virus stock was added to each well and incubated for 1 hour at 37°C. The virus was removed, and fresh complete growth medium was added. Mock infection was treated the same, but with complete growth media without virus. The cells grew for 48 hours before being used for immunofluorescent staining.

The complete growth media was removed from the cells at 48 HPI, and the cells were washed with PBS twice. To fixate the cells 200 μ L of 2% Pierce™ 16% Formaldehyde (w/v), Methanol-free (Thermo Fisher Scientific, US) diluted in 1x solution of Tris-buffered saline (TBS) with TWEEN® 20 (SIGMA-ALDRICH, US) (TBST) was added to each well and incubated for 10 min. The cells were then washed with 1x TBST for 5 min. To permeabilize the cells 200 μ L of 0.1% Triton™ X-100 (SIGMA-ALDRICH, US) diluted in 1x TBST was added to each well and incubated for 15 min. The cells were washed with 1x TBST and then blocked with 200 μ L of 1x TBST with 2% Skim Milk Powder (SIGMA-ALDRICH, US) for 1 hour. The cells were washed with 1x TBST. Porcine Circovirus Type 2 Capsid Polyclonal Antibody (Thermo Fisher Scientific, US) at a concentration of 7 μ g/mL was added to each well and incubated overnight at 4°C. The cells were then washed four times for 10 min each with 1x TBST. 200x Goat anti-Rabbit IgG (H+L) Highly Cross-Adsorbed Secondary Antibody, Alexa Fluor™ 647 (Thermo Fisher Scientific, US) was then added to each well and incubated for 2 hours. The cells were washed four times for 10 min each with 1x TBST. Alexa Fluor™ 488 phalloidin (Thermo Fisher Scientific, US) was prepared as described in the manufacturers protocol. Phalloidin staining was added to each well and incubated for 60 min in a covered container. The cells were washed three times in 1x TBST, and then DAPI (4',6-Diamidino-2-Phenylindole, Dilactate) (Thermo Fisher Scientific, US) staining was added to each well at a concentration of 300nM and incubated for 5 min. The solution was removed, and the cells were washed again 2-3 times with 1x TBST. The TBST was discarded, and the walls were removed from the slide. Three drops of ProLong™ Diamond Antifade Mountant (Thermo Fisher Scientific, US) were added to the coverslips, and each slide was placed on top of the coverslips. The slide was then analyzed under EVOS M5000 Imaging System (Thermo Fisher Scientific, US) to ensure proper staining.

2.5 BVDV detection in FBS

MDBK cells were thawed and passaged 2 times in FBS-G before they were seeded in 3 times 6-well plates. All different FBS are listed in **Table 4** and was used in the different wells at the next passage. Each FBS had two technical repeats and the supernatant was collected after the second passage and stored at -80°C until RNA extraction.

Table 4 – FBS used for BVDV contamination testing: The FBS name, name referred to in this study, supplier and reference number are listed.

FBS Name	Name (this study)	Supplier	Reference number	Lot number
Fetal Bovine Serum	1	SIGMA- ALDRICH	F2442	21G126
Fetal Bovine Serum	2	SIGMA- ALDRICH	F7524	0001665257
Fetal Bovine Serum	3	SIGMA- ALDRICH	F7524	0001665522
FBS Fetal bovine Serum, Certified Performance Plus	4	Gibco	16000-044	2208592RP
HyClone Characterized Fetal Bovine Serum (FBS), U.S. Origin	5	Cytiva/HyClone	SH30071.03	AG29692466
FBS Gold Plus – Very Low Endotoxin – Chromatographiert	FBS-G	Bio&SELL	FBS.GP.0500	Unknown
Fetal Bovine Serum	FBS-N	SIGMA- ALDRICH	F7524	Unknown

To test the samples for contaminations a nested RT-PCR was performed. RNA was extracted as described in 2.2.1 *Sample collection and DNA extraction* before the first PCR step was performed using QIAGEN® OneStep RT-PCR Kit (100) (Qiagen, Netherlands). RNA was amplified using 30 min cDNA synthesis at 45°C, before a hot start for 15 min at 95°C followed by 37 cycles of 30 sec denaturation at 94°C, 30 sec annealing at 55°C, and 1 min extension at 72°C ending with a 10 min final extension at 72°C. 1 µL of the first PCR product was used for the second PCR performed

using QIAGEN® Fast Cycling PCR Kit (200) (Qiagen, Netherlands). This was amplified using a hot start for 5 min at 95°C followed by 37 cycles of 5 sec denaturation at 96°C, 5 sec annealing at 60°C, and 6 sec extension at 68°C ending with a 1 min final extension at 72°C. Both were performed as described in the production manual and amplified on GeneAmp™ PCR system 9700. Primers used for all BVDV related research in this study is listed in **Table 5** and was ordered and produced by Thermo Fisher Scientific using Custom Standard DNA Oligos. The primers used for PCR, Nested RT-PCR and Real-Time PCR arrived dry and were diluted to a 100µM stock solution in ddH₂O. The 100µM stock solution was diluted to a 10µM working solution in ddH₂O. Both the Stock solution and the working solution were stored at -20°C until needed. An agarose gel electrophoresis was performed as described in 2.2.2 *PCR and Real-Time PCR* .

Table 5 - Primers used for BVDV research: Primer name, amplification site, organism, primer sequence and product size are listed. The primers are taken from the research paper published by Kadir et al. (Kadir et al., 2008).

Primer name	Amplification site/ Organism	Primer sequence	Product size
BVDV Step 1	5' UTR BVDV	Forward: BVDV-F1: 5` CATGCCCTCAGTAGGACTAGC 3` Reverse: BVDV-R1+R2: 5` CTCCATGTGCCATGTAGAGCAGAG 3`	283bp
BVDV Step 2	5' UTR BVDV	Forward: BVDV-F2: 5` TCGAGATGCCACGTGGACGAGG 3` Reverse: BVDV-R1+R2: 5` CTCCATGTGCCATGTAGAGCAGAG 3`	177bp

Since all samples were positive, the experiment was repeated on FBS 1, 3, 5 and FBS-G in a completely new MDBK cell line. This cell line is an engineered MDBK cell line with green fluorescent protein GFP and Cas9 induced by tetracycline-controlled transcriptional (TET) on promoter called MDBK clone 44. This cell line was kindly provided to us by our collaborators in Vienna and have been confirmed to be BVDV free. The Cells were passaged 5 times before the RNA from inside the cells were extracted using QIAGEN® RNeasy mini kit (Qiagen, Netherlands). The nested RT-PCR was performed as described earlier.

3 Results

3.1 Cultivation of PCV2

3.1.1 Investigating PCV1 contamination

The traditional PCR test conducted on the PK-15 cell line for PCV1 contamination yielded positive results as seen in **Figure 4**. This indicates a contamination of PCV1, which can have implications for downstream experiments. The PCR products were compared to a 100 kb ladder, and the results indicated a product size of approximately 300-400bp. This measurement is consistent with the expected size of 349 bp for the primer pair used on PCV1.

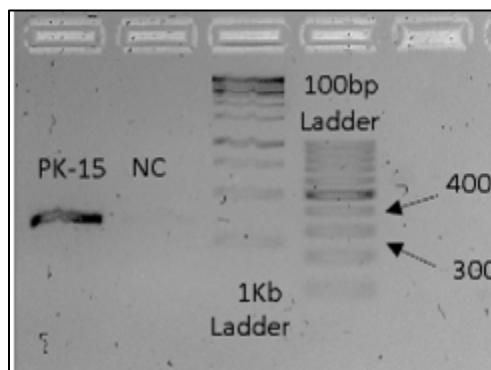


Figure 4 – PCR analysis of PCV1 contaminations in PK-15 cells: PCR product from DNA extracted from PK-15 cells at passage number 3 is in the first well. NC is negative control using DNA extracted from MDBK cells at passage number 4. A 1Kb and a 100bp on the right side as molecular weight markers.

3.1.2 PCV2 infection in PK-15 cells

Microscopic Insights

During the four-day observation of PK-15 cells infected with PCV2, significant cell death was observed throughout the early and late stages of the infection. Microscopic analysis of the cells revealed clear differences between mock infected and PCV2-infected cells, during the growth period. Mock infected cells appeared elongated with a rounded end and grew to a high density as seen in **Figure 5A** and **7C**. The mock infection showed a clear increase in density from 24 to 96 HPI, and by 72 hours, the density had reached 100%, resulting in overgrowth and observed cell

death from 72 to 96 HPI. Infected cells that survived the infection appeared similar in shape, but the density of the cells was noticeably lower due to the observed cell death as shown in *Figure 5B*. Additionally, the dead cells still attached to the surface of the cell culturing vial appeared rounded and porous as seen in *Figure 5D*, and there was a significant amount of floating cell debris in the supernatant. The cells infected with PCV2 showed early signs of cell death, and from 24 to 72 HPI, a significant decrease in density was observed. However, from 72 to 96 HPI, an increase in cell growth was observed again. It is worth noting that *Figure 5* only displays selection of mock infected and infected cells. While all infected cells showed a definite lower density, there were different amounts of cell death observed in the different wells. The cell death was observed both in cells infected with original PCV2 virus stock with an unknown concentration and in the 1:10 dilution of the original PCV2 virus stock. It is important to notice that even though the desired density was 70%, the density at point of infection was about 60%.

As shown in *Figure 6*, the presence of vacuolation in the cytoplasm of two infected cells is a clear indicator that these cells are undergoing apoptosis, due to a PCV2 infection. This observation was consistent across multiple time points, as vacuolation was observed at 24, 48, and 72 HPI, indicating continuous infection of PCV2 throughout these time points. Notably, vacuolation was not observed in any mock infected cells, further supporting the conclusion that this phenomenon is specific to PCV2 infection.

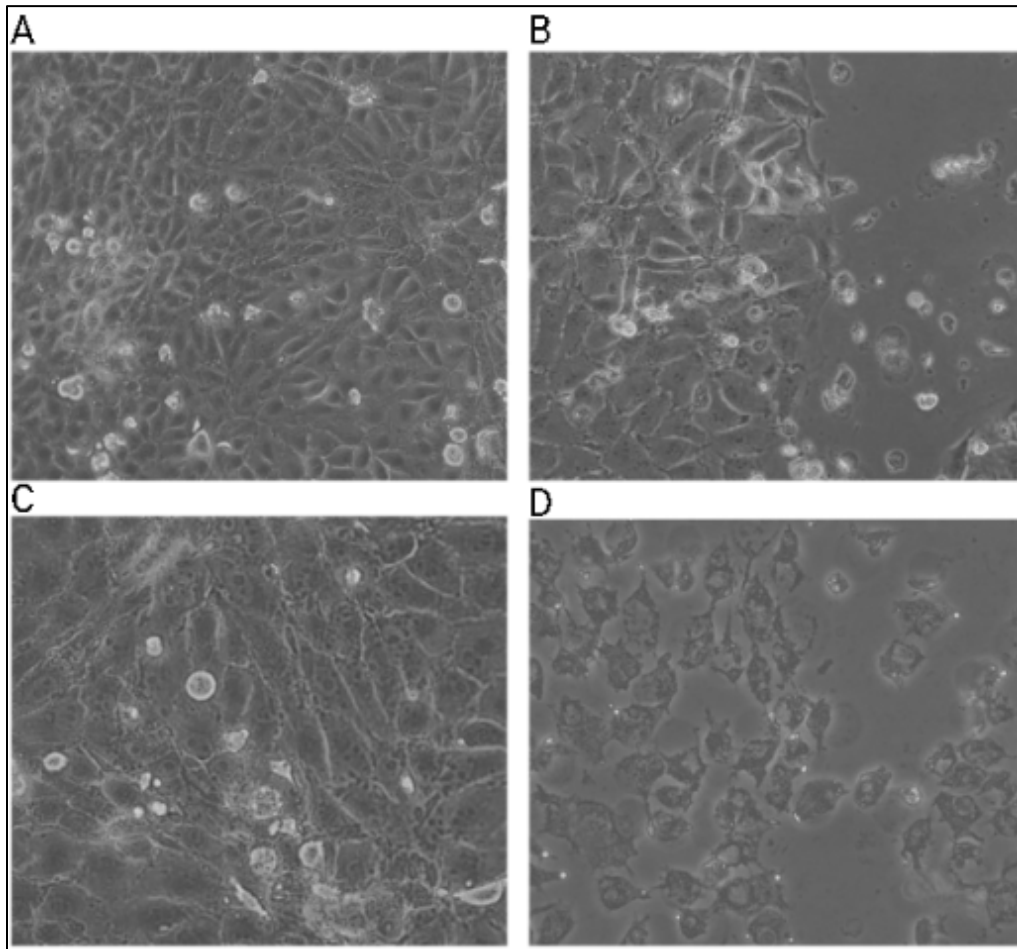


Figure 5 – Mock infected and PCV2 infected PK-15 cells: The picture is taken on ZEISS Axio Vert.A1 reverse microscope at magnification 20x (**A** and **B**) and 40x (**C** and **D**) 96 HPI. **A** and **C**: Mock infected PK-15 cells, **B**: PK-15 cells infected with original PCV2 virus stock, and **D**: PK-15 cells infected with 1:10 dilution of original PCV2 virus stock.

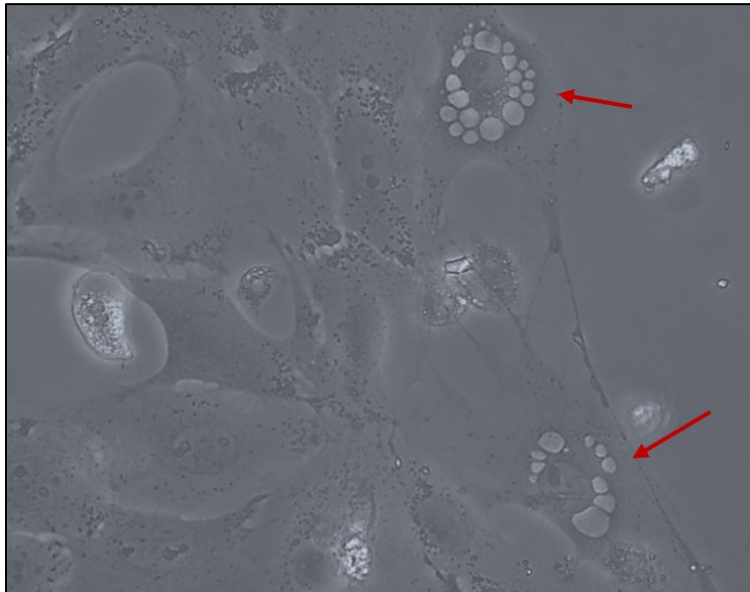


Figure 6 – PCV2 infected PK-15 cell: The picture is taken on ZEISS Axio Vert.A1 reverse microscope at magnification 40x. Two PK-15 cells (red arrows) infected with PCV2 undergoing apoptosis indicated by vacuolation in the cytoplasm observed at 24 HPI.

3.1.2.1 PCR

In this study, we first performed a PCR and agarose gel electrophoresis to confirm the presence of PCV2 in infected PK-15 cells. PCR and agarose gel electrophoresis were performed on DNA samples obtained from the first PCV2 infection in PK-15 cells with a detailed description of all samples listed in **Table 6**. All samples and positive control showed positive strong bands for PCV2, while the mock infection and negative control yielded negative results as seen in **Figure 7**. The PCR products were compared to a 100kb ladder, and the results indicated a product size of approximately 250-300bp. This measurement is consistent with the expected size of 263 bp for the primer pair used on PCV2. Strong bands were observed for all positive samples, apart from 48 HPI 1:10 dilution. A re-run of the PCR product from the 48 HPI 1:10 dilution resulted in a strong band, thus excluding any potential issues with the sample DNA that may have affected the initial results.

The negative control used in this experiment was PK-15 DNA and confirmed that the primers used in the PCR assay were specific for the target DNA. The positive control used for the PCR experiment was from the original PCV2 virus stock and confirms that the primer pair targets the target DNA. The negative mock infection indicates no cross-contamination of PCV2 during

growth, thus indicating good pipetting technique. It also indicates that any effects observed, such as alterations in cell viability, gene expression, or morphology, are not due to non-specific factors associated with the infection process.

Table 6 – Detailed description of samples used for the following PCR and Real-Time PCR

Name	Sample
0 HPI	0 HPI, 200µL Concentrated virus with 1h incubation at 37°C
24 HPI	24 HPI, 200µL Concentrated virus with 1h incubation at 37°C
48 HPI	48 HPI, 200µL Concentrated virus with 1h incubation at 37°C
72 HPI	72 HPI, 200µL Concentrated virus with 1h incubation at 37°C
96 HPI	96 HPI, 200µL Concentrated virus with 1h incubation at 37°C
0 HPI 1:10	0 HPI, 200µL 1:10 dilution of the virus with 1h incubation at 37°C
24 HPI 1:10	24 HPI, 200µL 1:10 dilution with 1h incubation at 37°C
48 HPI 1:10	48 HPI, 200µL 1:10 dilution with 1h incubation at 37°C
72 HPI 1:10	72 HPI, 200µL 1:10 dilution with 1h incubation at 37°C
96 HPI 1:10	96 HPI, 200µL 1:10 dilution with 1h incubation at 37°C
MI	96 HPI, Mock infection
Ladder	100 bp Ladder
NC 1	Negative control using uninfected PK-15
PC	Positive control using original PCV2 virus stock

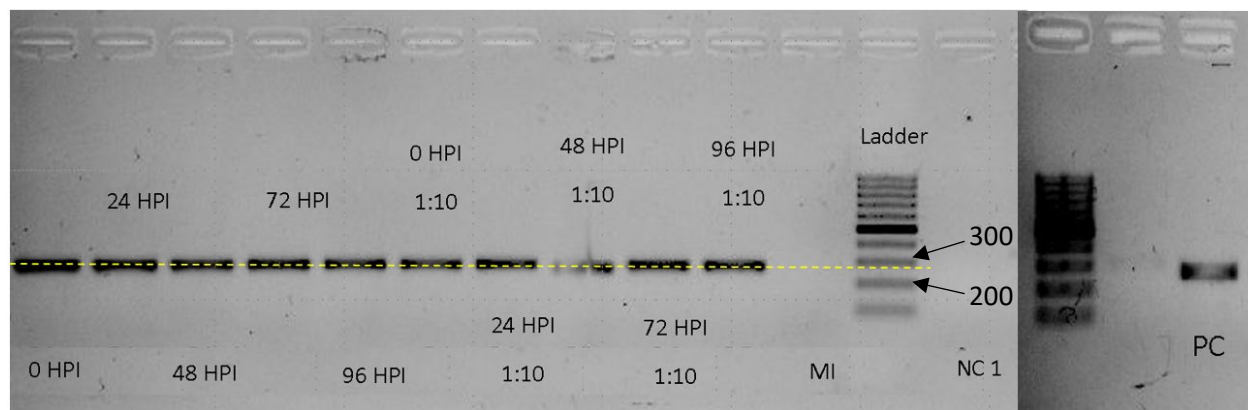


Figure 7 – PCR results testing extracted DNA from PK-15 cells infected with PCV2: Samples were collected at different times after infection and DNA was extracted. All samples were run on a PCR machine and then on a 2% agarose gel before the picture was taken. A more detailed description of the samples is listed in **Table 6**.

3.1.2.2 Real-Time PCR

Real-Time PCR was performed using the same samples from the previous PCR experiment, along with a 10-fold dilution series from the original PCV2 virus stock. Two negative controls and a mock infection were also included in the study. Negative controls both resulted in Ct values over 35 cycles. A no template control (NTC) resulted in a Ct value of 0. Standards 1 to 6 had increasing Ct values from 15 to 33, while standards 7 and 8 had a Ct value of 0. The standard curve generated from the Real-Time PCR software is displayed in **Figure 8** and had an efficiency of 91.2% with R² value of 0.999 and a slope value of -3.552.

A fold changes using Δ Ct values were calculated for all sample and the results are shown in **Figure 9**. The results of the Real-Time PCR experiment revealed that PK-15 cells infected with the original PCV2 stock grow over time, where 96 HPI showed the best results at 0.19 compared to the original PCV2 stock at 1.00. The results for undiluted infection showed an increase in viral DNA in the samples over time. The highest fold change Δ Ct value from the 1:10 diluted original PCV2 virus stock was observed after 72 hours post-infection, with 0.0106. The raw data from this and all Real-Time PCR experiment performed in this study is provided in **Appendix B: Real-time PCR raw data**.

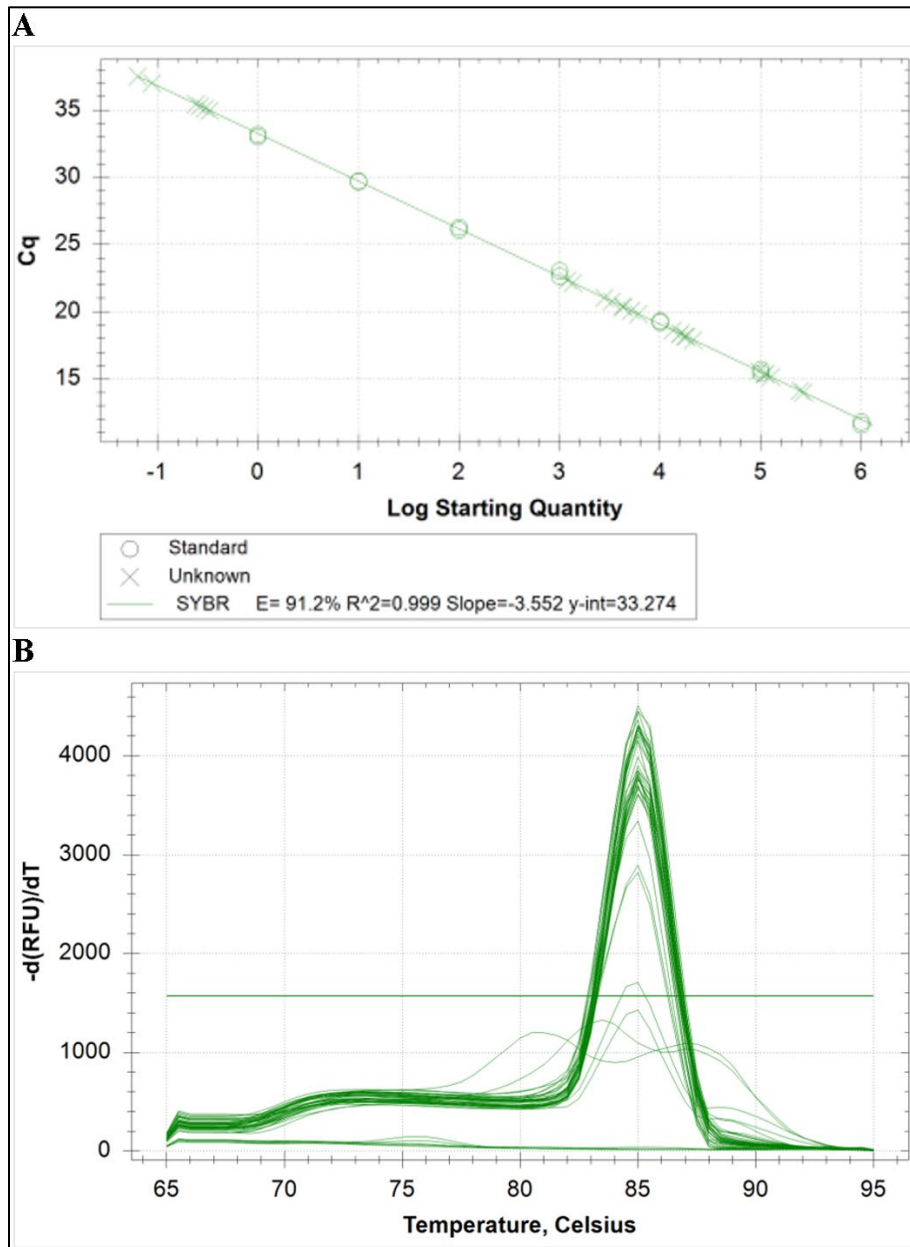


Figure 8 – Standard curve and melting curve for infecting PK-15 with PCV2: The standard curve (A) and melting curve (B) was generated by the CFX Maestro Software on the Real-Time PCR machine. To create the standard curve, an 8-point dilution series was performed using a 10-fold dilution from the original PCV2 virus stock, with Standard 1 (S1) being the first dilution. The standard curve (A) displays Ct (Cq) vs log starting quantity, while the melting curve (B) display Derivative reporter ($-Rn'$) vs. temperature. **Table 6** provides a detailed description of the samples used in the experiment.

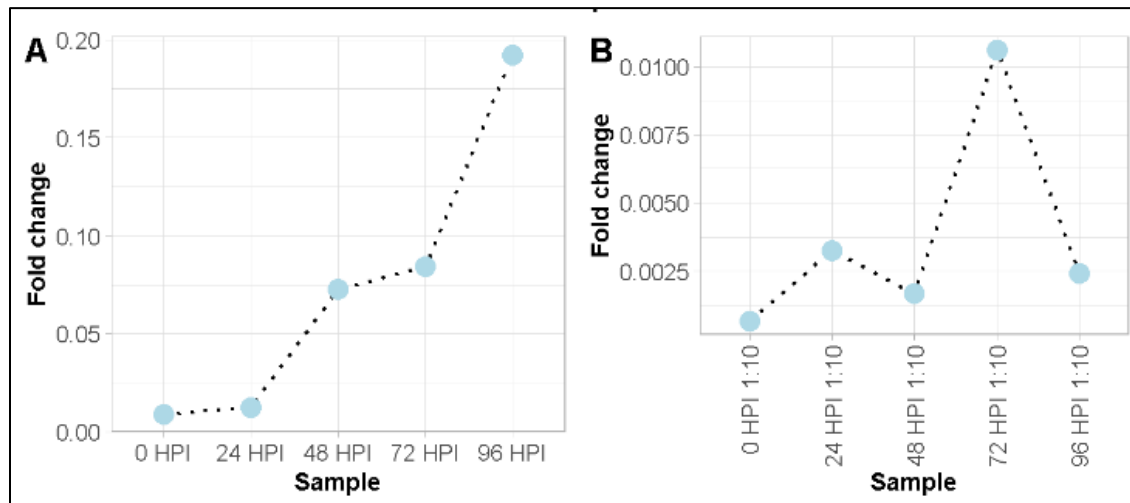


Figure 9 – Fold change: Shows the fold change calculated using ΔC_t values obtained from PK-15 cells infected with various concentrations of the original PCV2 virus stock collected different time points after infection. To determine ΔC_t of the infected samples, the mean C_t value of the original sample was used as the standard. **Panel A** shows the samples infected with the original virus stock, and **Panel B** displays cells infected with a 1:10 dilution of the original virus stock. **Table 1** provides a detailed description of the samples used in the experiment. The figure was created using R studio.

3.1.3 Concentrating PCV2 virus

Concentrating the produced virus stock is one possible solution to achieve a higher concentration of PCV2 stock, considering PCV2 has a low reproduction rate in PK-15 cells. While there are several possible methods to achieve this, ultrafiltration was performed on a non-usable PCV2 virus stock due to previous success with adenoviruses. The virus stock used for ultrafiltration was produced separately by infecting PK-15 cells that were treated with a CRISPR library. For this experiment, a 1:10 dilution of the original virus stock was used, and only the supernatant collected at 96 HPI. The stock was run through two filters with pore sizes of 100kDa and 10kDa, and the start and end volumes were recorded to calculate the expected concentration factor after filtration. A total volume of 4.5mL of collected virus stock was added to each filter, and the 100kDa filter resulted in an end volume of 450 μ L, giving a concentration factor of 10x. The 10kDa filter had an end volume of 550 μ L, resulting in a concentration factor of 8.2x. The DNA from unfiltered and filtered samples was then extracted, and a Real-Time PCR was performed. The results from the Real-Time PCR are presented in **Figure 10**, showed that the 100kDa filter had a concentration of

3.64x the unfiltered sample, indicating a virus loss of 66%, while the 10kDa filter had a concentration of 2.62x the unfiltered sample indicating a virus loss of 64%. There was not observed any virus in the flow through from either of the two filter sizes.

The final filtrated virus stock was compared to a 1:10 dilution of the original stock (refer to S1 in **Figure 10**) to calculate the relative concentrations. The initial volume of 1:10 dilution of the original PCV2 virus stock was 25mL and the virus stock collected at 96 HPI was 200mL. 25mL initial infection volume multiplied by the relative concentration of S1 at 8.54 gives a total relative concentration of 213.4. The relative concentration of the collected virus stock at 96 HPI was 200. Using the same calculation method, a total relative concentration in final volume of 100kDa is 1.628 and 10kDa at 1.441. These numbers can be used to calculate the total relative concentration if we filtered all 200 μ L using the two different cut off columns: 100kDa resulting in 72.8 and 10kDa resulting in 64.0. This indicates a virus loss of ca. 64% for 100kDa and 60% for 10kDa, further backing up the observations in **Figure 10** with small error.

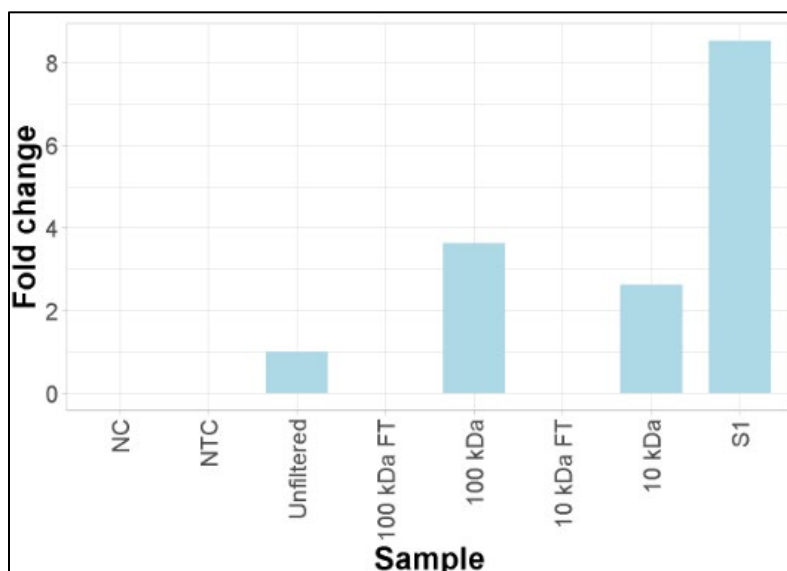


Figure 10 – Fold Change Calculation using Δ Ct values obtained from ultrafiltration of PCV2 Stock: The graph represents the fold change calculated from the Δ Ct values obtained using the ultra-filtered PCV2 stock. Two filters with 100kDa and 10kDa pore size were used to purify the virus stock. The unfiltered sample Ct value was used as the standard to calculate the Δ Ct values. The analysis includes negative control which consists of DNA from non-infected PK-15 cells, positive control from the original virus and no template control. S1 is a 1:10 dilution of the original PCV2 virus stock.

3.2 Cell viability

Due to the observed cell death in previous PCV2 infections of PK-15 cells (3.1.2 *PCV2 infection in PK-15 cells*, in **Figure 5**), a viability assay using cell titer glo was performed to assess the impact of PCV2 infection on cell viability at multiple time points (24, 48, 72, and 96 HPI). Two different seeding cell densities ($7.5 \cdot 10^3$ and $1.5 \cdot 10^4$) were used, resulting in distinct cell densities at the time of infection. Different concentrations of the original PCV2 virus stock were also used: 1:3, 1:6, 1:9, 1:12 and 1:15 dilutions. As the 96-well plate used had nontransparent white walls, the exact infection density is unknown.

To evaluate cell viability in the samples, we determined the mean luminescence percentage for each sample relative to the mean luminescence of the mock infection. The obtained results revealed that the luminescent signals of both mock infections, before and after heat-inactivation, were similar, suggesting comparable cell viability (**Figure 11**). A more unstable difference between infected and mock infected cells was observed in the different dilutions of PCV2 at higher seeding cell densities (**Figure 11B**) in comparison to lower seeding densities (**Figure 11A**). A notable difference in cell viability between infected and mock infected cells was evident at lower seeding cell densities, with infected cells exhibiting reduced viability (**Figure 11A**). When comparing mock infected and heat-inactivated virus-infected cells to infected cells in the higher seeding density experiment, a significant difference was observed only after 24 and 48 HPI. However, this difference diminished at 72 HPI and exceeded the mock infection level at 96 HPI (Figure 3A).

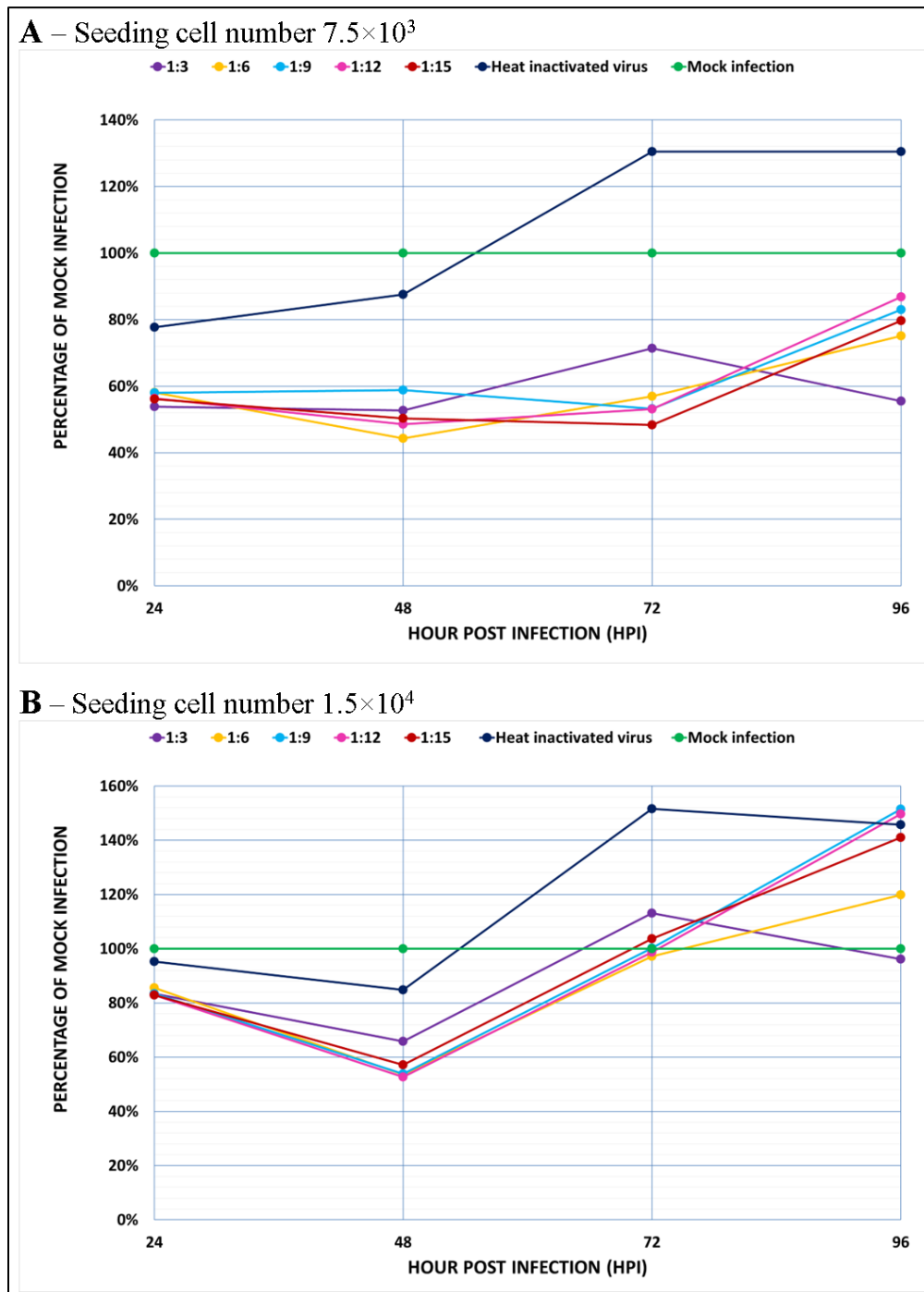


Figure 11 – Cell viability assay on PCV2-infected PK-15 cells: A cell viability assay was performed on PK-15 cells infected with different dilutions (1:3, 1:6, 1:9, 1:12, and 1:15) of original PCV2 virus stock, with measurements taken at 24, 48, 72, and 96 HPI. The results are presented in **Panel A** and **B**, where **A** corresponds to a seeding density of $7.5 \cdot 10^3$ cells and **B** corresponds to a seeding density of $1.5 \cdot 10^4$ cells. The Y-axis represents the percentage of mock infection calculated using the mean luminescence from two technical replicates.

3.3 Actin filament changes by fluorescence microscopy

The immunofluorescent staining experiment (*2.4 Actin filament changes by fluorescence microscopy*) using Alexa Fluor Phalloidin 488 and DAPI, along with virus staining, was unsuccessful. The cells were observed in the microscope after each step, and the fixed cells appeared to be in good condition. However, following the completion of all three staining procedures, only a weak DAPI staining was observed within the cells. While 6 to 7 cells exhibited strong actin staining, the majority of cells displayed no staining whatsoever.

3.4 BVDV detection in FBS

Initial nested RT-PCR analysis to detect BVDV contamination (*2.5 BVDV detection in FBS*) in the supernatant of MDBK cells grown with different FBS batches (listed in **Table 4**) resulted in all samples testing positive, while the negative control from PK-15 DNA resulted in a very weak positive band. As a result, a new approach was pursued using an engineered MDBK cell line provided by our collaborators in Vienna that has been confirmed to be BVDV-free called MDBK clone 44. This cell line was passaged five times with selected FBS batches based on the previous experiment (1, 3, 5, and FBS-G). RNA was extracted and subjected to nested RT-PCR and run on an agarose gel. All amplification products from the inner PCR were positive, except for the negative control (see **Figure 12**). After further consultation and collaboration with our collaborators in Vienna, we obtained a BVDV-free FBS batch that had been used successfully in their laboratory. We thereby solved our BVDV contamination issues by using the BVDV-free FBS batch and MDBK clone 44 cell line.

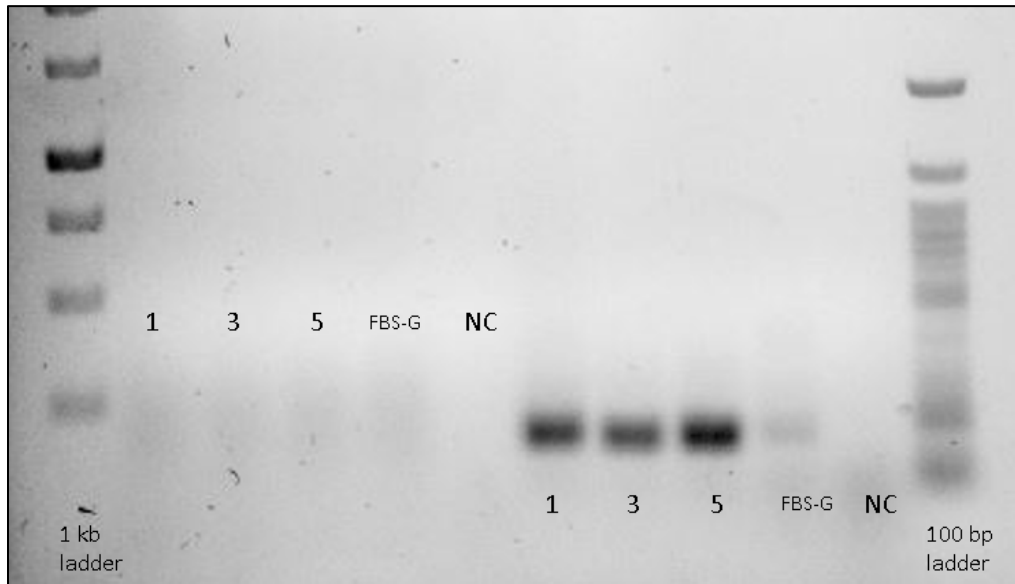


Figure 12 – Nested RT-PCR analysis of BVDV in MDBK cells provided by our collaborators in Vienna: The figure shows the results of nested RT-PCR analysis on four batches of FBS (FBS 1, 3, 5, and FBS-G) and on a negative control (NC) after 5 passages. The first row of samples shows the outer PCR amplification products using the first primer pair, while the second row shows the inner PCR amplification products using the second primer pair. A 1 Kb ladder was used on the left side of the gel, and a 100 bp ladder was used on the right side as a molecular weight marker.

4. Discussion

4.1 Cell viability assay

To evaluate whether cell death is a possible suitable phenotype for GeCKO screening in PCV2 infection experiments, a cell viability assay was performed on the PK-15 cells. The assay was performed four times at 24, 48, 72 and 96 HPI. **Figure 11** displays the percentage of infected cells compared to mock infected cells over time. **Figure 11A** and **11B** represent two different seeding densities, $7.5 \cdot 10^3$ and $1.5 \cdot 10^4$ cells per well, respectively, which resulted in different cell densities at the point of infection.

The heat-inactivated virus showed a closer resemblance to the mock infected cells in comparison to the significant differences observed in the infected cells. This finding suggests that the media utilized for the virus stock does not exert a significant influence on cell viability. However, it is worth noting that during the time period of 24 to 48 HPI, the cell viability was observed to be lower compared to the mock infected cells. In contrast, the cell viability grew above the mock infection at 72 to 96 HPI. It should be acknowledged that these differences in cell viability were smaller at 24 and 48 HPI when compared to the infected cells. It's interesting that the heat-inactivated virus culture started with around 20% below mock infection but resulted in around 40% above mock infection. The presence of heat-inactivated virus particles may trigger cellular responses that promote cell growth or survival in the treated culture. Heat-inactivated virus is a normal way of creating a viral vaccine and during these studies it has been shown that there is a less significant cellular response after injection, compared to the active virus (Louten, 2023; Yang et al., 2022). The activation of certain signaling pathways or the production of specific cytokines or growth factors might enhance cell proliferation in this culture compared to the normal mock infection. Additionally, it is also plausible that these differences could be influenced by variations in the initial seeding of the wells, especially connected to cell counting errors. Further research needs to be conducted to find a specific cause for the heat-inactivated PCV2 effect on PK-15.

Both the low- and high-density cell populations demonstrated an initial discrepancy between infected and mock infected cells at 24 to 48 hours post-infection (HPI). The viability of low cell density infected with PCV2 (**Figure 11A**) exhibited approximately 60% relative cell viability compared to mock infection, resulting in a difference of approximately 40% at both 24 and 48 HPI. The viability of high cell density infected with PCV2 (**Figure 11B**) exhibited approximately 80%

relative cell viability compared to mock infection, resulting in a difference of approximately 20% at both 24 and 48 HPI. These observations indicate that the variation in cell viability is more pronounced for cells cultured at a lower density. Furthermore, it is important to note that the lower cell density population consistently maintains a difference of 40% up to 72 HPI, with a slight increase to around 20% observed at 96 HPI. This suggests that the variation in cell viability between infected and mock infected cells remains relatively stable and is more prominent when starting with a low-density cell population at the time of infection. Starting with a higher density at the point of infection resulted in a more rapid recovery of PK-15 cells compared to the lower cell density, as shown in *Figure 11B*. After 72 HPI, the cell viability of the higher-density population reached levels similar to that of the mock infected cells with no significant difference. Subsequently, the cell viability further increased to a difference of around 40% above the mock infection. These findings suggest that the cells not only recovered quickly after infection but also exhibited enhanced growth compared to the mock infected cells. The observed difference between lower and higher densities suggests that cell density is an important factor, where the lower density shows a bigger difference between mock infected and infected cells. This suggests that a lower cell density makes it harder for the cells to grow during viral infection.

The greater difference in cell viability observed when cells are infected at a lower density compared to a higher density at the point of infection can potentially be explained by various factors. When the initial cell density is low, there are fewer cells available for the virus to infect. This results in a higher virus-to-cell ratio, which increases the likelihood of individual cells being infected with multiple viral particles. Consequently, cells may experience a more robust viral replication, ultimately leading to increased cytopathic effect and cell death. When cells are less confluent, they have less contact with neighboring cells, which could affect their ability to maintain homeostasis and resist stress. This increased vulnerability may make them more prone to the cytopathic effects of viral infection and result in increased cell death. In a low-density culture, there is generally more nutrient availability per cell, which could promote higher viral replication within infected cells (Kamen & Henry, 2004). As the virus replicates more efficiently, it can cause more severe cytopathic effects and increased cell death. Researchers have investigated substances known as interferons that are released by host cells in response to viral infections. Interferons can induce an antiviral state in nearby cells, making them more resistant to viral replication, thus a higher cell density can cause more cell to cell communication causing better resistance to the virus (Samuel,

2001). Considering these possible reasons further research is required to identify the specific cause underlying the greater difference in cell viability observed when cells are infected at a lower density.

The concentration of virus used to infect the cells was shown to be a less pronounced factor affecting the cell viability. However, we can clearly see that the highest concentration of virus (1:3 dilution) maintain the difference of 40% also at 96 HPI both for low and high cell densities (**Figure 11**). This suggests that a too high virus concentration will make it harder for the cells to survive for a longer period of time. The 1:6, 1:9, 1:12, and 1:15 dilutions have a lower viral load compared to the 1:3 dilution. As a result, there might be less robust viral replication in the cells, leading to reduced cellular stress and lower cytopathic effects. This allows the cells to better tolerate the infection and maintain their viability.

To determine whether a cytopathic effect is a suitable phenotype for GeCKO screening, several factors should be considered, including time course, magnitude of cytopathic effect, specificity, and reproducibility (Bock et al., 2022). The optimal time course for the cytopathic effect will depend on the specific virus and cell line being used. Generally, the time course should be long enough to allow for sufficient cell proliferation to occur, but not so long that the cells become too damaged or die and should be around 24-72 HPI. In the low-density experiment, differences between infected and mock infected were visible already after 24 HPI and remained consistent until 72 HPI, indicating that a cytopathic effect was present at an optimal time course. This is consistent with the PCV2 replication cycle that is reported to be around 24 to 36 HPI (Meerts et al., 2005). The magnitude of the cytopathic effect should be sufficient to distinguish infected cells from mock infected cells, a difference between 25 to 50 % in cell growth or viability of infected cells relative to mock infected cells (Bock et al., 2022). As discussed above the most promising difference is observed in the lower density experiment with a significant difference of 40 % (**Figure 11A**). It is however important to note that this effect was not as stable and significantly different in the high-density experiment.

The cytopathic effect should be specific to viral infection and not due to other factors such as toxicity or stress. To ensure that observed effects were specific to the viral infection, mock infected cells were used, one with complete growth media without virus and one where the virus stock was heat inactivated. Using heat inactivated virus excludes any stress response caused by the media the

virus is stored in. Additionally, the cytopathic effect should be reproducible across multiple experimental replicates to ensure that the effects are consistent and reliable. While the experiment has not been repeated, scaling up the infection using a 1:10 dilution of the original PCV2 virus stock in 175cm² T-flasks showed that cell death observed in a previous separate experiment did not occur. It is important to notice that the cell density in this experiment was high at point of infection which further confirm that cell density is an important factor in inducing cytopathic effects in PK-15 cells infected by PCV2.

4.2 Actin filament changes by fluorescence microscopy

At point of staining no difference between mock infected and PCV2 infected IPEC-J2 cells was observed in the microscope, suggesting that the virus does not cause apoptosis in IPEC-J2 cell line. Therefore, a possible fluorescence staining method published by Yan et al. (2014) was attempted. The results of the immunofluorescent staining experiment using Alexa Fluor™ Phalloidin 488 and DAPI, along with virus staining, were unsuccessful. Despite the cells appearing to be in good condition following fixation, only a weak DAPI staining was observed within the cells. The weak staining of the majority of cells, along with the lack of virus staining, suggests a potential issue with the experimental protocol or the quality of the staining reagents. The failure of the staining experiment could be attributed to several factors, especially since immunofluorescence staining can be complex and subject to various experimental variables.

One potential factor that may contribute to suboptimal staining is the use of inadequate fixation and permeabilization methods. In the present study, 2% formaldehyde was used for fixation, and this concentration has been a successful method used in CIGENEs laboratory. After fixation and during all staining the cells appeared in good condition. 0.1% Triton X-100 were used for permeabilization, and IPEC-J2 have successfully been permeabilized using 0.1% Triton X-100 previously (Yuan et al., 2022). It is important to note that the duration and concentration of the permeabilization step can impact the success of the staining experiment. While insufficient permeabilization can result in poor antibody penetration and reduced staining, longer or higher concentrations of permeabilization may result in non-specific background staining.

In addition to permeabilization, the blocking step is critical for reducing non-specific antibody binding, which can result in high background staining. The use of 2% skim milk powder in 1x

TBST is a commonly used blocking agent. The blocking step can also interfere with the binding of subsequent staining reagents if the blocking agent is not completely removed from the sample. Incomplete washing after blocking can result in residual blocking agent interfering with the binding of subsequent antibodies or staining reagents, leading to decreased staining intensity or specificity. Therefore, it is important to ensure thorough washing after each step in an immunofluorescent staining protocol.

Finally, the concentration of staining solutions used in immunofluorescent staining experiments can also impact the success of the staining. Using too high or too low concentrations of staining reagents can result in non-specific background staining, low signal-to-noise ratios, or poor penetration of the staining. Therefore, it is recommended to perform a series of pilot experiments to determine the optimal concentration of each staining reagent for the specific cellular targets and experimental conditions. Gradually titrating the concentration of each staining reagent and evaluating the staining intensity and specificity can help to identify the optimal staining conditions. In this study the protocol for Alexa Flour™ 488 phalloidin staining was followed, however the concentration used (300 nM) can be considered too low.

4.3 BVDV contaminations in FBS

Contamination of FBS with BVDV presents a significant challenge in conducting BVDV diagnostics and research using the MDBK cell line (Bolin et al., 1991). Although FBS suppliers certify their serum as BVDV-free, there is still a risk of contamination if the method used for certification is not sensitive enough. Typically, FBS is directly tested by suppliers, but even small BVDV contamination in FBS can infect and replicate in MDBK cells. Therefore, if the FBS is contaminated with a BVDV below the detection limit of the certification method, it can lead to the accumulation of BVDV in MDBK cells after a certain number of passages, considering that MDBK cells are highly susceptible to BVDV infection. Moreover, the contaminations can be of a non-cytopathic strain of BVDV, and therefore may not produce any visible effects on the cell line. This can make it challenging to detect the presence of the virus in MDBK cells and to determine the cause of any observed changes in the cells. Contamination with BVDV can significantly affect the reproducibility and reliability of experimental results, leading to incorrect conclusions and wasted resources. As a result, it is crucial to ensure that both the MDBK cell

line, and the FBS used is entirely BVDV-free when conducting BVDV experiments. This will ensure the accuracy and validity of research results.

The main purpose of using nested RT-PCR in this study was to detect BVDV contamination in MDBK cell cultures. The enhanced sensitivity and specificity provided by nested RT-PCR allowed for the accurate detection of low levels of BVDV RNA, which is critical in maintaining the integrity of cell cultures and ensuring reliable experimental results. The results of our initial testing for BVDV contamination in the supernatant of MDBK cells grown with different FBS batches yielded positive results including FBS-G that was expected to be our negative control. This is indicating a contamination problem, suggesting that the MDBK cell line may have been contaminated from the beginning and that the commercial FBS test did not have sufficient sensitivity to detect the contaminations. To address this, we used a new cell line that had been confirmed to be BVDV-free. Since the initial testing used supernatant samples, it is possible that inactivated BVDV was present in the complete growth media, as nested RT-PCR is highly sensitive and can detect even small amounts of virus. Since inactivated BVDV cannot infect the cells, it is not a concern for investigations, and to eliminate the possibility of detecting inactivated virus, we modified our approach by extracting RNA from inside the cells rather than from the supernatant.

Our subsequent approach, which involved using an engineered BVDV-free MDBK cell line and selected FBS batches, yielded positive results for all FBS tested, including a weak band for FBS-G. This indicated that the BVDV contamination was from the FBS, and that the virus had activated and infected the MDBK cells. Consequently, none of the FBS listed in **Table 4** were used to solve the contamination problem. Fortunately, we were able to obtain a batch of FBS from the providers of the engineered MDBK cell line, which was confirmed to be free of BVDV contamination. This batch of FBS and MDBK cell line can be used in future research of BVDV including GeCKO screening.

4.4 Cultivation of PCV2

4.4.1 PCV1 contamination

The propagation of PCV2 in PK-15 cells has been extensively studied, with a focus on enhancing replication due to the low viral titer produced by PCV2 in PK-15 cells (Chen et al., 2013; Gilpin et al., 2003; Hua et al., 2018; Yang et al., 2013; Zhu et al., 2007). One proposed method to enhance

PCV2 replication is the creation of a PCV1-free PK-15 cell line, as PCV1 has been shown to interfere with PCV2 replication (Chen et al., 2013). Although no co-infection studies on PCV-free PK-15 cells have been conducted, it has been demonstrated that a created PCV-free PK-15 cell line can enhance PCV2 replication (Chen et al., 2013). Another suggested approach to enhance PCV2 replication in PK-15 cells is treatment with Interleukin-2 protein, Concanavalin A, D-glucosamine, and methyl-beta-cyclodextrin 24 HPI (Yang et al., 2013).

4.4.2 Microscopic insights

Our four-day observation of PK-15 cells infected with PCV2 demonstrated significant differences in cell growth and viability compared to mock infected cells. This finding implies that PCV2 infection substantially affects the health and survival of the infected cells, which prompted us to conduct a cell viability assay as described in section 2.3 *Cell viability assay*. **Figure 5** clearly illustrates these differences in cell density between mock infected and PCV2-infected cells. While mock infected cells exhibited high cell density, reaching 100% by 72 HPI, PCV2-infected cells showed a significant decrease in density from 24 to 72 HPI. These observations are consistent with the findings of Karuppanan et al. (2016), who reported a similar decline in cell density and viability in PCV2-infected PK-15 cells as represented in figure 6 in their research paper also showed in **Figure 3**. Interestingly, cell growth in infected cells increased again from 72 to 96 HPI, suggesting a potential adaptation or recovery process in the surviving cells. This phenomenon is also observed in the cell viability assay as shown in **Figure 5**. It is worth noting that the actual cell density at the point of infection was closer to 60% instead of the desired 70%, which might have influenced the observed results to some extent.

The presence of vacuolation in the cytoplasm of PCV2-infected cells (**Figure 6**) strongly indicates apoptosis induced by the viral infection. Apoptosis through vacuolization is a well-known cellular response to viral infections, including PCV2, and is characterized by distinct changes in the cytoplasm, typically associated with cell death (Shubin et al., 2016). The observation of vacuolation in infected cells at multiple time points (24, 48, and 72 HPI) suggests a continuous PCV2 infection and ongoing induction of apoptosis during this period. The lack of vacuolation in mock infected cells supports the conclusion that this phenomenon is specifically associated with PCV2 infection, rather than non-specific cellular stress or experimental artifacts. Our findings align with previous

studies that reported cytopathic effects and apoptosis in PCV2-infected cells (Karuppanan et al., 2016). Moreover, the presence of vacuolation in infected cells is likely to contribute to the reduced cell density and viability observed in PCV2-infected cells compared to mock infected cells, as discussed earlier. Similar observations of apoptosis have been reported in multiple other studies on PCV2-infected PK-15 cells (Misinzo et al., 2005; Wang et al., 2021).

4.4.3 PCR

The PCR and agarose gel electrophoresis results provided conclusive evidence of PCV2 presence in the infected PK-15 cells. Positive bands observed for all infected samples, except for the initial 48 HPI 1:10 dilution, confirmed that PCV2 is present in PK-15 cells. The strong bands for the positive control, along with negative results for the mock infection and negative control, further validated the reliability and specificity of the PCR assay provided by Larochelle et al (Larochelle et al., 1999). The PCR assay yielded product sizes of approximately 250-300 bp, which is consistent with the expected size of 263 bp for the primer pair targeting PCV2. This consistency in PCR product sizes supports the accuracy of the selected primers and confirms the assay's specificity, ensuring that the primers only amplify the specific PCV2 gene and are not influenced by DNA from PK-15 cells. The initial absence of a strong band for the 48 HPI 1:10 dilution sample could have resulted from various factors such as pipetting errors or low DNA concentration. However, after re-running the PCR assay for this sample, a strong band was observed, alleviating any concerns regarding the sample DNA's integrity. The negative control using PK-15 DNA demonstrated the primers' specificity for PCV2, ensuring that the PCR assay only amplified the target DNA. Additionally, the negative mock infection results confirmed that there was no cross-contamination of PCV2 during the growth process. This is crucial, as it ensures that any observed effects on cell viability, gene expression, or morphology in the PCV2-infected PK-15 cells are directly attributable to the viral infection and not due to non-specific factors or experimental artifacts.

4.4.4 Real-Time PCR

Since the PCR showed that the primers were specific for the target DNA they were used in Real-Time PCR. The Real-Time PCR results confirmed successful amplification of PCV2 viral DNA

from the PK-15 cell samples. The standard curve generated by the Real-Time PCR software exhibits a high efficiency (91.2%) and R² value (0.999), suggesting consistent and reliable PCR reactions across various dilutions as seen in **Figure 8**. The slope value of -3.552 falls within the range of -3.1 (110%) to -3.58 (90%), indicating good amplification efficiency (Bivins et al., 2021). Negative controls yielded Ct values over 35 cycles, demonstrating the assay's specificity and the absence of non-specific amplification or contamination. The no template control (NTC) produced a Ct value of 0, further supporting the specificity of the assay. Melting curve analysis verifies the specificity of the Real-Time PCR assay, revealing only a few non-specific amplification products or primer-dimer artifacts with a different melting temperature than the target product at 85°C. The presence of non-specific products can interfere with the accurate amplification of the target template in Real-Time PCR, so it is crucial to verify the reaction's specificity. A few of the negative controls display a melting temperature at 85°C; however, these curves are substantially shorter than the samples. This suggests minor contamination in these wells; however, since the other parallels of the negative samples are negative, this is most likely due to cross-contamination during pipetting.

In the viral infection experiment using the concentrated PCV2 virus stock, an increasing amount of viral DNA is observed from 0 to 96 HPI as seen in **Figure 9A**. This suggests an increase in viral DNA in the samples over time, indicating that the PCV2 virus is replicating within the PK-15 cells. However, the values are only around 20% compared to the original virus stock used for infection, signifying that the replication is slow. This observation aligns with previous research on PK-15 cells infected with PCV2 (Zhu et al., 2007). This can also suggest that the infection method might not be optimal.

The viral infection experiment utilizing a 1:10 dilution of the original PCV2 virus stock yielded unexpected results, showing a relatively low and inconsistent pattern in viral DNA levels over time as seen in **Figure 9B**. The observed values remained minimal across different time points, making it challenging to discern any clear trends. The highest value recorded at 72 hours post infection (HPI) was 0.01, indicating a potential increase in viral DNA content over time, albeit to a lesser extent compared to the undiluted stock. This outcome aligns with the expectation that a lower initial viral concentration would result in slower replication kinetics and potentially lower overall viral DNA content. However, it is worth noting that the viral DNA levels at 96 HPI were unexpectedly similar to those observed at 48 HPI. Given the small magnitude of the observed differences and the inherent limitations of the technique employed, it is crucial to consider the uncertainty and potential

errors associated with the measurements. In such cases, drawing definitive conclusions or establishing clear patterns based on these subtle differences may not be reliable or accurate. As illustrated in Figure 9A, the data might only appear as a straight line at the bottom, indicating minimal variation.

Despite the low and inconsistent viral DNA levels observed with the 1:10 dilution, cytopathic effects were still observed in both the cells infected with the original PCV2 virus stock and the diluted version. Considering the limited availability of the original virus stock, it seems reasonable to continue utilizing the 1:10 dilution for further experiments. This decision assumes that even though the values are low, the presence of PCV2 virus in the PK-15 cells suggests that the infection can still provide valuable information for the study. Nonetheless, it is important to acknowledge and consider potential factors that might have contributed to the observed low and inconsistent values, such as variations in infection efficiency, viral replication rate, or experimental conditions.

4.4.5 Concentrating PCV2

Concentrating the PCV2 virus stock can be a potential solution for producing a high concentrated PCV2 stock using PK-15 cells. Due to PCV2's low reproduction rate in PK-15 cells, the viral titers may be insufficient for subsequent experiments. In this study, ultrafiltration was investigated as a potential concentration strategy, drawing on previous success with adenoviruses in our laboratory. The Real-Time PCR results, presented in *Figure 10*, demonstrated that both filters led to an increased concentration of the virus stock. The 100kDa filter yielded a 3x concentration increase compared to the unfiltered sample, while the 10kDa filter resulted in a 2.6x increase. However, the concentration factors were lower than expected based on the starting and ending volumes (10x for the 100kDa filter and 8.2x for the 10kDa filter). This discrepancy suggests significant virus loss during the ultrafiltration process, with 66% and 64% virus loss for the 100kDa and 10kDa filters, respectively. The 1:10 dilution from the original PCV2 virus stock was used to compare the relative concentrations and further supports these observations, suggesting that virus loss during ultrafiltration is a critical concern that should be addressed to improve the efficiency of virus concentration. The absence of virus in the flow-through from both filters indicates that no viral loss occurred during the first filtration step. The filtration was performed in two steps, and the second

flow-through was not tested, which could potentially account for the greater virus loss. Additionally, the virus may have been retained within the filter material, resulting in viral loss.

4.5 Further Work

4.5.1 Cell viability

The results depicted in *Figure 11A* provide promising evidence of a phenotype suitable for GeCKO screening in PCV2 infected PK-15 cells. However, it is important to note that further development and optimization of the experimental procedure are necessary, particularly when considering scaling up the experiment. Scaling up would involve an increased number of flasks containing cells with a low cell density to generate an adequate quantity of cells for the GeCKO screening process. Additionally, for a successful scale-up, it becomes imperative to acquire a new high concentrated batch of virus. This consideration arises from the fact that our current replication method is insufficient to generate the required virus concentration essential for expanded experiment.

4.5.2 Actin filament changes

Although we were unable to repeat the experiment due to time constraints, there are several modifications that could potentially enhance the results. Specifically, I recommend increasing the concentration of Triton X-100 used and duration of the permeabilization step, as well as doubling the concentration of DAPI staining and considering a higher concentration of Alexa Flour™ 488 phalloidin to improve the intensity of the fluorescence signals. It should be considered to increase the staining duration as well. Considering the complexity of the immunofluorescent staining, it may be beneficial to simplify the experiment by eliminating the blocking and antibody staining steps. This modification could reduce the number of potential sources of error and improve the reproducibility of the results. Additionally, a lower concentration of Triton X-100 in the staining solution could help to ensure that the staining reaches the inside of the cells. These modifications should be carefully evaluated in future studies to determine their effectiveness in improving the quality and reproducibility of the experimental results.

4.5.3 Cultivation of PCV2

For PCV2 cultivation, it might be worth trying to increase the period of infection to enhance viral replication. However, a method of removing viruses after a specific period is often employed to reduce background noise and prevent potential cytotoxic effects associated with a high viral load. It can be considered testing different time points for virus removal to determine the optimal conditions for PCV2 replication in PK-15 cells. Additionally, other factors may improve viral replication, such as optimizing cell culture conditions, using different virus concentrations, or employing alternative infection strategies.

According to Merck, the recommended pore size for viruses measuring 17 nm in diameter is 50kDa, with a recommended diameter range of 15 to 30 nm (*Virus Concentration by Ultrafiltration*, n.d.). Therefore, it could be worthwhile to test the same method using 50kDa ultrafiltration cutoff columns to achieve higher virus titers for downstream experiments. To enhance virus concentration efficiency and minimize virus loss, it is crucial to optimize the ultrafiltration method by testing different pore sizes and exploring alternative concentration techniques, such as ultracentrifugation. Ultracentrifugation, a high-speed centrifugation at approximately 30 000-100 000xg, can be used together with a low-density gradient such as sucrose or glycerol gradient to create a concentrated virus pellet (Eskelin, 2021; Homberger, 1994; Payne, 2017; Ueba, 1978). However, this requires specialized equipment. Additionally, the process can be time-consuming and requires careful optimization to achieve the desired level of virus concentration and purity.

6 Conclusion

This study aimed to identify a cell line capable of exhibiting detectable cytopathic effects upon PCV2 infection, find a suitable FBS source free from BVDV contaminations, and develop a protocol for PCV2 cultivation in PK-15 cells. The findings and outcomes of this research will potentially be used as a part of the GeneInnovate project.

Firstly, the evaluation of cell viability as a phenotype for GeCKO screening in PCV2 infection experiments suggests that it is a suitable indicator of cytopathic effects. Differences in cell viability between infected and mock infected cells were observed, particularly at lower cell densities, indicating the presence of a viral-induced cytopathic effect. However, further optimization and scaling up of the experimental procedure are needed to ensure reproducibility and reliability for GeCKO screening applications.

Secondly, the immunofluorescent staining experiment using Alexa Fluor™ Phalloidin 488 and DAPI, along with virus staining, was unsuccessful in this study. Possible factors contributing to the suboptimal staining results include inadequate fixation and permeabilization methods, insufficient blocking and washing steps, and potentially low concentrations of staining reagents. Optimization of these factors, such as using a higher concentration of permeabilization agent, thorough washing, and titration of staining reagent concentrations, may improve the staining results. Previous studies have demonstrated the potential of detecting cytopathic effects of PCV2 infection through F-actin staining, providing a potential target for GeCKO screening using flow cytometry. However, further optimization and validation are needed to achieve the desired difference between infected and mock infected cells for successful GeCKO screening.

A summary of all findings using the PCV2 virus is presented in *Figure 13*, encompassing both the results from PK-15 experiments and potential outcomes using IPEC-J2.

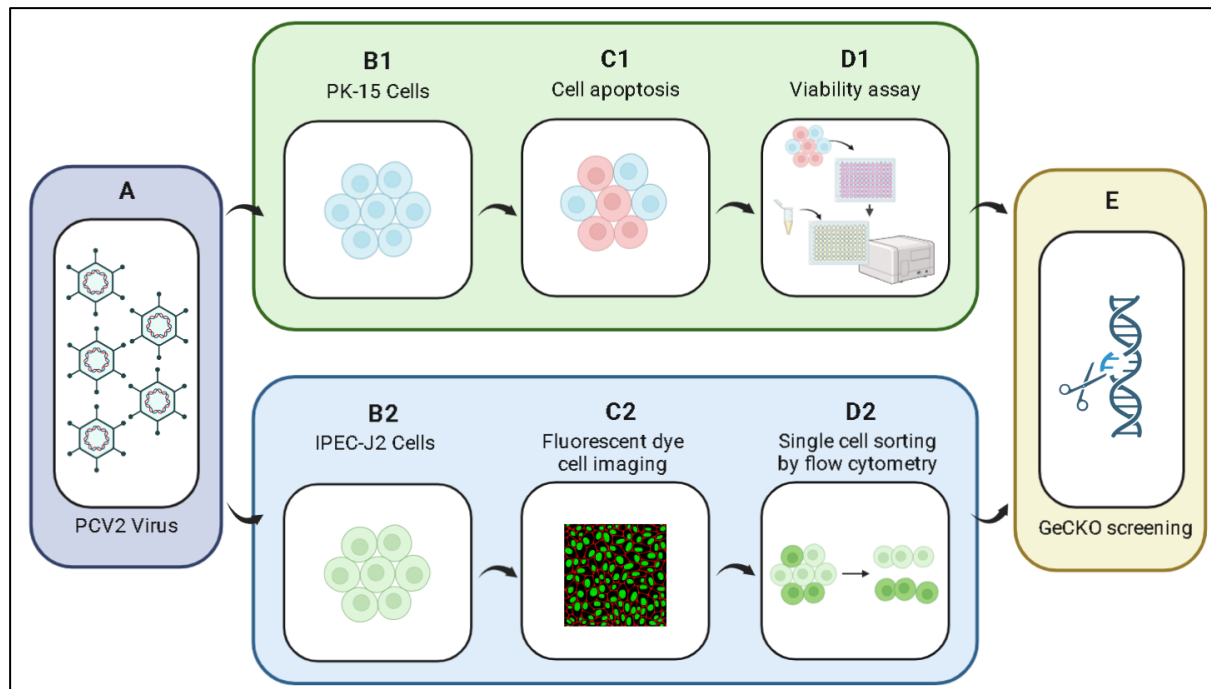


Figure 13 – Overview of the workflow for identifying a suitable cytopathic effect for GeCKO screening: PCV2 (A) was used to infect both PK-15 and IPEC-J2 cells. In PK-15 cells (B1), cell death was observed (C1), leading to the performance of a cell viability assay (D1). The cell viability assay confirmed that PCV2 induced cell death as a potential screenable cytopathic effect in PK-15 cells (E). In IPEC-J2 cells (B2), infection and staining attempts were made (C2) but were unsuccessful. Consequently, the staining protocol requires optimization before it can be used for flow cytometry to sort infected and non-infected cells into two distinct populations (D2). If successfully performed, this sorting method can potentially be applied in GeCKO screening (E).

Thirdly, the initial testing for BVDV contamination in MDBK cells grown with different FBS batches showed positive results, indicating a contamination problem. Subsequent testing using a BVDV free MDBK cell line confirmed FBS as the source of contamination. However, a BVDV-free batch of FBS was obtained from the providers of the BVDV free MDBK cell line, resolving the contamination issue for future research, including GeCKO screening.

Lastly, the observation of PK-15 cells infected with PCV2 revealed significant differences in cell growth and viability compared to mock infected cells, indicating the substantial impact of PCV2 infection on cellular health. Vacuolation in the cytoplasm of PCV2-infected cells further supported

the induction of apoptosis by viral infection. PCR and agarose gel electrophoresis confirmed the presence of PCV2 in infected PK-15 cells, with high specificity and reliability of the assay. Real-Time PCR demonstrated successful amplification of PCV2 viral DNA, with a standard curve exhibiting high efficiency and reliable reactions. Viral replication was observed in the infected cells, albeit at a slow rate, and the 1:10 dilution of the virus stock resulted in low and inconsistent viral DNA levels. However, cytopathic effects were still observed in both the original and diluted virus-infected cells. Concentrating the PCV2 virus stock using ultrafiltration showed increased virus concentration, but with significant virus loss during the process. Further optimization of concentration methods is necessary to enhance efficiency and minimize virus loss.

7 Bibliography

- 4.5: The Cytoskeleton. (2023). In *General Biology 1e (OpenStax)*.
[https://bio.libretexts.org/Bookshelves/Introductory_and_General_Biology/General_Biology_1e_\(OpenStax\)/2%3A_The_Cell/04%3A_Cell_Structure/4.5%3A_The_Cytoskeleton](https://bio.libretexts.org/Bookshelves/Introductory_and_General_Biology/General_Biology_1e_(OpenStax)/2%3A_The_Cell/04%3A_Cell_Structure/4.5%3A_The_Cytoskeleton)
- Alarcon, P., Rushton, J., & Wieland, B. (2013). Cost of post-weaning multi-systemic wasting syndrome and porcine circovirus type-2 subclinical infection in England - an economic disease model. *Prev Vet Med*, 110(2), 88-102. <https://doi.org/10.1016/j.prevetmed.2013.02.010>
- Allan, G. M., Kennedy, S., McNeilly, F., Foster, J. C., Ellis, J. A., Krakowka, S. J., Meehan, B. M., & Adair, B. M. (1999). Experimental reproduction of severe wasting disease by co-infection of pigs with porcine circovirus and porcine parvovirus. *J Comp Pathol*, 121(1), 1-11.
<https://doi.org/10.1053/jcpa.1998.0295>
- Allan, G. M., McNeilly, F., Ellis, J., Krakowka, S., Meehan, B., McNair, I., Walker, I., & Kennedy, S. (2000). Experimental infection of colostrum deprived piglets with porcine circovirus 2 (PCV2) and porcine reproductive and respiratory syndrome virus (PRRSV) potentiates PCV2 replication. *Arch Virol*, 145(11), 2421-2429. <https://doi.org/10.1007/s007050070031>
- Allan, G. M., McNeilly, F., Ellis, J., Krakowka, S., Meehan, B., McNair, I., & Walker, I. (1998). Experimental infection of colostrum deprived piglets with porcine circovirus 2 (PCV2) and porcine reproductive and respiratory syndrome virus (PRRSV) potentiates PCV2 replication. *Canadian Veterinary Journal*, 39(1), 44-51.
- Anderson, D. J., & Le Grand, R. (2014). Cell-associated HIV mucosal transmission: the neglected pathway. *J Infect Dis*, 210 Suppl 3(Suppl 3), S606-608. <https://doi.org/10.1093/infdis/jiu538>
- Annie Zhang Bargsten, I. R. (2020). *The first step to a successful CRISPR screen: Making the right choice between arrayed or pooled library*. <https://horizondiscovery.com/en/blog/2020/arrayed-vs-pooled-CRISPR-screening>
- Baer, A., & Kehn-Hall, K. (2014). Viral concentration determination through plaque assays: using traditional and novel overlay systems. *J Vis Exp*(93), e52065. <https://doi.org/10.3791/52065>
- Barber, G. N. (2001). Host defense, viruses and apoptosis. *Cell Death Differ*, 8(2), 113-126.
<https://doi.org/10.1038/sj.cdd.4400823>
- Bivins, A., Kaya, D., Bibby, K., Simpson, S. L., Bustin, S. A., Shanks, O. C., & Ahmed, W. (2021). Variability in RT-qPCR assay parameters indicates unreliable SARS-CoV-2 RNA quantification for wastewater surveillance. *Water Res*, 203, 117516. <https://doi.org/10.1016/j.watres.2021.117516>
- Bock, C., Datlinger, P., Chardon, F., Coelho, M. A., Dong, M. B., Lawson, K. A., Lu, T., Maroc, L., Norman, T. M., Song, B., Stanley, G., Chen, S., Garnett, M., Li, W., Moffat, J., Qi, L. S., Shapiro, R. S., Shendure, J., Weissman, J. S., & Zhuang, X. (2022). High-content CRISPR screening. *Nature Reviews Methods Primers*, 2(1). <https://doi.org/10.1038/s43586-021-00093-4>
- Bolin, S. R., Matthews, P. J., & Ridpath, J. F. (1991). Methods for detection and frequency of contamination of fetal calf serum with bovine viral diarrhoea virus and antibodies against bovine viral diarrhoea virus. *J Vet Diagn Invest*, 3(3), 199-203.
<https://doi.org/10.1177/104063879100300302>
- Bolin, S. R., Stoffregen, W. C., Nayar, G. P., & Hamel, A. L. (2001). Postweaning multisystemic wasting syndrome induced after experimental inoculation of cesarean-derived, colostrum-deprived piglets with type 2 porcine circovirus. *J Vet Diagn Invest*, 13(3), 185-194.
<https://doi.org/10.1177/104063870101300301>
- Brosnahan, A. J., & Brown, D. R. (2012). Porcine IPEC-J2 intestinal epithelial cells in microbiological investigations. *Vet Microbiol*, 156(3-4), 229-237. <https://doi.org/10.1016/j.vetmic.2011.10.017>
- Brunstein, J. (2013). *Process controls: internal and external*. <https://www.mlo-online.com/home/article/13005863/process-controls-internal-and-external>

- Bürki, F., König, H., & Schmid, H. R. (1964). Kasuistischer Beitrag zur Mucosal Disease. Isolierung des Virus der bovinen Virus-Diarrhöe aus einem typischen Fall. *Schweiz Arch Tierheilkd*, *106*, 473-477.
- Carr, J., Williams, D. G., & Hayden, R. T. (2010). Molecular Detection of Multiple Respiratory Viruses. In *Molecular Diagnostics* (pp. 289-300). Academic Press. <https://doi.org/10.1016/b978-0-12-369428-7.00024-0>
- CellSaurus PK-15 (CVCL_2160). (2023). https://www.cellosaurus.org/CVCL_2160
- CellTiter-Glo® Luminescent Cell Viability Assay. (2023). <https://ch.promega.com/-/media/files/resources/protocols/technical-bulletins/0/celltiter-glo-luminescent-cell-viability-assay-protocol.pdf>
- Chen, H. C., Kuo, T. Y., Yang, Y. C., Wu, C. C., & Lai, S. S. (2013). Highly permissive subclone of the porcine kidney cell line for porcine circovirus type 2 production. *J Virol Methods*, *187*(2), 380-383. <https://doi.org/10.1016/j.jviromet.2012.11.013>
- Childs, T. (1946). X disease of Cattle—Saskatchewan. *Canadian journal of comparative medicine and veterinary science*, *10*(11), 316.
- Cruz, T. F., & Araujo, J. P., Jr. (2014). Cultivation of PCV2 in swine testicle cells using the shell vial technique and monitoring of viral replication by qPCR and RT-qPCR. *J Virol Methods*, *196*, 82-85. <https://doi.org/10.1016/j.jviromet.2013.10.025>
- Cui, H., Liang, W., Wang, D., Guo, K., & Zhang, Y. (2019). Establishment and Characterization of an Immortalized Porcine Oral Mucosal Epithelial Cell Line as a Cytopathogenic Model for Porcine Circovirus 2 Infection. *Front Cell Infect Microbiol*, *9*, 171. <https://doi.org/10.3389/fcimb.2019.00171>
- Cytoskeleton. (2022). *Encyclopedia Britannica*. <https://www.britannica.com/science/cytoskeleton>
- da Silva Silveira, C., Maya, L., Casaux, M. L., Schild, C., Caffarena, D., Araoz, V., da Costa, R. A., Macias-Rioseco, M., Perdomo, Y., Castells, M., Colina, R., Fraga, M., Riet-Correa, F., & Giannitti, F. (2020). Diseases associated with bovine viral diarrhea virus subtypes 1a and 2b in beef and dairy cattle in Uruguay. *Braz J Microbiol*, *51*(1), 357-368. <https://doi.org/10.1007/s42770-019-00170-7>
- Dede, M., McLaughlin, M., Kim, E., & Hart, T. (2020). Multiplex enCas12a screens detect functional buffering among paralogs otherwise masked in monogenic Cas9 knockout screens. *Genome Biol*, *21*(1), 262. <https://doi.org/10.1186/s13059-020-02173-2>
- Downey, N. (2016). *Interpreting melt curves: An indicator, not a diagnosis*. Coralville. <http://www.science.smith.edu/cmbs/wp-content/uploads/sites/36/2015/09/Interpreting-melt-curves.pdf>
- Driskell, E. A., & Ridpath, J. F. (2006). A survey of bovine viral diarrhea virus testing in diagnostic laboratories in the United States from 2004 to 2005. *Journal of veterinary diagnostic investigation* (18(6)), 600-605.
- Fang, C. Y., Wu, C. C., Fang, C. L., Chen, W. Y., & Chen, C. L. (2017). Long-term growth comparison studies of FBS and FBS alternatives in six head and neck cell lines. *PLoS One*, *12*(6), e0178960. <https://doi.org/10.1371/journal.pone.0178960>
- Faurez, F., Dory, D., Grasland, B., & Jestin, A. (2009). Replication of porcine circoviruses. *Virology*, *6*, 60. <https://doi.org/10.1186/1743-422X-6-60>
- Fay, P. C., Cook, C. G., Wijesiriwardana, N., Tore, G., Comtet, L., Carpentier, A., Shih, B., Freimanis, G., Haga, I. R., & Beard, P. M. (2020). Madin-Darby bovine kidney (MDBK) cells are a suitable cell line for the propagation and study of the bovine poxvirus lumpy skin disease virus. *J Virol Methods*, *285*, 113943. <https://doi.org/10.1016/j.jviromet.2020.113943>
- Fensterbusch, T., Steinfeldt, T., Caliskan, R., & Mankertz, A. (2005). Analysis of the subcellular localization of the proteins Rep, Rep¹ and Cap of porcine circovirus type 1. *Virology*, *343*(1), 36-46. <https://doi.org/10.1016/j.virol.2005.08.021>

- Fort, M., Sibila, M., Nofrarias, M., Perez-Martin, E., Olvera, A., Mateu, E., & Segales, J. (2012). Evaluation of cell-mediated immune responses against porcine circovirus type 2 (PCV2) Cap and Rep proteins after vaccination with a commercial PCV2 sub-unit vaccine. *Vet Immunol Immunopathol*, *150*(1-2), 128-132. <https://doi.org/10.1016/j.vetimm.2012.09.001>
- Fort, M., Sibila, M., Perez-Martin, E., Nofrarias, M., Mateu, E., & Segales, J. (2009). One dose of a porcine circovirus 2 (PCV2) sub-unit vaccine administered to 3-week-old conventional piglets elicits cell-mediated immunity and significantly reduces PCV2 viremia in an experimental model. *Vaccine*, *27*(30), 4031-4037. <https://doi.org/10.1016/j.vaccine.2009.04.028>
- Gao, Y., Wang, S., Du, R., Wang, Q., Sun, C., Wang, N., Zhang, P., & Zhang, L. (2011). Isolation and identification of a bovine viral diarrhoea virus from sika deer in china. *Virology*, *8*, 83. <https://doi.org/10.1186/1743-422X-8-83>
- Gilpin, D. F., McCullough, K., Meehan, B. M., McNeilly, F., McNair, I., Stevenson, L. S., Foster, J. C., Ellis, J. A., Krakowka, S., Adair, B. M., & Allan, G. M. (2003). In vitro studies on the infection and replication of porcine circovirus type 2 in cells of the porcine immune system. *Vet Immunol Immunopathol*, *94*(3-4), 149-161. [https://doi.org/10.1016/s0165-2427\(03\)00087-4](https://doi.org/10.1016/s0165-2427(03)00087-4)
- Green, M. R., & Sambrook, J. (2019). Nested Polymerase Chain Reaction (PCR). *Cold Spring Harb Protoc*, *2019*(2). <https://doi.org/10.1101/pdb.prot095182>
- Harms, P. A., Sorden, S. D., Halbur, P. G., Bolin, S. R., Lager, K. M., Morozov, I., & Paul, P. S. (2001). Experimental reproduction of severe disease in CD/CD pigs concurrently infected with type 2 porcine circovirus and porcine reproductive and respiratory syndrome virus. *Vet Pathol*, *38*(5), 528-539. <https://doi.org/10.1354/vp.38-5-528>
- Heaton, N. S. (2017). Revisiting the concept of a cytopathic viral infection. *PLoS Pathog*, *13*(7), e1006409. <https://doi.org/10.1371/journal.ppat.1006409>
- Hosono, S., Shiokawa, M., Kobayashi, T., Fukusho, A., & Aoki, H. (2019). Porcine circovirus type 2 induces a strong cytopathic effect in the serum-free culture cell line CPK-NS. *J Virol Methods*, *273*, 113706. <https://doi.org/10.1016/j.jviromet.2019.113706>
- Houe, H. (2003). Economic impact of BVDV infection in dairies. *Biologicals*, *31*(2), 137-143. [https://doi.org/10.1016/s1045-1056\(03\)00030-7](https://doi.org/10.1016/s1045-1056(03)00030-7)
- Hu, Y., Cai, X., Zhan, Y., Yuan, X., Liu, T., Tan, L., Li, Y., Zhang, L., Yang, L., Liu, W., Deng, Z., Wang, N., Yang, Y., Guo, S., & Wang, A. (2019). Truncated Rep protein of porcine circovirus 2 (PCV2) caused by a naturally occurring mutation reduced virus replication in PK15 cells. *BMC Vet Res*, *15*(1), 248. <https://doi.org/10.1186/s12917-019-1984-8>
- Hua, T., Zhang, X., Tang, B., Chang, C., Liu, G., Feng, L., Yu, Y., Zhang, D., & Hou, J. (2018). Tween-20 transiently changes the surface morphology of PK-15 cells and improves PCV2 infection. *BMC Vet Res*, *14*(1), 138. <https://doi.org/10.1186/s12917-018-1457-5>
- Huang, L., Van Renne, N., Liu, C., & Nauwynck, H. J. (2015). A sequence of basic residues in the porcine circovirus type 2 capsid protein is crucial for its co-expression and co-localization with the replication protein. *J Gen Virol*, *96*(12), 3566-3576. <https://doi.org/10.1099/jgv.0.000302>
- Jedrzejczak-Silicka, M. (2017). History of Cell Culture. *New Insights into Cell Culture Technology*. <https://doi.org/10.5772/66905>
- Jiang, S., Li, F., Li, X., Wang, L., Zhang, L., Lu, C., Zheng, L., & Yan, M. (2019). Transcriptome analysis of PK-15 cells in innate immune response to porcine deltacoronavirus infection. *PLoS One*, *14*(10), e0223177. <https://doi.org/10.1371/journal.pone.0223177>
- Jochems, C. E., van der Valk, J. B., Stafleu, F. R., & Baumans, V. (2002). The use of fetal bovine serum: ethical or scientific problem? *Altern Lab Anim*, *30*(2), 219-227. <https://doi.org/10.1177/026119290203000208>
- Kadir, Y., Christine, F., Barbara, B. W., Zeki, Y., Feray, A., Aykut, O., Ibrahim, B., Sibilina Cedillo, R., Heinz-Jurgen, T., & Matthias, K. (2008). Genetic heterogeneity of bovine viral diarrhoea virus (BVDV)

- isolates from Turkey: identification of a new subgroup in BVDV-1. *Vet Microbiol*, 130(3-4), 258-267. <https://doi.org/10.1016/j.vetmic.2008.01.016>
- Kamen, A., & Henry, O. (2004). Development and optimization of an adenovirus production process. *J Gene Med*, 6 Suppl 1, S184-192. <https://doi.org/10.1002/jgm.503>
- Karuppappan, A. K., Ramesh, A., Reddy, Y. K., Ramesh, S., Mahaprabhu, R., Jaisree, S., Roy, P., Sridhar, R., Pazhanivel, N., Sakthivelan, S. M., Sreekumar, C., Murugan, M., Jaishankar, S., Gopi, H., Purushothaman, V., Kumanan, K., & Babu, M. (2016). Emergence of Porcine Circovirus 2 Associated Reproductive Failure in Southern India. *Transbound Emerg Dis*, 63(3), 314-320. <https://doi.org/10.1111/tbed.12276>
- Keilová, H. (1948). The effect of streptomycin on tissue cultures. *Experientia*, 4(12), 483-484. <https://doi.org/10.1007/bf02164510>
- Kekarainen, T., McCullough, K., Fort, M., Fossum, C., Segales, J., & Allan, G. M. (2010). Immune responses and vaccine-induced immunity against Porcine circovirus type 2. *Vet Immunol Immunopathol*, 136(3-4), 185-193. <https://doi.org/10.1016/j.vetimm.2010.03.025>
- Kennedy, S., Moffett, D., McNeilly, F., Meehan, B., Ellis, J., Krakowka, S., & Allan, G. M. (2000). Reproduction of lesions of postweaning multisystemic wasting syndrome by infection of conventional pigs with porcine circovirus type 2 alone or in combination with porcine parvovirus. *J Comp Pathol*, 122(1), 9-24. <https://doi.org/10.1053/jcpa.1999.0337>
- Khodakaram-Tafti, A., & Farjanikish, G. H. (2017). Persistent bovine viral diarrhoea virus (BVDV) infection in cattle herds. *P. Iranian journal of veterinary research*, 18(3), 154-163.
- Koksharov, M. I., & Ugarova, N. N. (2011). Thermostabilization of firefly luciferase by in vivo directed evolution. *Protein Eng Des Sel*, 24(11), 835-844. <https://doi.org/10.1093/protein/gzr044>
- Krakowka, S., Ellis, J. A., Meehan, B., Kennedy, S., McNeilly, F., & Allan, G. (2000). Viral wasting syndrome of swine: experimental reproduction of postweaning multisystemic wasting syndrome in gnotobiotic swine by coinfection with porcine circovirus 2 and porcine parvovirus. *Vet Pathol*, 37(3), 254-263. <https://doi.org/10.1354/vp.37-3-254>
- Lanyon, S. R., Hill, F. I., Reichel, M. P., & Brownlie, J. (2014). Bovine viral diarrhoea: pathogenesis and diagnosis. *Vet J*, 199(2), 201-209. <https://doi.org/10.1016/j.tvjl.2013.07.024>
- Larochelle, R., Antaya, M., Morin, M., & Magar, R. (1999). Typing of porcine circovirus in clinical specimens by multiplex PCR. *Journal of Virological Methods*, 80(1), 69-75. [https://doi.org/10.1016/s0166-0934\(99\)00032-4](https://doi.org/10.1016/s0166-0934(99)00032-4)
- Louten, J. (2023). Vaccines, antivirals, and the beneficial uses of viruses. In *Essential Human Virology* (pp. 145-168). Academic Press. <https://doi.org/10.1016/b978-0-323-90565-7.00008-3>
- Mah, A. (2021). *Pooled Versus Arrayed Screens: Considerations Before Choosing a Screening Format*. <https://www.synthego.com/blog/pooled-versus-arrayed-screens-considerations-before-choosing-a-screening-format>
- Mariani, V., Palermo, S., Fiorentini, S., Lanubile, A., & Giuffra, E. (2009). Gene expression study of two widely used pig intestinal epithelial cell lines: IPEC-J2 and IPI-2I. *Vet Immunol Immunopathol*, 131(3-4), 278-284. <https://doi.org/10.1016/j.vetimm.2009.04.006>
- Matsumura, K., Hayashi, F., Nagashima, T., Rajan, R., & Hyon, S.-H. (2021). Molecular mechanisms of cell cryopreservation with polyampholytes studied by solid-state NMR. *Communications Materials*, 2(1). <https://doi.org/10.1038/s43246-021-00118-1>
- Meade, O., Clark, J., McCutchen, M., & Kerwin, J. (2021). Exploring the design space of AAV transient-transfection in suspension cell lines. *Methods Enzymol*, 660, 341-360. <https://doi.org/10.1016/bs.mie.2021.08.003>
- Meerts, P., Misinzo, G., McNeilly, F., & Nauwynck, H. J. (2005). Replication kinetics of different porcine circovirus 2 strains in PK-15 cells, fetal cardiomyocytes and macrophages. *Arch Virol*, 150(3), 427-441. <https://doi.org/10.1007/s00705-004-0444-2>

- Ménard, J. (2006). PMWS interventions preventive measures: Canadian approach. In
- Mettlen, M., Chen, P. H., Srinivasan, S., Danuser, G., & Schmid, S. L. (2018). Regulation of Clathrin-Mediated Endocytosis. *Annu Rev Biochem*, *87*, 871-896. <https://doi.org/10.1146/annurev-biochem-062917-012644>
- Miroslaw, P., Rola-Luszczak, M., Kuzmak, J., & Polak, M. P. (2022). Transcriptomic Analysis of MDBK Cells Infected with Cytopathic and Non-Cytopathic Strains of Bovine Viral Diarrhea Virus (BVDV). *Viruses*, *14*(6). <https://doi.org/10.3390/v14061276>
- Misinzio, G., Delputte, P. L., Lefebvre, D. J., & Nauwynck, H. J. (2009). Porcine circovirus 2 infection of epithelial cells is clathrin-, caveolae- and dynamin-independent, actin and Rho-GTPase-mediated, and enhanced by cholesterol depletion. *Virus Res*, *139*(1), 1-9. <https://doi.org/10.1016/j.virusres.2008.09.005>
- Misinzio, G., Delputte, P. L., Meerts, P., Lefebvre, D. J., & Nauwynck, H. J. (2006). Porcine circovirus 2 uses heparan sulfate and chondroitin sulfate B glycosaminoglycans as receptors for its attachment to host cells. *J Virol*, *80*(7), 3487-3494. <https://doi.org/10.1128/JVI.80.7.3487-3494.2006>
- Misinzio, G., Delputte, P. L., & Nauwynck, H. J. (2008). Inhibition of endosome-lysosome system acidification enhances porcine circovirus 2 infection of porcine epithelial cells. *J Virol*, *82*(3), 1128-1135. <https://doi.org/10.1128/JVI.01229-07>
- Misinzio, G., Meerts, P., Bublot, M., Mast, J., Weingartl, H. M., & Nauwynck, H. J. (2005). Binding and entry characteristics of porcine circovirus 2 in cells of the porcine monocytic line 3D4/31. *J Gen Virol*, *86*(Pt 7), 2057-2068. <https://doi.org/10.1099/vir.0.80652-0>
- Mo, Y., Wan, R., & Zhang, Q. (2012). Application of reverse transcription-PCR and real-time PCR in nanotoxicity research. *Methods Mol Biol*, *926*, 99-112. https://doi.org/10.1007/978-1-62703-002-1_7
- Moennig, V., & Becher, P. (2018). Control of Bovine Viral Diarrhea. *Pathogens*, *7*(1). <https://doi.org/10.3390/pathogens7010029>
- Neidler, S. (2017). What are the differences between PCR, RT-PCR, qPCR, and RT-qPCR? <https://www.enzolifesciences.com/science-center/technotes/2017/march/what-are-the-differences-between-pcr-rt-pcr-qpcr-and-rt-qpcr?/>
- Nuttall, P. A., Luther, P. D., & Stott, E. J. (1977). Viral contamination of bovine foetal serum and cell cultures. *Nature*, *266*(5605), 835-837. <https://doi.org/10.1038/266835a0>
- Ouyang, Y., & Nauwynck, H. J. (2023). PCV2 Uptake by Porcine Monocytes Is Strain-Dependent and Is Associated with Amino Acid Characteristics on the Capsid Surface. *Microbiol Spectr*, e0380522. <https://doi.org/10.1128/spectrum.03805-22>
- Payne, S. (2017). Methods to Study Viruses. *Viruses*, 37-52. <https://doi.org/10.1016/B978-0-12-803109-4.00004-0>
- Puck, T. T., Cieciura, S. J., & Robinson, A. (1958). Genetics of somatic mammalian cells. III. Long-term cultivation of euploid cells from human and animal subjects. *J Exp Med*, *108*(6), 945-956. <https://doi.org/10.1084/jem.108.6.945>
- Puschnik, A. S., Majzoub, K., Ooi, Y. S., & Carette, J. E. (2017). A CRISPR toolbox to study virus-host interactions. *Nat Rev Microbiol*, *15*(6), 351-364. <https://doi.org/10.1038/nrmicro.2017.29>
- Ramamoorthy, S., & Pineyro, P. (2019). Porcine Circoviruses. In *Porcine Viruses: From Pathogenesis to Strategies for Control* (pp. 81-106). <https://doi.org/10.21775/9781910190913.04>
- Rayaprolu, V., Ramsey, J., Wang, J. C., & Mukhopadhyay, S. (2018). Alphavirus Purification Using Low-speed Spin Centrifugation. *Bio Protoc*, *8*(6), e2772. <https://doi.org/10.21769/BioProtoc.2772>
- Real-Time PCR Application Guide*. (2006). https://www.bio-rad.com/webroot/web/pdf/lsr/literature/Bulletin_5279.pdf
- Riss TL, M. R., Niles AL, et al. . (2013). *Cell Viability Assays*. <https://www.ncbi.nlm.nih.gov/books/NBK144065/>

- Rodriguez-Arrioja, G. M., Segales, J., Calsamiglia, M., Resendes, A. R., Balasch, M., Plana-Duran, J., Casal, J., & Domingo, M. (2002). Dynamics of porcine circovirus type 2 infection in a herd of pigs with postweaning multisystemic wasting syndrome. *Am J Vet Res*, 63(3), 354-357. <https://doi.org/10.2460/ajvr.2002.63.354>
- Saif, L. J., Heckert, R. A., Miller, K. L., & Tarek, M. M. (1988). Cell culture propagation of bovine coronavirus. *J Tissue Cult Methods*, 11(3), 139-145. <https://doi.org/10.1007/bf01404267>
- Samuel, C. E. (2001). Antiviral actions of interferons. *Clin Microbiol Rev*, 14(4), 778-809, table of contents. <https://doi.org/10.1128/CMR.14.4.778-809.2001>
- Segales, J. (2012). Porcine circovirus type 2 (PCV2) infections: clinical signs, pathology and laboratory diagnosis. *Virus Res*, 164(1-2), 10-19. <https://doi.org/10.1016/j.virusres.2011.10.007>
- Segales, J., & Domingo, M. (2002). Postweaning multisystemic wasting syndrome (PMWS) in pigs. A review. *Vet Q*, 24(3), 109-124. <https://doi.org/10.1080/01652176.2002.9695132>
- Segeritz, C. P., & Vallier, L. (2017). Cell Culture: Growing Cells as Model Systems In Vitro. In *Basic Science Methods for Clinical Researchers* (pp. 151–172). <https://doi.org/10.1016/B978-0-12-803077-6.00009-6>
- Shubin, A. V., Demidyuk, I. V., Komissarov, A. A., Rafieva, L. M., & Kostrov, S. V. (2016). Cytoplasmic vacuolization in cell death and survival. *Oncotarget*, 7(34), 55863-55889. <https://doi.org/10.18632/oncotarget.10150>
- Synthego. (n.d.). *CRISPR Screening 101 - Strategies for Target Identification* <https://hubs.ly/H0pBGTk0>
- Taylor, M. P., Koyuncu, O. O., & Enquist, L. W. (2011). Subversion of the actin cytoskeleton during viral infection. *Nat Rev Microbiol*, 9(6), 427-439. <https://doi.org/10.1038/nrmicro2574>
- Tischer, I., Peters, D., Rasch, R., & Pociuli, S. (1987). Replication of porcine circovirus: induction by glucosamine and cell cycle dependence. *Arch Virol*, 96(1-2), 39-57. <https://doi.org/10.1007/BF01310989>
- Tischer, I., Rasch, R., & Tochtermann, G. (1974). Characterization of papovavirus-and picornavirus-like particles in permanent pig kidney cell lines. . In *Zentralblatt fur Bakteriologie, Parasitenkunde, Infektionskrankheiten und Hygiene. Erste Abteilung Originale. Reihe A: Medizinische Mikrobiologie und Parasitologie* (Vol. 2, pp. 153–167).
- Udayangani, D. S. (2021). *Difference Between Immortalized and Transformed Cells*. <https://www.differencebetween.com/difference-between-immortalized-and-transformed-cells/>
- Vergauwen, H. (2015). The IPEC-J2 cell line. In K. Verhoeckx, P. Cotter, I. Lopez-Exposito, C. Kleiveland, T. Lea, A. Mackie, T. Requena, D. Swiatecka, & H. Wichers (Eds.), *The Impact of Food Bioactives on Health: in vitro and ex vivo models* (pp. 125-134). <https://doi.org/10.1007/978-3-319-16104-4>
- Virus Concentration by Ultrafiltration*. (n.d.). <https://www.sigmaaldrich.com/NO/en/technical-documents/technical-article/analytical-chemistry/filtration/viral-concentration-amicon-ultrafiltration>
- Wang, H., La Russa, M., & Qi, L. S. (2016). CRISPR/Cas9 in Genome Editing and Beyond. *Annu Rev Biochem*, 85, 227-264. <https://doi.org/10.1146/annurev-biochem-060815-014607>
- Wang, J. C., Chen, C., Rayaprolu, V., Mukhopadhyay, S., & Zlotnick, A. (2015). Self-Assembly of an Alphavirus Core-like Particle Is Distinguished by Strong Intersubunit Association Energy and Structural Defects. *ACS Nano*, 9(9), 8898-8906. <https://doi.org/10.1021/acs.nano.5b02632>
- Wang, P., Huang, S., Hao, C., Wang, Z., Zhao, H., Liu, M., Tian, X., Ge, L., Wu, W., & Peng, C. (2021). Establishment of a Suspension MDBK Cell Line in Serum-Free Medium for Production of Bovine Alphaherpesvirus-1. *Vaccines (Basel)*, 9(9). <https://doi.org/10.3390/vaccines9091006>
- Wang, S., Li, C., Sun, P., Shi, J., Wu, X., Liu, C., Peng, Z., Han, H., Xu, S., Yang, Y., Tian, Y., Li, J., He, H., Li, J., & Wang, Z. (2021). PCV2 Triggers PK-15 Cell Apoptosis Through the PLC-IP3R-Ca(2+) Signaling Pathway. *Front Microbiol*, 12, 674907. <https://doi.org/10.3389/fmicb.2021.674907>

- Wang, T. E., Chao, T. L., Tsai, H. T., Lin, P. H., Tsai, Y. L., & Chang, S. Y. (2020). Differentiation of Cytopathic Effects (CPE) induced by influenza virus infection using deep Convolutional Neural Networks (CNN). *PLoS Comput Biol*, *16*(5), e1007883. <https://doi.org/10.1371/journal.pcbi.1007883>
- Xia, H., Vijayaraghavan, B., Belak, S., & Liu, L. (2011). Detection and identification of the atypical bovine pestiviruses in commercial foetal bovine serum batches. *PLoS One*, *6*(12), e28553. <https://doi.org/10.1371/journal.pone.0028553>
- Xu, Y., & Li, Z. (2020). CRISPR-Cas systems: Overview, innovations and applications in human disease research and gene therapy. *Comput Struct Biotechnol J*, *18*, 2401-2415. <https://doi.org/10.1016/j.csbj.2020.08.031>
- Yan, M., Zhu, L., & Yang, Q. (2014). Infection of porcine circovirus 2 (PCV2) in intestinal porcine epithelial cell line (IPEC-J2) and interaction between PCV2 and IPEC-J2 microfilaments. *Virology*, *11*, 193. <https://doi.org/10.1186/s12985-014-0193-0>
- Yang, N., Garcia, A., Meyer, C., Tuschl, T., Merghoub, T., Wolchok, J. D., & Deng, L. (2022). Heat-inactivated modified vaccinia virus Ankara boosts Th1 cellular and humoral immunity as a vaccine adjuvant. *NPJ Vaccines*, *7*(1), 120. <https://doi.org/10.1038/s41541-022-00542-5>
- Yang, X., Chen, F., Cao, Y., Pang, D., Ouyang, H., & Ren, L. (2013). Comparative analysis of different methods to enhance porcine circovirus 2 replication. *J Virol Methods*, *187*(2), 368-371. <https://doi.org/10.1016/j.jviromet.2012.11.001>
- Yarnall, M. J., & Thrusfield, M. V. (2017). Engaging veterinarians and farmers in eradicating bovine viral diarrhoea: a systematic review of economic impact. *Vet Rec*, *181*(13), 347. <https://doi.org/10.1136/vr.104370>
- Yitagesu, E., Jackson, W., Kebede, N., Smith, W., & Fentie, T. (2021). Prevalence of bovine abortion, calf mortality, and bovine viral diarrhoea virus (BVDV) persistently infected calves among pastoral, peri-urban, and mixed-crop livestock farms in central and Northwest Ethiopia. *BMC Vet Res*, *17*(1), 87. <https://doi.org/10.1186/s12917-021-02798-w>
- Yu, J. S. L., & Yusa, K. (2019). Genome-wide CRISPR-Cas9 screening in mammalian cells. *Methods*, *164-165*, 29-35. <https://doi.org/10.1016/j.ymeth.2019.04.015>
- Yuan, C., Sun, L., Chen, L., Li, L., Yao, Z., Wang, Y., Guo, H., Li, T., & Song, Q. (2022). Differences in cytokines expression between Vero cells and IPEC-J2 cells infected with porcine epidemic diarrhoea virus. *Front Microbiol*, *13*, 1002349. <https://doi.org/10.3389/fmicb.2022.1002349>
- Zabal, O., Kobrak, A. L., Lager, I. A., Schudel, A. A., & Weber, E. L. (2000). Contaminación del suero fetal bovino con virus de la diarrea viral bovina [Contamination of bovine fetal serum with bovine viral diarrhoea virus]. *32*(1), 27-32.
- Zhu, Y., Feng, F., Hu, G., Wang, Y., Yu, Y., Zhu, Y., Xu, W., Cai, X., Sun, Z., Han, W., Ye, R., Qu, D., Ding, Q., Huang, X., Chen, H., Xu, W., Xie, Y., Cai, Q., Yuan, Z., & Zhang, R. (2021). A genome-wide CRISPR screen identifies host factors that regulate SARS-CoV-2 entry. *Nat Commun*, *12*(1), 961. <https://doi.org/10.1038/s41467-021-21213-4>
- Zhu, Y., Lau, A., Lau, J., Jia, Q., Karuppanan, A. K., & Kwang, J. (2007). Enhanced replication of porcine circovirus type 2 (PCV2) in a homogeneous subpopulation of PK15 cell line. *Virology*, *369*(2), 423-430. <https://doi.org/10.1016/j.virol.2007.08.014>

Appendix A: Cell lines, Materials, Reagents, and Instruments

Tabell 1 - Cell lines and virus used during this study.

Cell line	Supplier
MDBK	ATCC – CCL-22
PK-15	ATCC – CCL-33
IPEC-J2	Lab collection
Virus	Supplier
PCV2	Professor Lars E. Larsen

Tabell 2 - Cell culturing products used during this study.

Product	Supplier	Reference number
Dulbecco's Modified Eagles Medium (DMEM) – high glucose	SIGMA-ALDRICH	D6429-500ML
FBS Gold Plus – Very Low Endotoxin – Chromatographiert	Bio&SELL	FBS.GP.0500
Fetal Bovine Serum	SIGMA-ALDRICH	F7524
Penicillin-Streptomycin (10,000 U/mL)	Thermo Fisher Scientific	15140122
Trypsin-EDTA (0.25%), phenol red	Thermo Fisher Scientific	2520072
Phosphate buffered saline	SIGMA-ALDRICH	P3813
Dimethyl sulfoxide	SIGMA-ALDRICH	41639
Fetal Bovine Serum	SIGMA-ALDRICH	F2442
Fetal Bovine Serum, certified, United States	Gibco	16000-044
HyClone Characterized Fetal Bovine Serum (FBS), U.S. Origin	Cytiva/HyClone	SH30071.03

Tabell 3 - Materials and reagents used in diverse methods during this project.

Product	Supplier	Reference number
Mr. Frosty™ Freezing Container	Thermo Fisher Scientific	5100-0036
Cell scraper, 2-position blade, size: S	Sarstedt	83.3950
0.45 µm pore size Filtropur S syringe filter	Sarstedt	83.1826
BD Luer-Lok™ syringe, with concentric tip and PC barrel, 1mL	VWR	309628
Purelink™ Viral RNA/DNA Mini Kit	Thermo Fisher Scientific	12280-050
DNeasy Blood and tissue	Qiagen	69504
50x TAE Electrophoresis Buffer	Thermo Fisher Scientific	B49
Standard Agarose – Type LE	BioNordika	BN50004
Gel Loading Solution	SIGMA-ALDRICH	G7654
SsoAdvanced Universal SYBR® Green Supermix	BIO-RAD	1725271
Hard-Shell® PCR Plates, 96-Well, thin-wall	BIO-RAD	HSP9655
Amicon® Ultra-15 Centrifugal Filter Unit 10kDa	Merck Millipore	UFC901024
Amicon® Ultra-15 Centrifugal Filter Unit 100kDa	Merck Millipore	UFC910024
CellTiter-Glo® Luminescent Cell Viability Assay	Pomega	G7570
8 Well Chamber, removable	Ibidi	80841
Pierce™ 16% Formaldehyde (w/v), Methanol-free	Thermo Fisher Scientific	28906
TWEEN® 20	SIGMA-ALDRICH	P1379
Triton™ X-100	SIGMA-ALDRICH	X100
Skim Milk Powder	SIGMA-ALDRICH	70166
Porcine Circovirus Type 2 Capsid Polyclonal Antibody	Thermo Fisher Scientific	PA5-34969
Goat anti-Rabbit IgG (H+L) Highly Cross-Adsorbed Secondary Antibody, Alexa Fluor™ 647	Thermo Fisher Scientific	A-21245
Alexa Flour™ 488 phalloidin	Thermo Fisher Scientific	A12379
DAPI (4',6-Diamidino-2-Phenylindole, Dilactate)	Thermo Fisher Scientific	D3571
ProLong™ Diamond Antifade Mountant	Thermo Fisher Scientific	P36961
QIAGEN® OneStep RT-PCR Kit (100)	Qiagen	210212
QIAGEN® Fast Cycling PCR Kit (200)	Qiagen	203743

RNeasy mini kit	Qiagen	74104
-----------------	--------	-------

Tabell 4 - Instruments used during this project.

Product	Supplier
Countess™ 3 FL Automated Cell Counter	Thermo Fisher Scientific
IKA Digital Orbital Plate Shaker	IKA
Synergy H1 Hybrid Multi-Mode Reader	BioTek
EVOS M5000 Imaging System	Thermo Fisher Scientific
GeneAmp™ PCR system 9700	Applied Biosystems
Qubit 4 Fluorimeter	Thermo Fisher Scientific
NanoDrop™ 8000 Spectrophotometer	Thermo Fisher Scientific
Horizontal Electrophoresis Systems	BIO-RAD
PowerPac™ Basic Power Supply	BIO-RAD
ChemiDoc XRS+ Gel Imaging System	BIO-RAD
C1000 Touch™ Thermal Cycler CFX96™ Real-Time System	BIO-RAD

Appendix B: Real-time PCR raw data



02.12.2022: PCV2 infection in PK-15 cells.pcrd

02/22/2023 18:36

Protocol

1: 98.0°C for 3:00

2: 95.0°C for 0:15

3: 60.0°C for 1:00

Plate Read

4: GOTO 2, 39 more times

5: Melt Curve 65.0°C to 95.0°C: Increment 0.5°C 0:05

Plate Read

Quantification

Step #: 3

Analysis Mode: Fluorophore

Cq Determination: Single Threshold

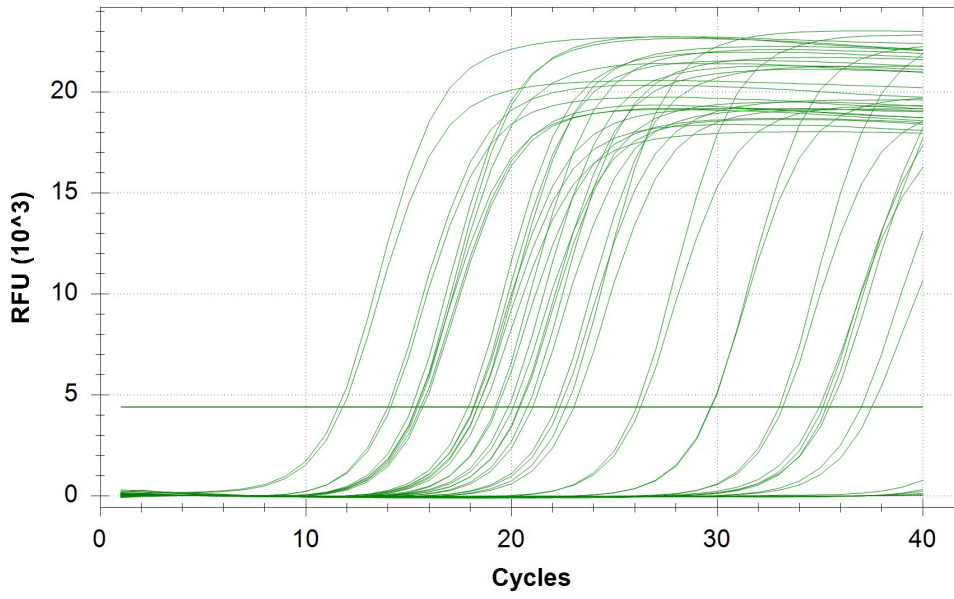
Baseline Method:

SYBR: Auto Calculated

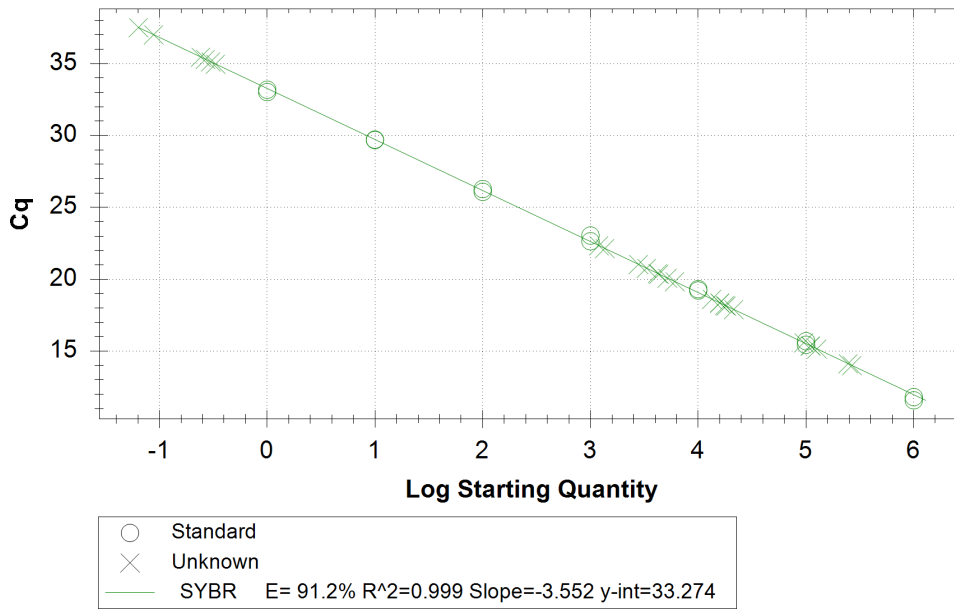
Threshold Setting:

SYBR: 4410.88, Auto Calculated

Amplification



Standard Curve



Quantification Data

Well	Fluor	Target	Content	Sample	Cq	Cq Mean	Cq Std. Dev	Starting Quantity (SQ)	Log Starting Quantity	SQ Mean	SQ Std. Dev
B04	SYBR	PCV2	Unkn-01	B1	18.62	18.49	0.182	1.340E+04	4.127	1.46E+04	1.72E+03
B05	SYBR	PCV2	Unkn-02	B2	18.19	18.04	0.204	1.771E+04	4.248	1.95E+04	2.58E+03
B06	SYBR	PCV2	Unkn-03	B3	15.59	15.48	0.157	9.545E+04	4.980	1.03E+05	1.05E+04
B07	SYBR	PCV2	Unkn-04	B4	15.36	15.26	0.148	1.104E+05	5.043	1.18E+05	1.14E+04
B08	SYBR	PCV2	Unkn-05	B5	14.13	14.07	0.089	2.459E+05	5.391	2.56E+05	1.48E+04
B09	SYBR	PCV2	NTC-01		N/A	0.00	0.000	N/A	N/A	0.00E+00	0.00E+00
B10	SYBR	PCV2	Neg Ctrl-01	PK-15	34.97	35.22	0.344	3.320E-01	-0.479	2.87E-01	6.35E-02
C04	SYBR	PCV2	Unkn-01	B1	18.36	18.49	0.182	1.584E+04	4.200	1.46E+04	1.72E+03
C05	SYBR	PCV2	Unkn-02	B2	17.90	18.04	0.204	2.136E+04	4.330	1.95E+04	2.58E+03
C06	SYBR	PCV2	Unkn-03	B3	15.36	15.48	0.157	1.103E+05	5.042	1.03E+05	1.05E+04
C07	SYBR	PCV2	Unkn-04	B4	15.15	15.26	0.148	1.265E+05	5.102	1.18E+05	1.14E+04
C08	SYBR	PCV2	Unkn-05	B5	14.00	14.07	0.089	2.668E+05	5.426	2.56E+05	1.48E+04
C09	SYBR	PCV2	NTC-01		N/A	0.00	0.000	N/A	N/A	0.00E+00	0.00E+00
C10	SYBR	PCV2	Neg Ctrl-01	PK-15	35.46	35.22	0.344	2.422E-01	-0.616	2.87E-01	6.35E-02
D03	SYBR	PCV2	Neg Ctrl-03	MDBK	37.52	37.27	0.353	6.397E-02	-1.194	7.62E-02	1.73E-02
D04	SYBR	PCV2	Unkn-06	D1	22.34	22.24	0.140	1.196E+03	3.078	1.28E+03	1.15E+02
D05	SYBR	PCV2	Unkn-07	D2	20.09	19.96	0.173	5.169E+03	3.713	5.61E+03	6.29E+02
D06	SYBR	PCV2	Unkn-08	D3	21.04	20.90	0.188	2.789E+03	3.445	3.05E+03	3.72E+02
D07	SYBR	PCV2	Unkn-09	D4	18.35	18.25	0.149	1.587E+04	4.201	1.70E+04	1.64E+03
D08	SYBR	PCV2	Unkn-10	D5	20.40	20.38	0.032	4.208E+03	3.624	4.27E+03	8.85E+01
D09	SYBR	PCV2	Neg Ctrl-02	Mock infection	35.13	35.22	0.123	2.998E-01	-0.523	2.84E-01	2.27E-02
D10	SYBR		Std-01	Original PCV2	11.80	11.69	0.159	1.000E+06	6.000	1.00E+06	0.00E+00
E03	SYBR	PCV2	Neg Ctrl-03	MDBK	37.02	37.27	0.353	8.843E-02	-1.053	7.62E-02	1.73E-02
E04	SYBR	PCV2	Unkn-06	D1	22.15	22.24	0.140	1.360E+03	3.133	1.28E+03	1.15E+02

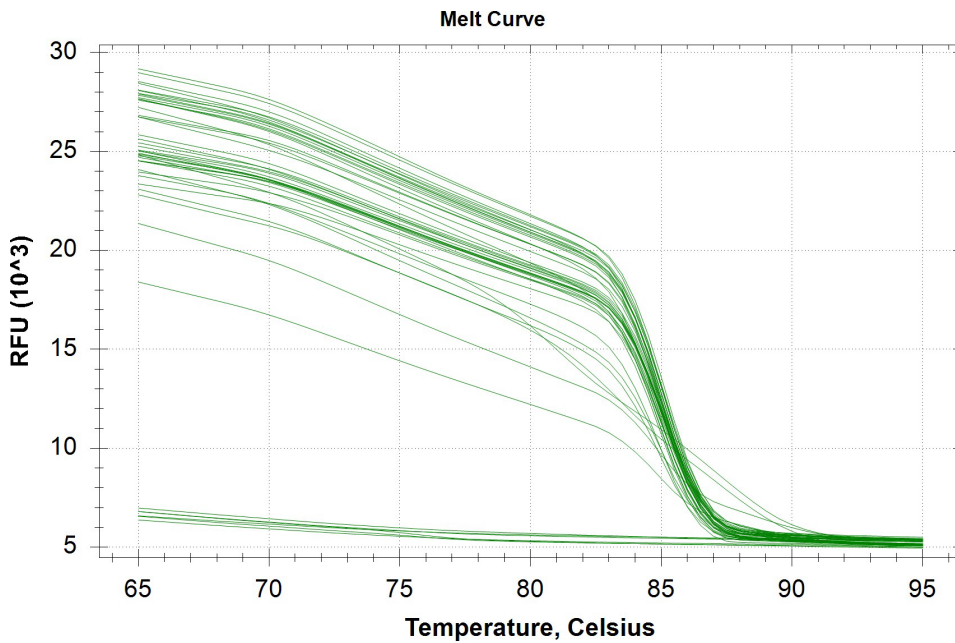
Quantification Data

Well	Fluor	Target	Content	Sample	Cq	Cq Mean	Cq Std. Dev	Starting Quantity (SQ)	Log Starting Quantity	SQ Mean	SQ Std. Dev
E05	SYBR	PCV2	Unkn-07	D2	19.84	19.96	0.173	6.059E+03	3.782	5.61E+03	6.29E+02
E06	SYBR	PCV2	Unkn-08	D3	20.77	20.90	0.188	3.315E+03	3.521	3.05E+03	3.72E+02
E07	SYBR	PCV2	Unkn-09	D4	18.14	18.25	0.149	1.819E+04	4.260	1.70E+04	1.64E+03
E08	SYBR	PCV2	Unkn-10	D5	20.36	20.38	0.032	4.333E+03	3.637	4.27E+03	8.85E+01

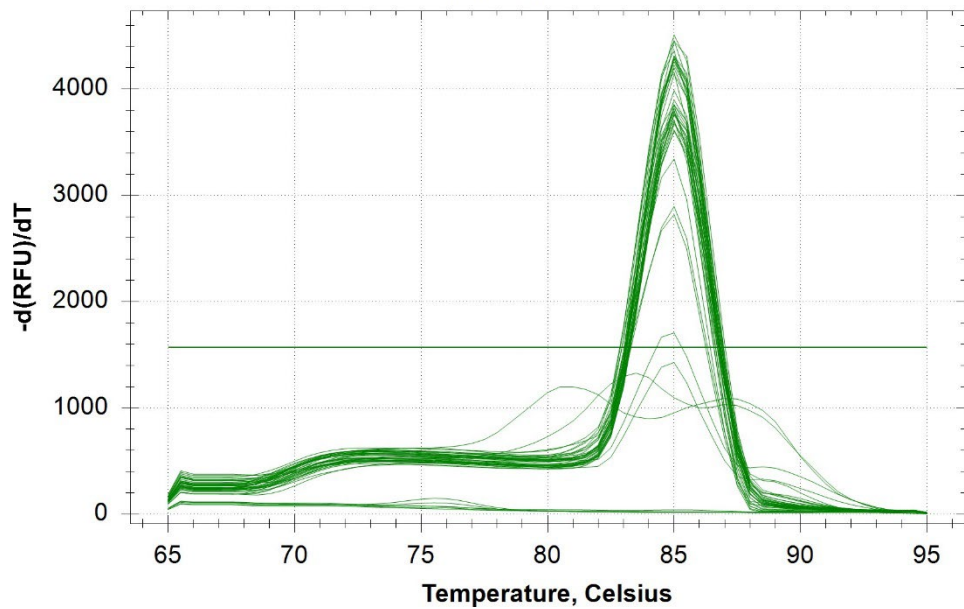
E09	SYBR	PCV2	Neg Ctrl-02	Mock infection	35.31	35.22	0.123	2.677E-01	-0.572	2.84E-01	2.27E-02
E10	SYBR		Std-01	Original PCV2	11.57	11.69	0.159	1.000E+06	6.000	1.00E+06	0.00E+00
F03	SYBR		Std-02		15.69	15.56	0.177	1.000E+05	5.000	1.00E+05	0.00E+00
F04	SYBR		Std-03		19.31	19.26	0.068	1.000E+04	4.000	1.00E+04	0.00E+00
F05	SYBR		Std-04		23.04	22.84	0.281	1.000E+03	3.000	1.00E+03	0.00E+00
F06	SYBR		Std-05		26.27	26.18	0.136	1.000E+02	2.000	1.00E+02	0.00E+00
F07	SYBR		Std-06		29.68	29.70	0.023	1.000E+01	1.000	1.00E+01	0.00E+00
F08	SYBR		Std-07		33.19	33.10	0.119	1.000E+00	0.000	1.00E+00	0.00E+00
F09	SYBR		Std-08		N/A	0.00	0.000	1.000E-01	-1.000	0.00E+00	0.00E+00
F10	SYBR		Std-09		N/A	0.00	0.000	1.000E-02	-2.000	0.00E+00	0.00E+00
G03	SYBR		Std-02		15.44	15.56	0.177	1.000E+05	5.000	1.00E+05	0.00E+00
G04	SYBR		Std-03		19.22	19.26	0.068	1.000E+04	4.000	1.00E+04	0.00E+00
G05	SYBR		Std-04		22.64	22.84	0.281	1.000E+03	3.000	1.00E+03	0.00E+00
G06	SYBR		Std-05		26.08	26.18	0.136	1.000E+02	2.000	1.00E+02	0.00E+00
G07	SYBR		Std-06		29.72	29.70	0.023	1.000E+01	1.000	1.00E+01	0.00E+00
G08	SYBR		Std-07		33.02	33.10	0.119	1.000E+00	0.000	1.00E+00	0.00E+00
G09	SYBR		Std-08		N/A	0.00	0.000	1.000E-01	-1.000	0.00E+00	0.00E+00
G10	SYBR		Std-09		N/A	0.00	0.000	1.000E-02	-2.000	0.00E+00	0.00E+00

Melt Curve

Step #: 5



Melt Peak



Melt Curve Data

Well	Fluor	Target	Content	Sample	Melt Temp
B04	SYBR	PCV2	Unkn-01	B1	85.00
B05	SYBR	PCV2	Unkn-02	B2	85.00
B06	SYBR	PCV2	Unkn-03	B3	85.00
B07	SYBR	PCV2	Unkn-04	B4	85.00
B08	SYBR	PCV2	Unkn-05	B5	85.00
B09	SYBR	PCV2	NTC-01		None
B10	SYBR	PCV2	Neg Ctrl-01	PK-15	None
C04	SYBR	PCV2	Unkn-01	B1	85.00
C05	SYBR	PCV2	Unkn-02	B2	85.00
C06	SYBR	PCV2	Unkn-03	B3	85.00
C07	SYBR	PCV2	Unkn-04	B4	85.00
C08	SYBR	PCV2	Unkn-05	B5	85.00
C09	SYBR	PCV2	NTC-01		None
C10	SYBR	PCV2	Neg Ctrl-01	PK-15	None
D03	SYBR	PCV2	Neg Ctrl-03	MDBK	None
D04	SYBR	PCV2	Unkn-06	D1	85.00
D05	SYBR	PCV2	Unkn-07	D2	85.00
D06	SYBR	PCV2	Unkn-08	D3	85.00
D07	SYBR	PCV2	Unkn-09	D4	85.00
D08	SYBR	PCV2	Unkn-10	D5	85.00
D09	SYBR	PCV2	Neg Ctrl-02	Mock infection	85.00
D10	SYBR		Std-01	Original PCV2	85.00
E03	SYBR	PCV2	Neg Ctrl-03	MDBK	85.00
E04	SYBR	PCV2	Unkn-06	D1	85.00
E05	SYBR	PCV2	Unkn-07	D2	85.00

Well	Fluor	Target	Content	Sample	Melt Temp
E06	SYBR	PCV2	Unkn-08	D3	85.00
E07	SYBR	PCV2	Unkn-09	D4	85.00
E08	SYBR	PCV2	Unkn-10	D5	85.00
E09	SYBR	PCV2	Neg Ctrl-02	Mock infection	85.00
E10	SYBR		Std-01	Original PCV2	85.00
F03	SYBR		Std-02		85.00
F04	SYBR		Std-03		85.00
F05	SYBR		Std-04		85.00
F06	SYBR		Std-05		85.00
F07	SYBR		Std-06		85.00
F08	SYBR		Std-07		85.00
F09	SYBR		Std-08		None
F10	SYBR		Std-09		None
G03	SYBR		Std-02		85.00
G04	SYBR		Std-03		85.00
G05	SYBR		Std-04		85.00
G06	SYBR		Std-05		85.00
G07	SYBR		Std-06		85.00
G08	SYBR		Std-07		85.00
G09	SYBR		Std-08		None
G10	SYBR		Std-09		None



01.03.2022: Concentrating PCV2 virus.pcrd

03/09/2023 14:47

Protocol

1: 98.0°C for 3:00

2: 95.0°C for 0:15

3: 60.0°C for 1:00

Plate Read

4: GOTO 2, 39 more times

5: Melt Curve 65.0°C to 95.0°C: Increment 0.5°C 0:05

Plate Read

Plate Display

Quantification

Step #: 3

Analysis Mode: Fluorophore

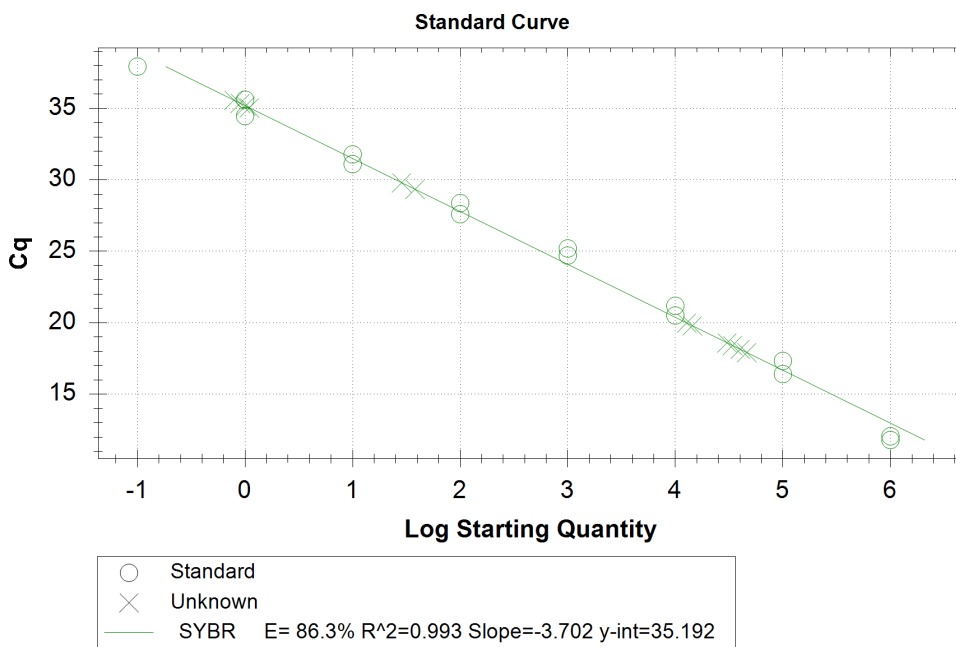
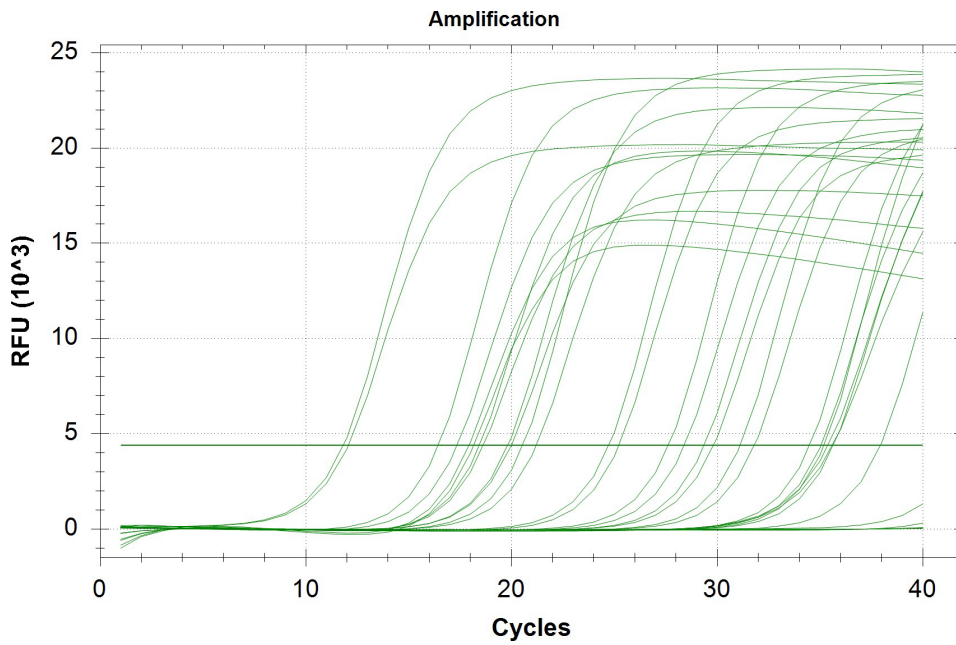
Cq Determination: Single Threshold

Baseline Method:

SYBR: Auto Calculated

Threshold Setting:

SYBR: 4391.08, Auto Calculated



Quantification Data

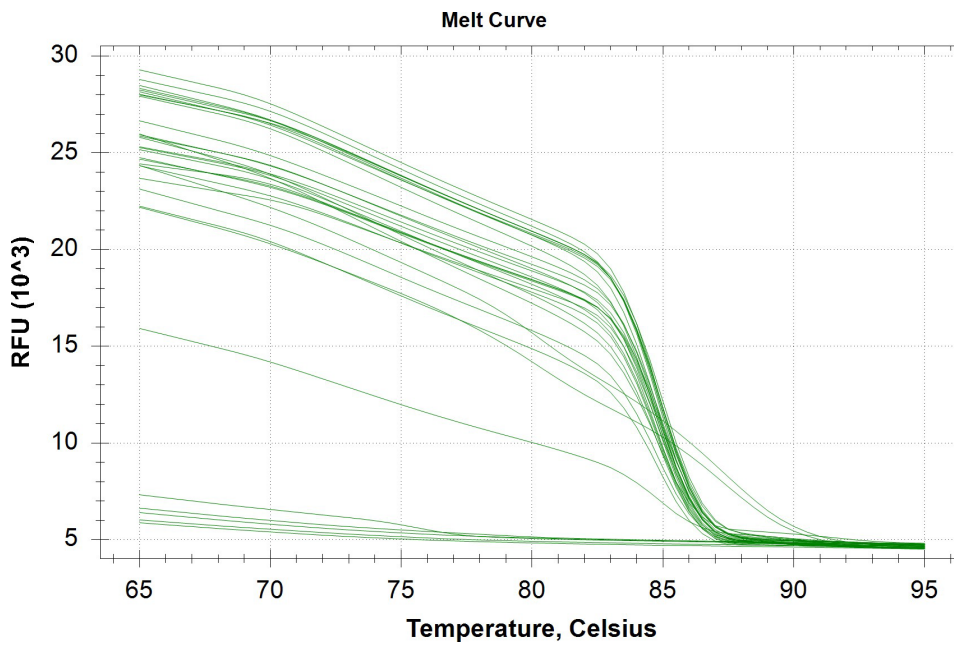
Well	Fluor	Target	Content	Sample	Cq	Cq Mean	Cq Std. Dev	Starting Quantity (SQ)	Log Starting Quantity	SQ Mean	SQ Std. Dev
B04	SYBR		Unkn-1	1	19.99	19.90	0.138	1.275E+04	4.106	1.36E+04	1.16E+03
B05	SYBR		Unkn-2	2	29.80	29.57	0.325	2.860E+01	1.456	3.33E+01	6.69E+00
B06	SYBR		Unkn-3	3	35.04	35.11	0.092	1.097E+00	0.040	1.05E+00	6.04E-02
B07	SYBR		Unkn-4	4	18.15	18.04	0.160	4.012E+04	4.603	4.32E+04	4.29E+03
B08	SYBR		Unkn-5	5	18.60	18.51	0.133	3.025E+04	4.481	3.21E+04	2.66E+03
C04	SYBR		Unkn-1	1	19.80	19.90	0.138	1.439E+04	4.158	1.36E+04	1.16E+03
C05	SYBR		Unkn-2	2	29.34	29.57	0.325	3.805E+01	1.580	3.33E+01	6.69E+00
C06	SYBR		Unkn-3	3	35.17	35.11	0.092	1.012E+00	0.005	1.05E+00	6.04E-02
C07	SYBR		Unkn-4	4	17.92	18.04	0.160	4.618E+04	4.664	4.32E+04	4.29E+03
C08	SYBR		Unkn-5	5	18.42	18.51	0.133	3.401E+04	4.532	3.21E+04	2.66E+03
D05	SYBR		Std-1	PC	12.06	11.93	0.184	1.000E+06	6.000	1.00E+06	0.00E+00
D06	SYBR		NTC	NTC	N/A	0.00	0.000	N/A	N/A	0.00E+00	0.00E+00
D07	SYBR		Neg Ctrl	NC	35.58	35.58	0.000	7.878E-01	-0.104	7.88E-01	0.00E+00
E05	SYBR		Std-1	PC	11.80	11.93	0.184	1.000E+06	6.000	1.00E+06	0.00E+00
E06	SYBR		NTC	NTC	N/A	0.00	0.000	N/A	N/A	0.00E+00	0.00E+00
E07	SYBR		Neg Ctrl	NC	35.36	35.36	0.000	9.004E-01	-0.046	9.00E-01	0.00E+00
F03	SYBR		Std-2		17.33	16.87	0.650	1.000E+05	5.000	1.00E+05	0.00E+00
F04	SYBR		Std-3		21.19	20.85	0.478	1.000E+04	4.000	1.00E+04	0.00E+00
F05	SYBR		Std-4		25.20	24.95	0.351	1.000E+03	3.000	1.00E+03	0.00E+00
F06	SYBR		Std-5		28.37	27.99	0.548	1.000E+02	2.000	1.00E+02	0.00E+00
F07	SYBR		Std-6		31.78	31.44	0.482	1.000E+01	1.000	1.00E+01	0.00E+00
F08	SYBR		Std-7		35.62	35.04	0.816	1.000E+00	0.000	1.00E+00	0.00E+00
F09	SYBR		Std-8		37.92	37.92	0.000	1.000E-01	-1.000	1.00E-01	0.00E+00
F10	SYBR		Std-9		N/A	0.00	0.000	1.000E-02	-2.000	0.00E+00	0.00E+00
G03	SYBR		Std-2		16.41	16.87	0.650	1.000E+05	5.000	1.00E+05	0.00E+00
G04	SYBR		Std-3		20.51	20.85	0.478	1.000E+04	4.000	1.00E+04	0.00E+00
G05	SYBR		Std-4		24.71	24.95	0.351	1.000E+03	3.000	1.00E+03	0.00E+00
G06	SYBR		Std-5		27.60	27.99	0.548	1.000E+02	2.000	1.00E+02	0.00E+00

Quantification Data

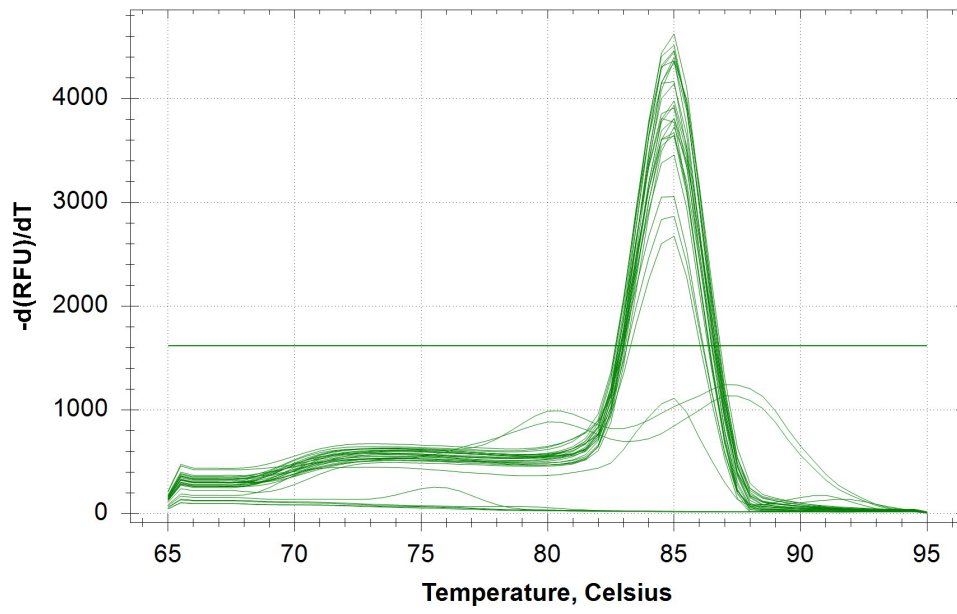
Well	Fluor	Target	Content	Sample	Cq	Cq Mean	Cq Std. Dev	Starting Quantity (SQ)	Log Starting Quantity	SQ Mean	SQ Std. Dev
G07	SYBR		Std-6		31.10	31.44	0.482	1.000E+01	1.000	1.00E+01	0.00E+00
G08	SYBR		Std-7		34.46	35.04	0.816	1.000E+00	0.000	1.00E+00	0.00E+00
G09	SYBR		Std-8		N/A	0.00	0.000	1.000E-01	-1.000	0.00E+00	0.00E+00
G10	SYBR		Std-9		N/A	0.00	0.000	1.000E-02	-2.000	0.00E+00	0.00E+00

Melt Curve

Step #: 5



Melt Peak



Melt Curve Data

Well	Fluor	Target	Content	Sample	Melt Temp
B04	SYBR		Unkn-1	1	85.00
B05	SYBR		Unkn-2	2	85.00
B06	SYBR		Unkn-3	3	85.00
B07	SYBR		Unkn-4	4	85.00
B08	SYBR		Unkn-5	5	85.00
C04	SYBR		Unkn-1	1	85.00
C05	SYBR		Unkn-2	2	84.50
C06	SYBR		Unkn-3	3	85.00
C07	SYBR		Unkn-4	4	85.00
C08	SYBR		Unkn-5	5	85.00
D05	SYBR		Std-1	PC	85.00
D06	SYBR		NTC	NTC	None
D07	SYBR		Neg Ctrl	NC	None
E05	SYBR		Std-1	PC	85.00
E06	SYBR		NTC	NTC	None
E07	SYBR		Neg Ctrl	NC	None
F03	SYBR		Std-2		85.00
F04	SYBR		Std-3		85.00
F05	SYBR		Std-4		85.00
F06	SYBR		Std-5		85.00
F07	SYBR		Std-6		85.00
F08	SYBR		Std-7		85.00
F09	SYBR		Std-8		None
F10	SYBR		Std-9		None
G03	SYBR		Std-2		85.00
G04	SYBR		Std-3		85.00
G05	SYBR		Std-4		85.00
G06	SYBR		Std-5		85.00
G07	SYBR		Std-6		85.00

Well	Fluor	Target	Content	Sample	Melt Temp
G08	SYBR		Std-7		85.00
G09	SYBR		Std-8		None
G10	SYBR		Std-9		None



Norges miljø- og biovitenskapelige universitet
Noregs miljø- og biovitenskapelige universitet
Norwegian University of Life Sciences

Postboks 5003
NO-1432 Ås
Norway